Imaging by wave-equation inversion

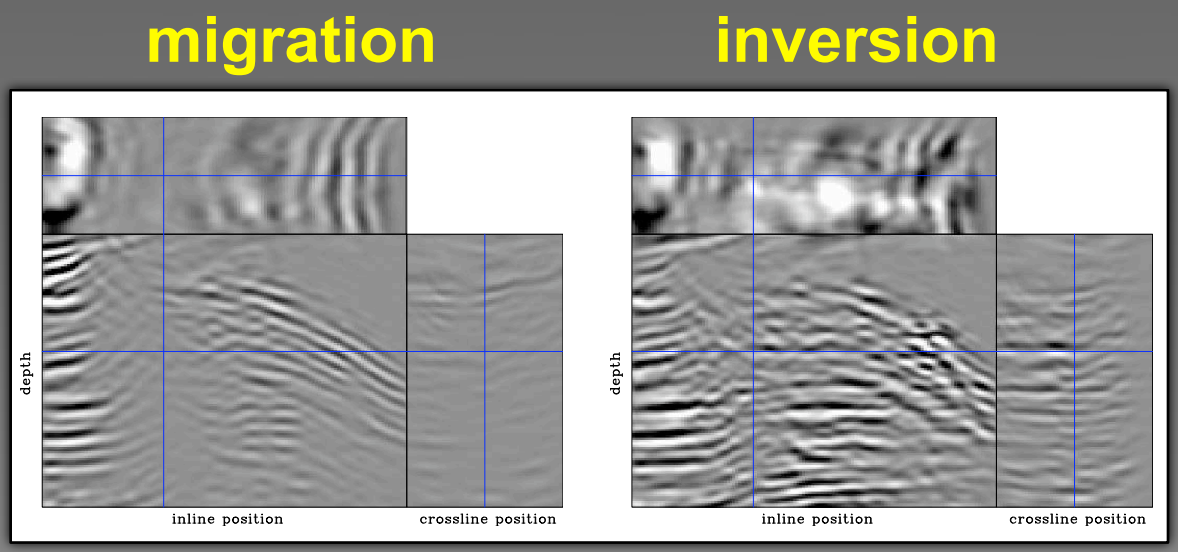

Alejandro A. Valenciano

Subsalt hydrocarbon field

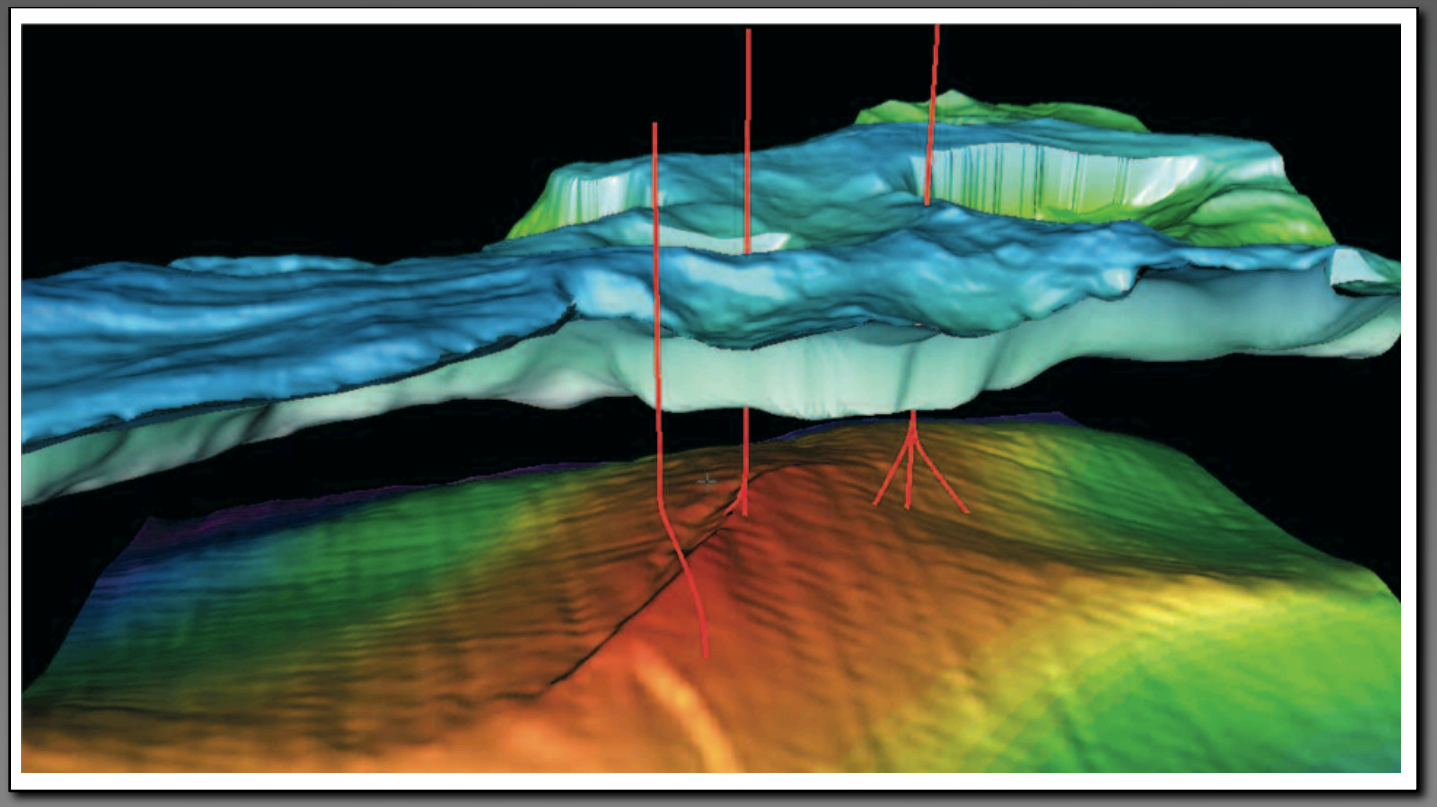

(from bp frontiers, www.bp.com)

Worldwide distribution of offshore salt sheets

[from Farmer et al., (Oilfield Review, 1996), adapted from Ward et al. The Leading Edge (1994)]

Reflectivity image

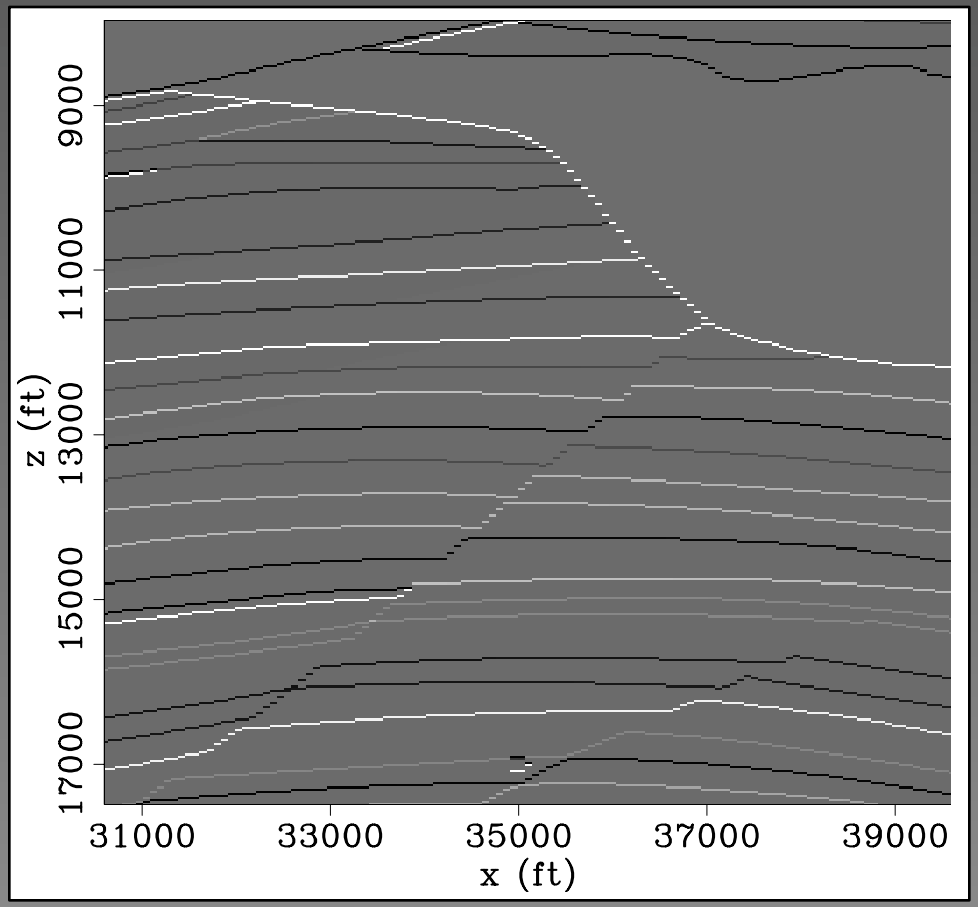

Migrated image

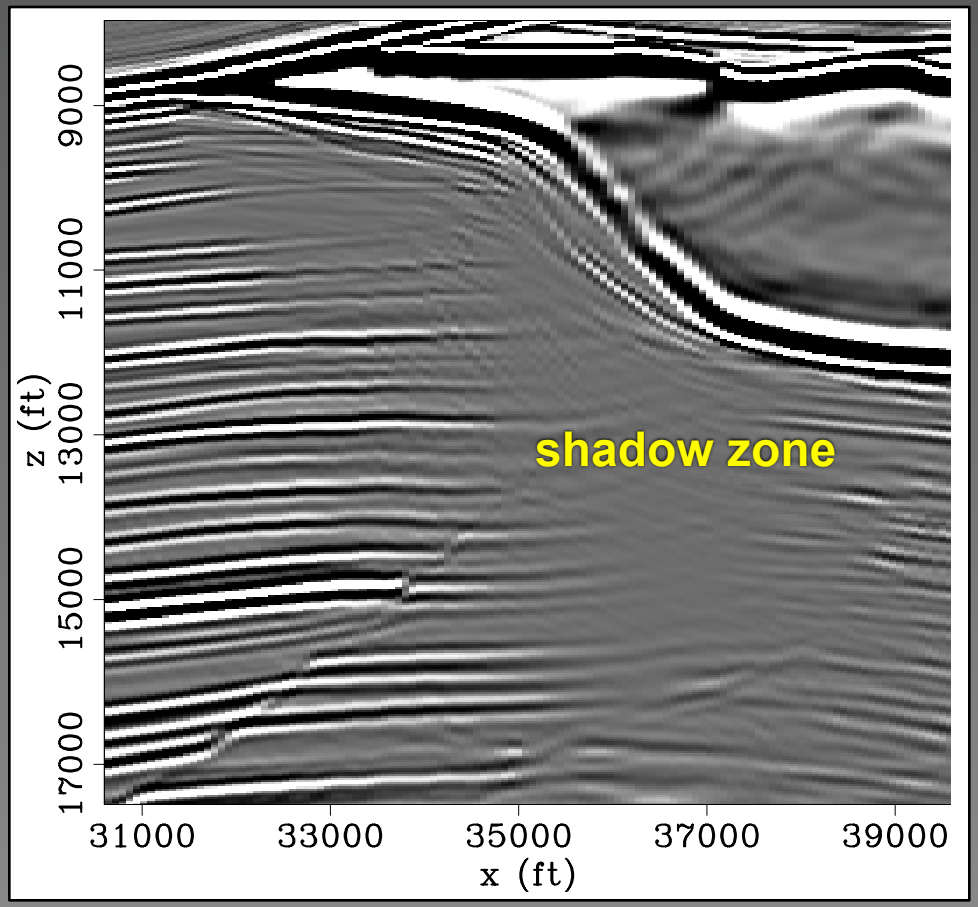

Propagation through salt

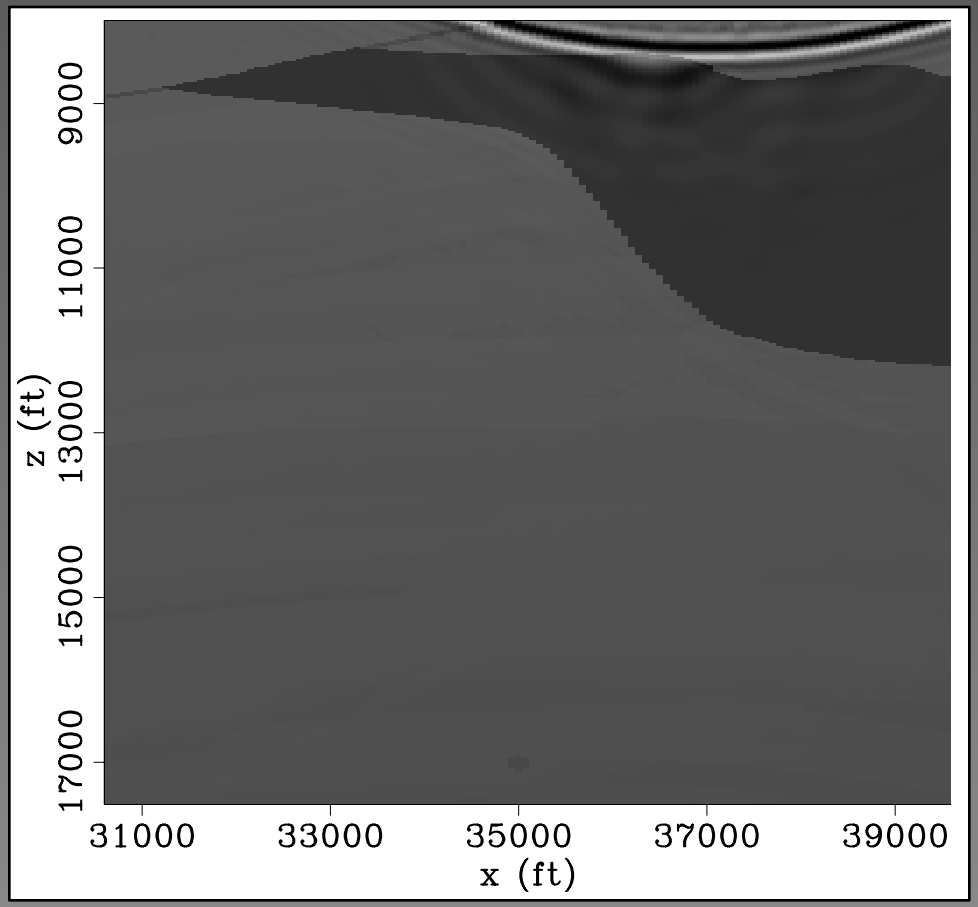

Propagation through salt

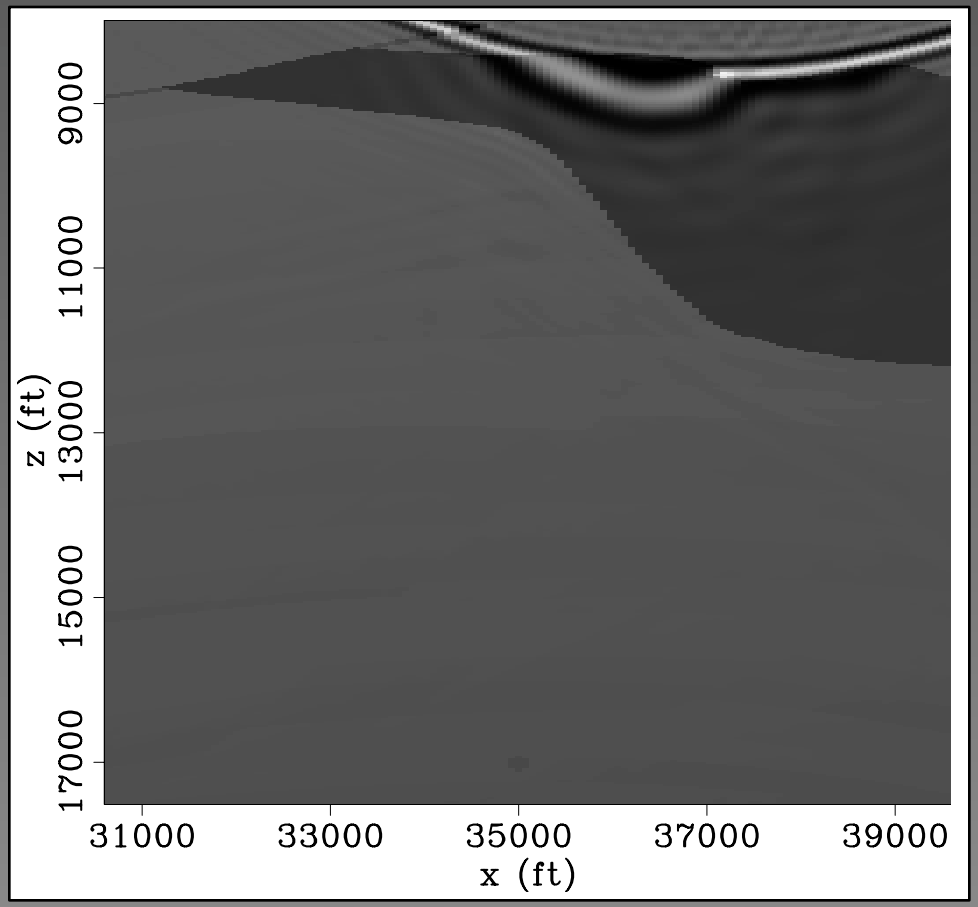

Propagation through salt

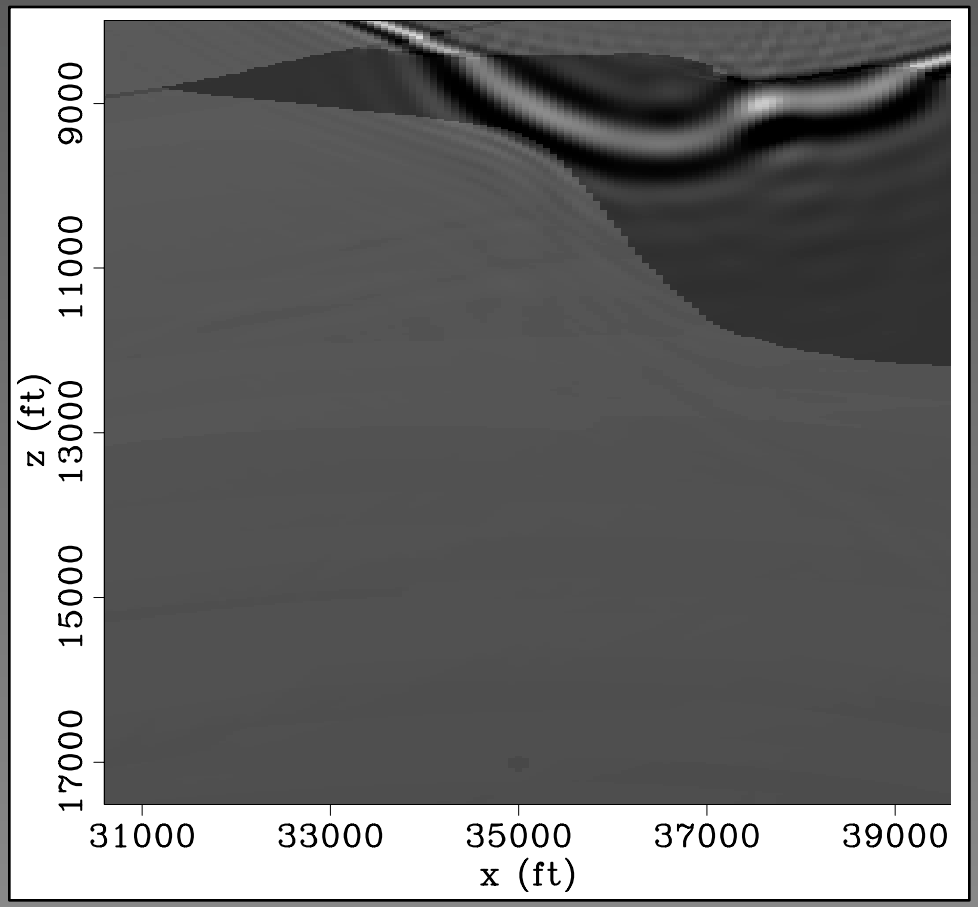

Propagation through salt

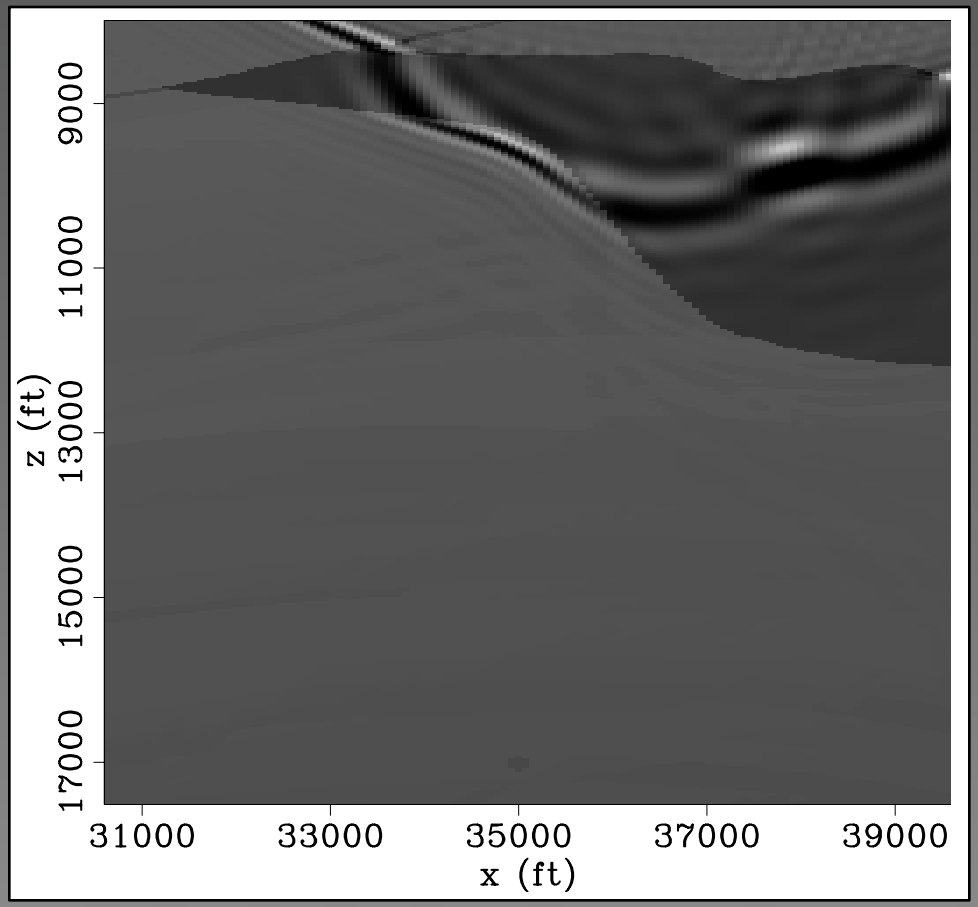

Propagation through salt

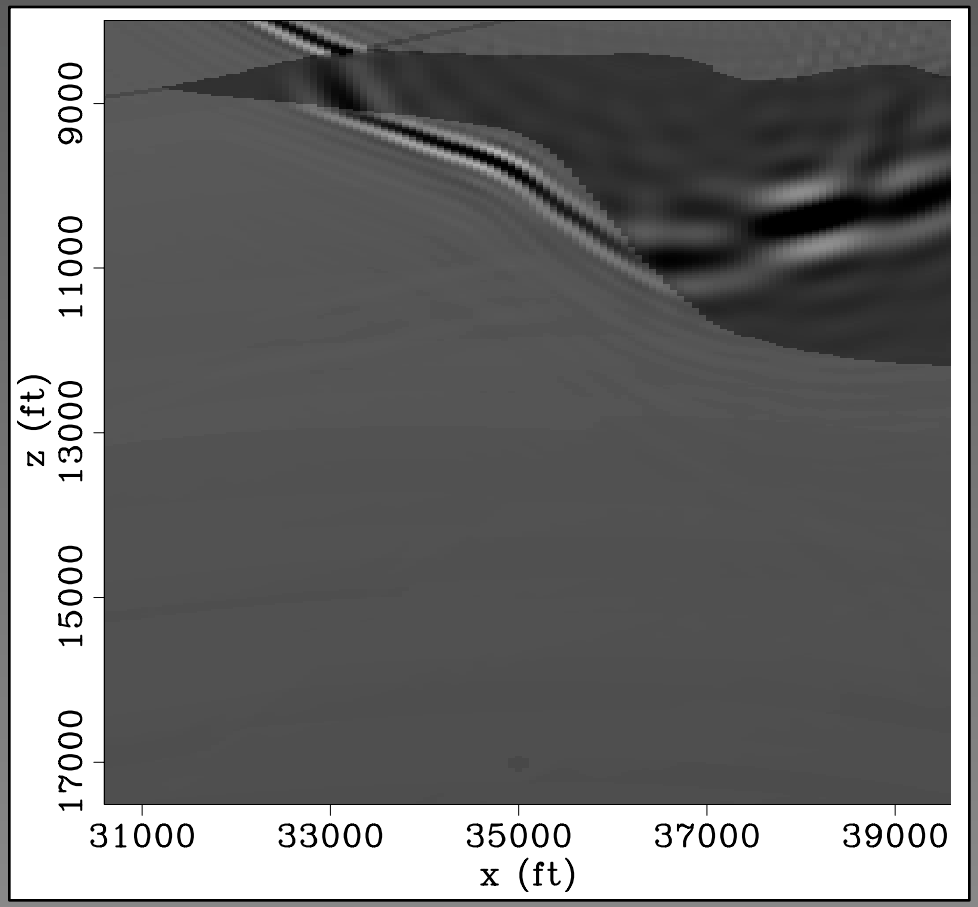

Propagation through salt

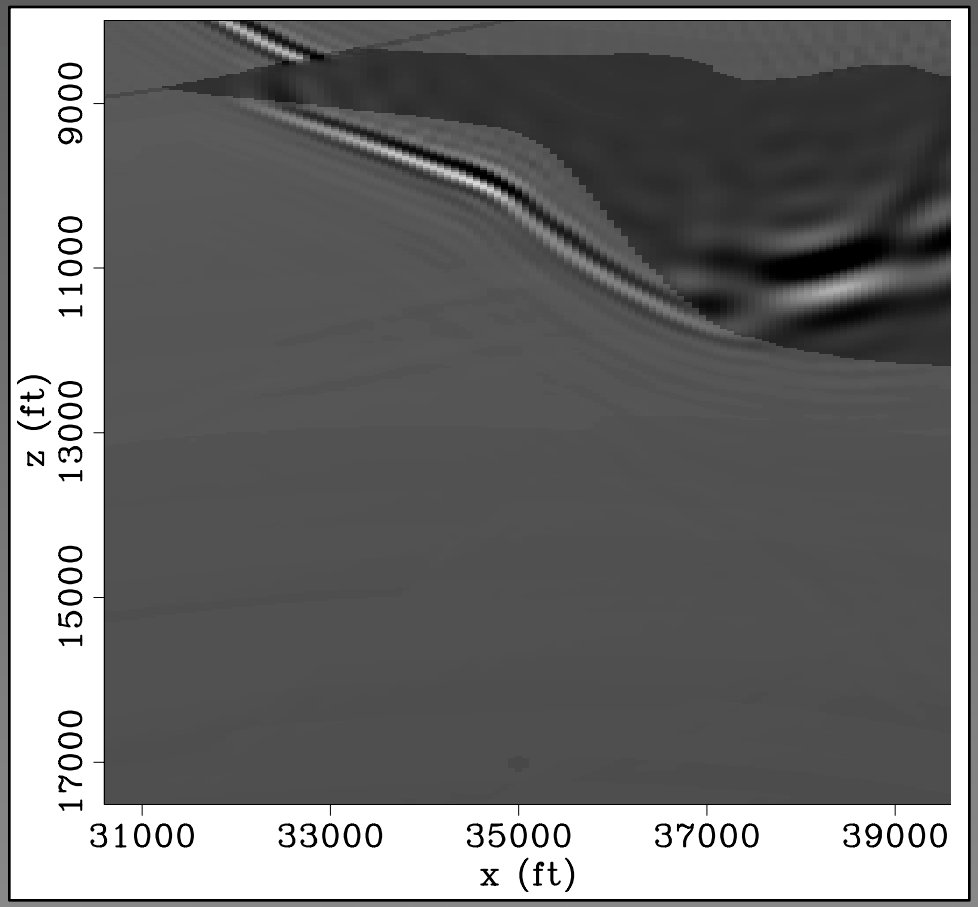

Propagation through salt

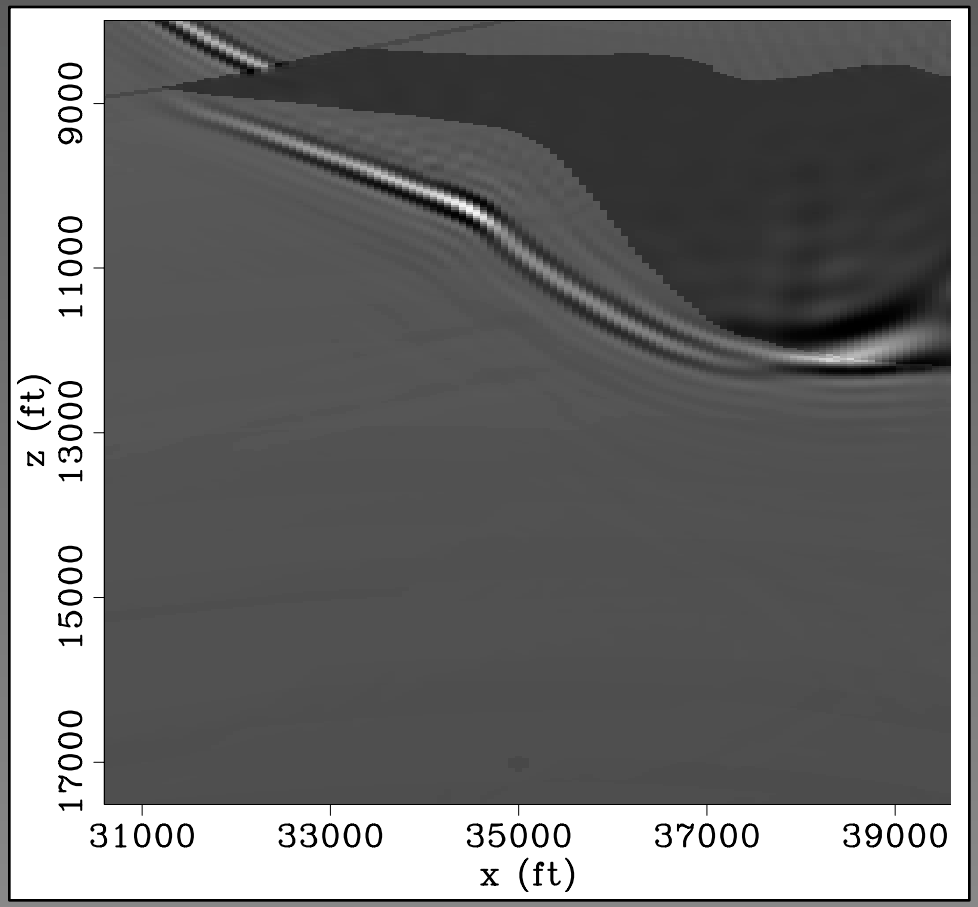

Propagation through salt

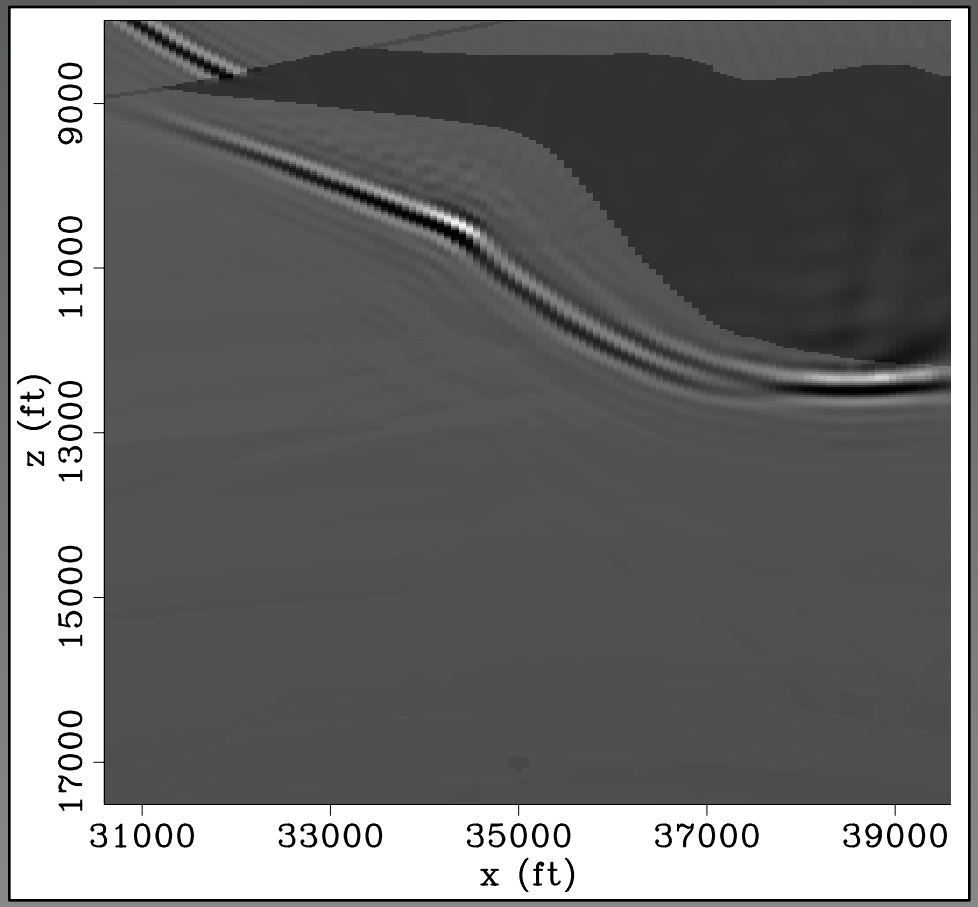

Propagation through salt

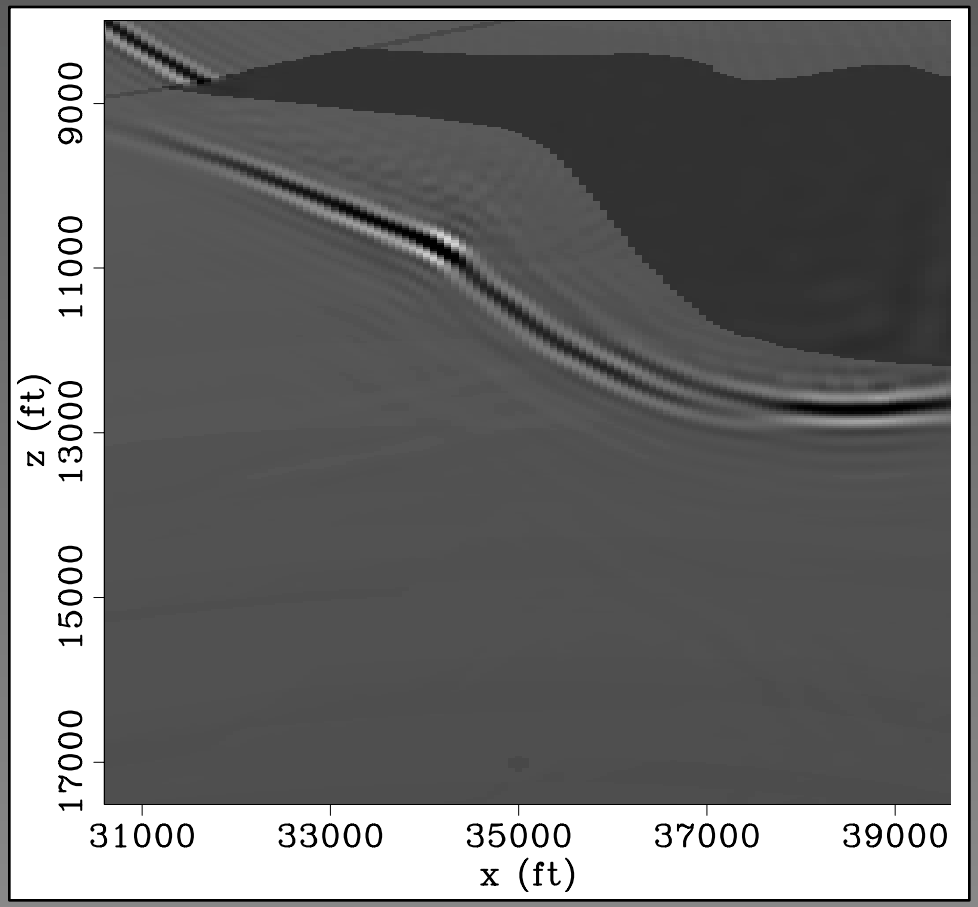

Propagation through salt

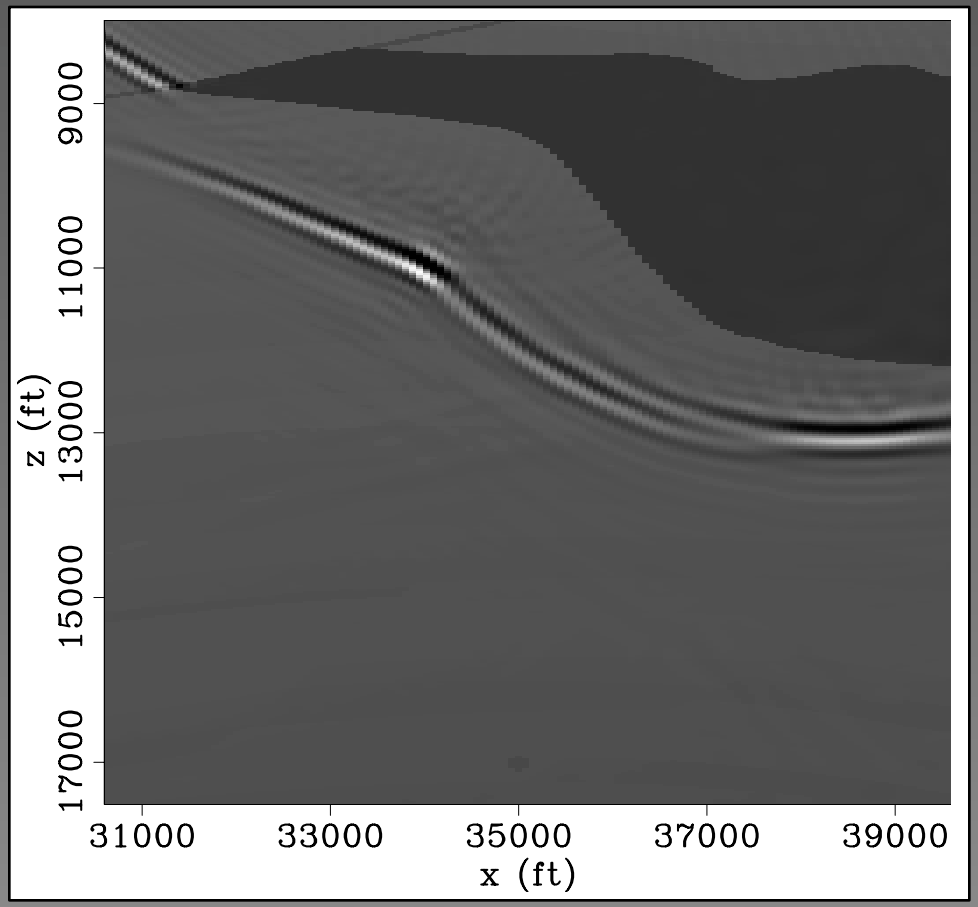

Propagation through salt

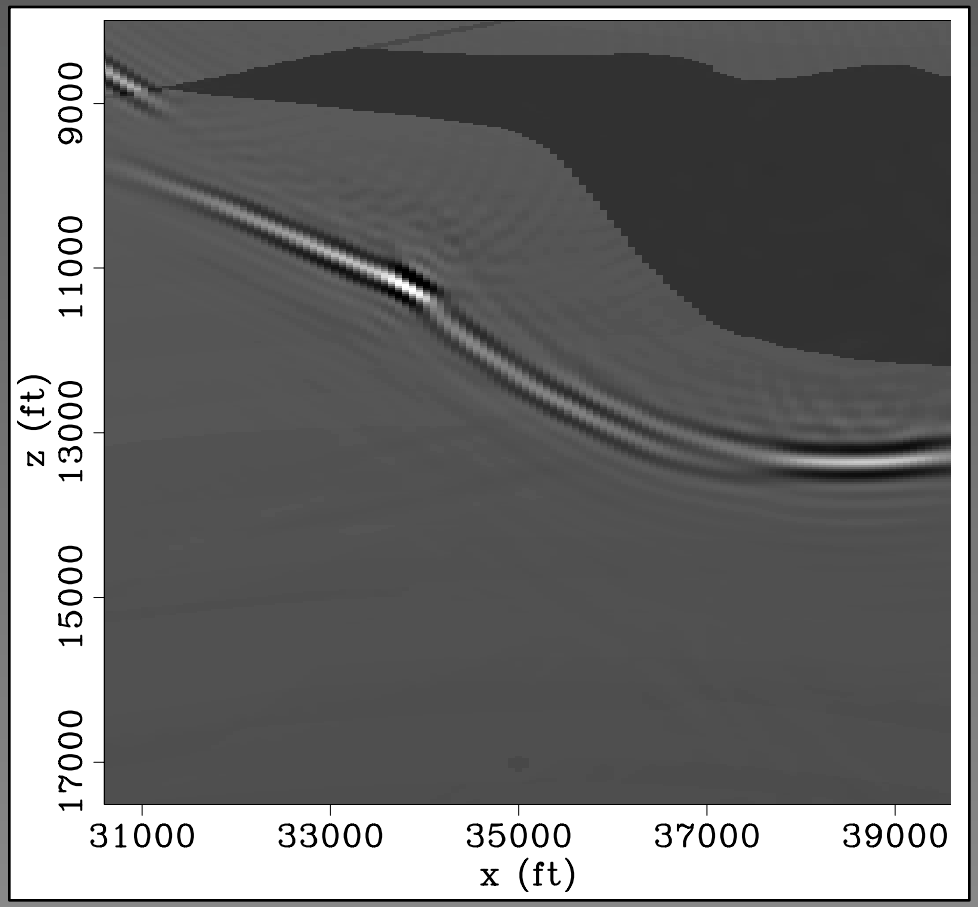

Propagation through salt

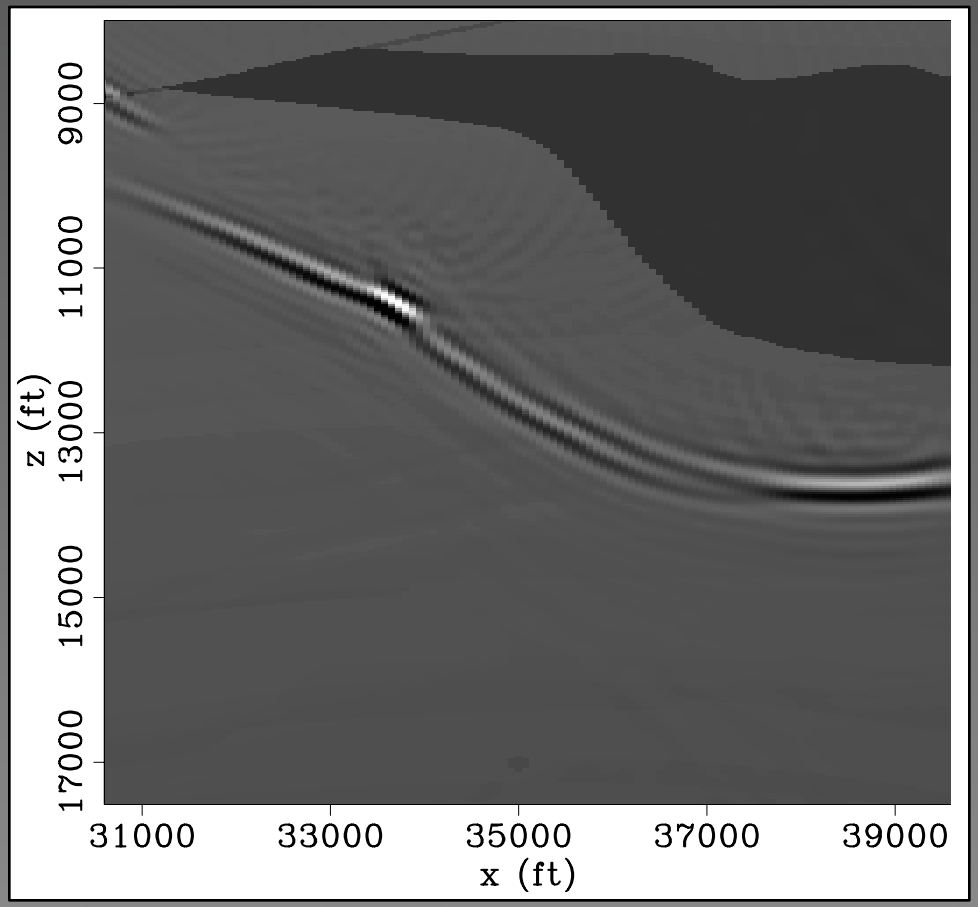

Propagation through salt

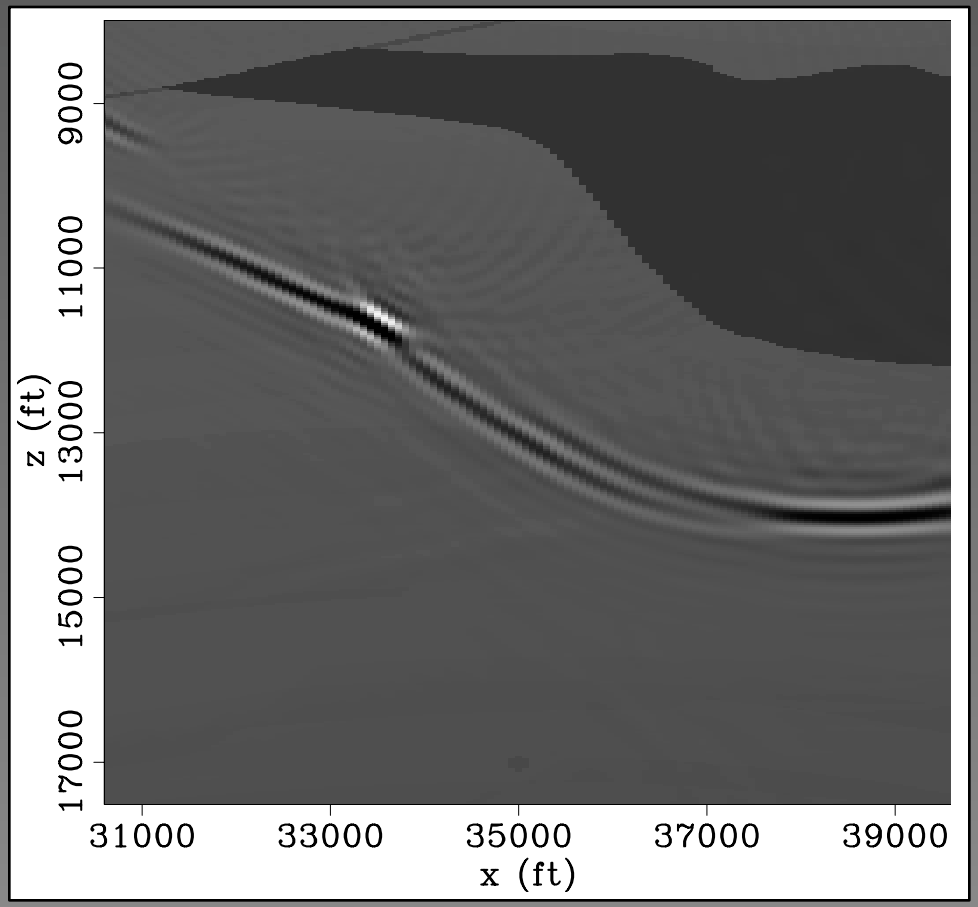

“illumination” constant velocity

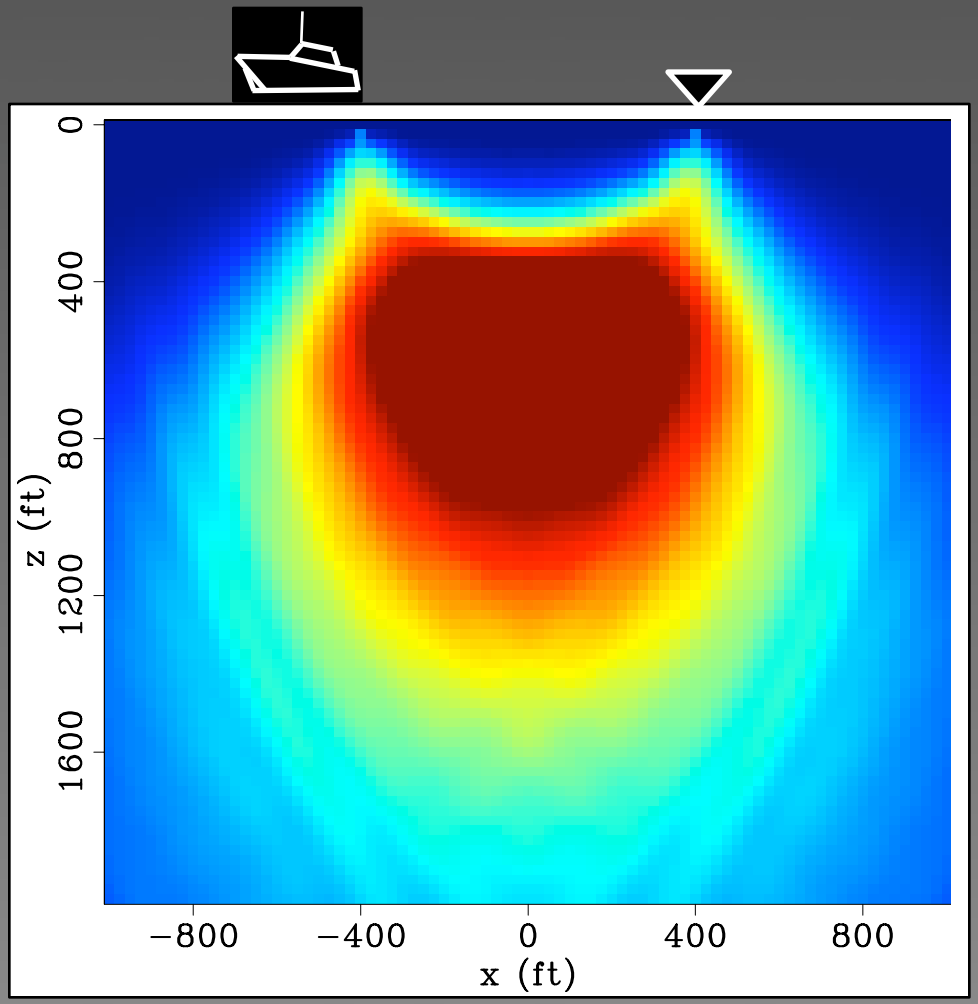

“illumination” constant velocity

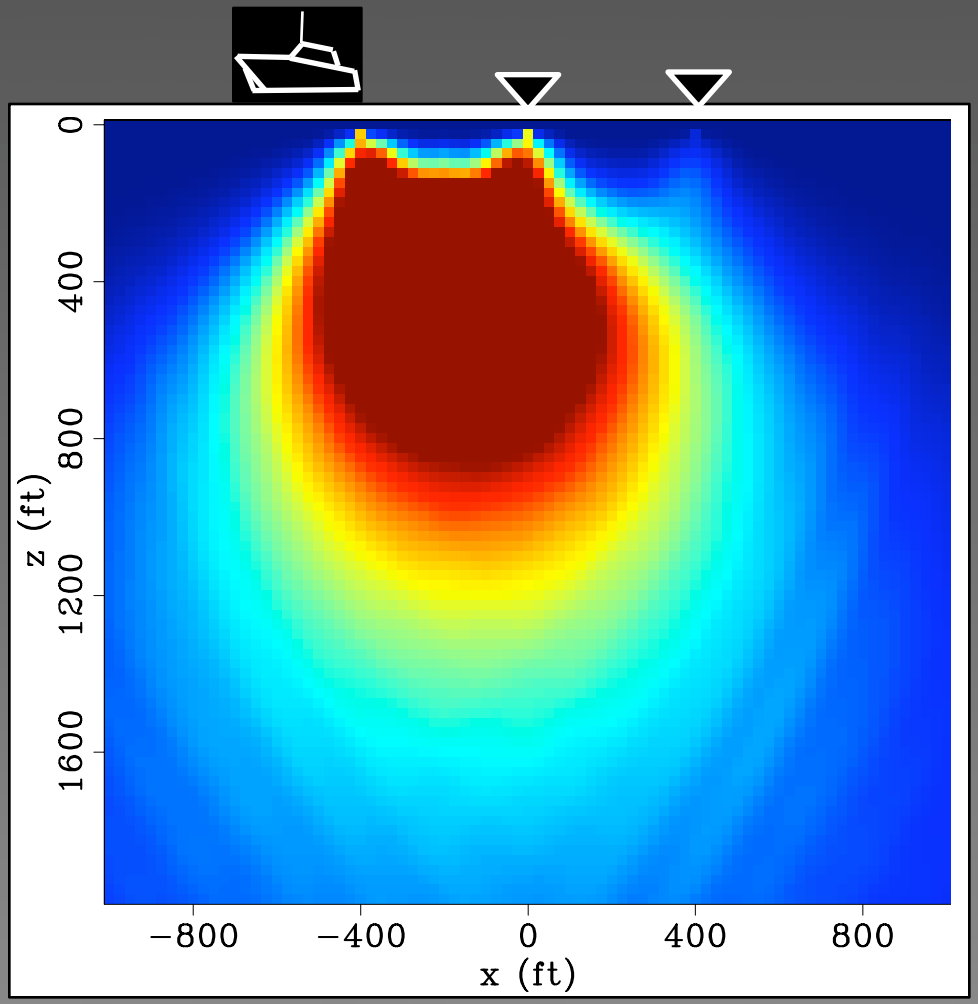

“illumination” constant velocity

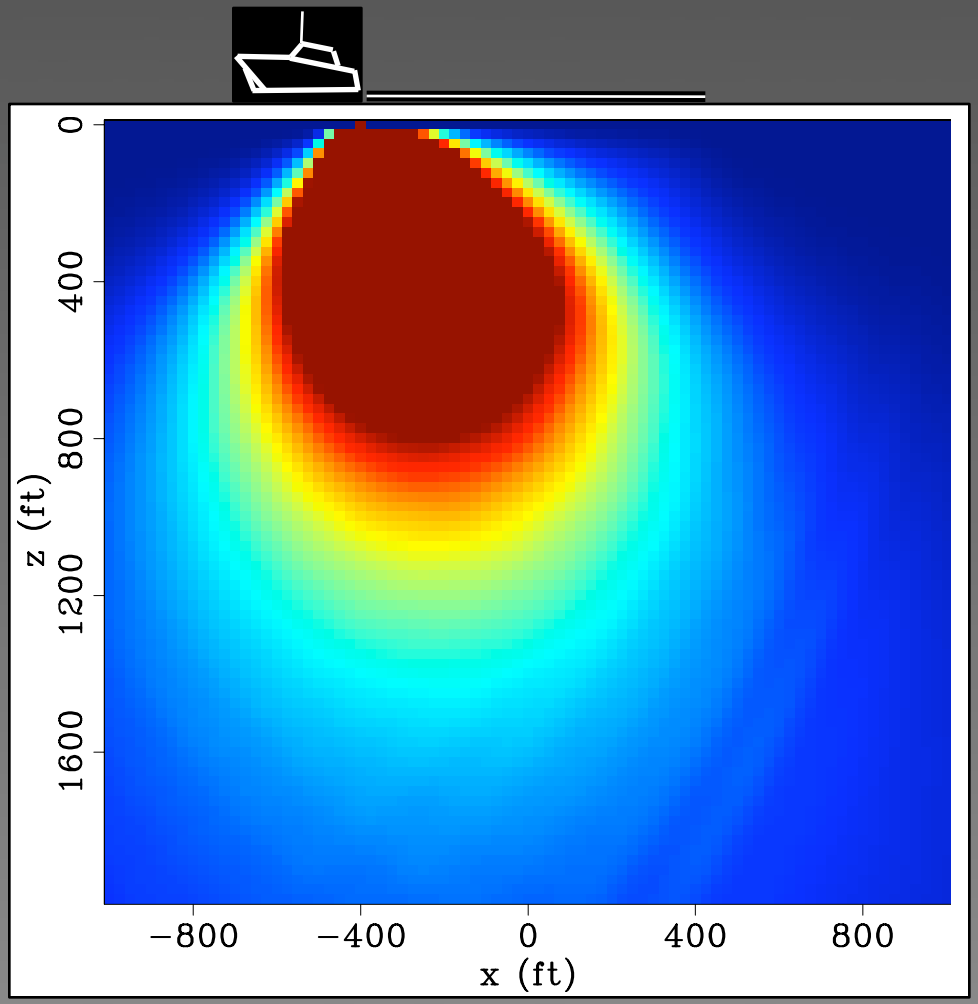

“illumination” from shot at x=40000 ft

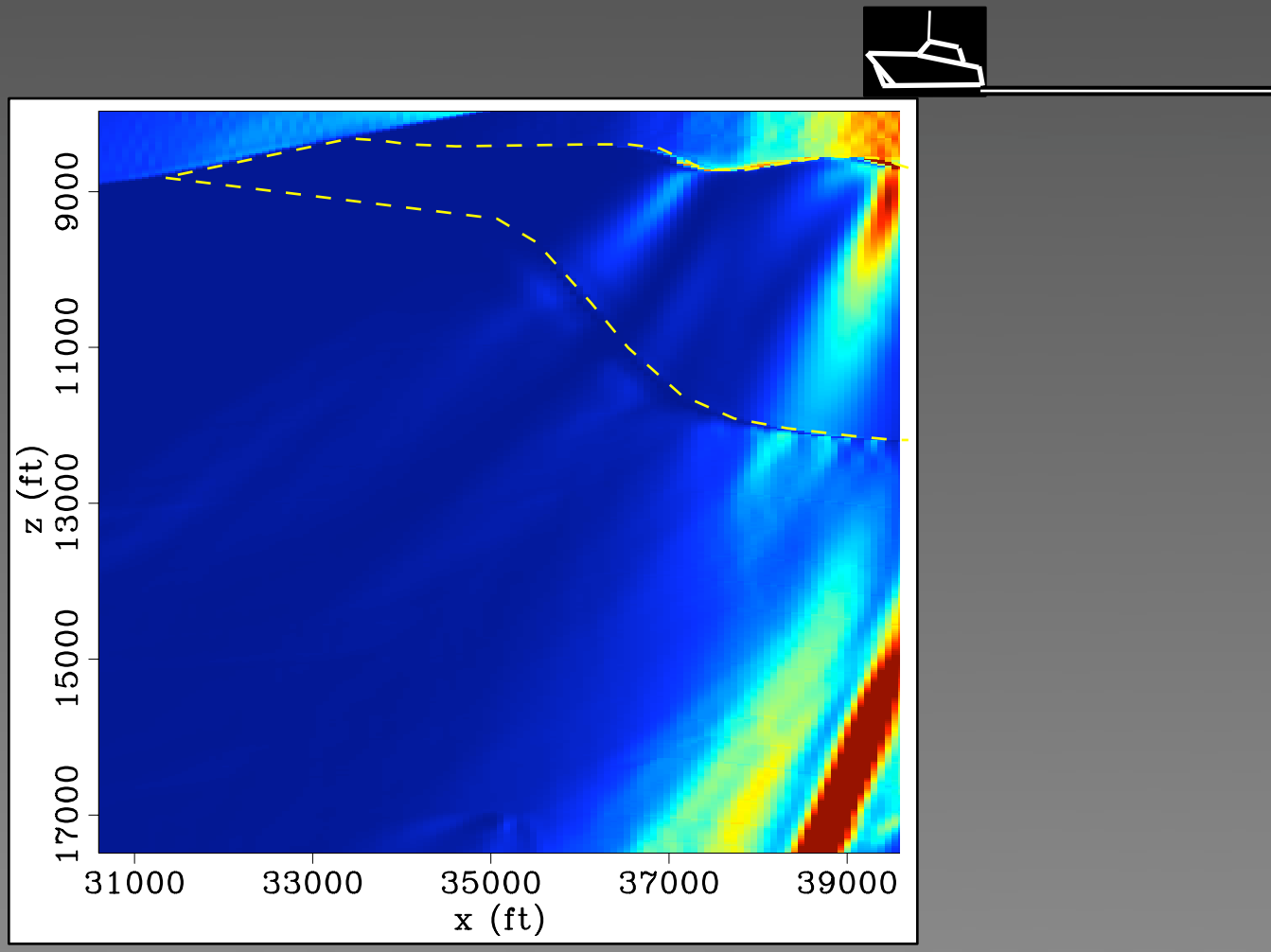

“illumination” from shot at x=39000 ft

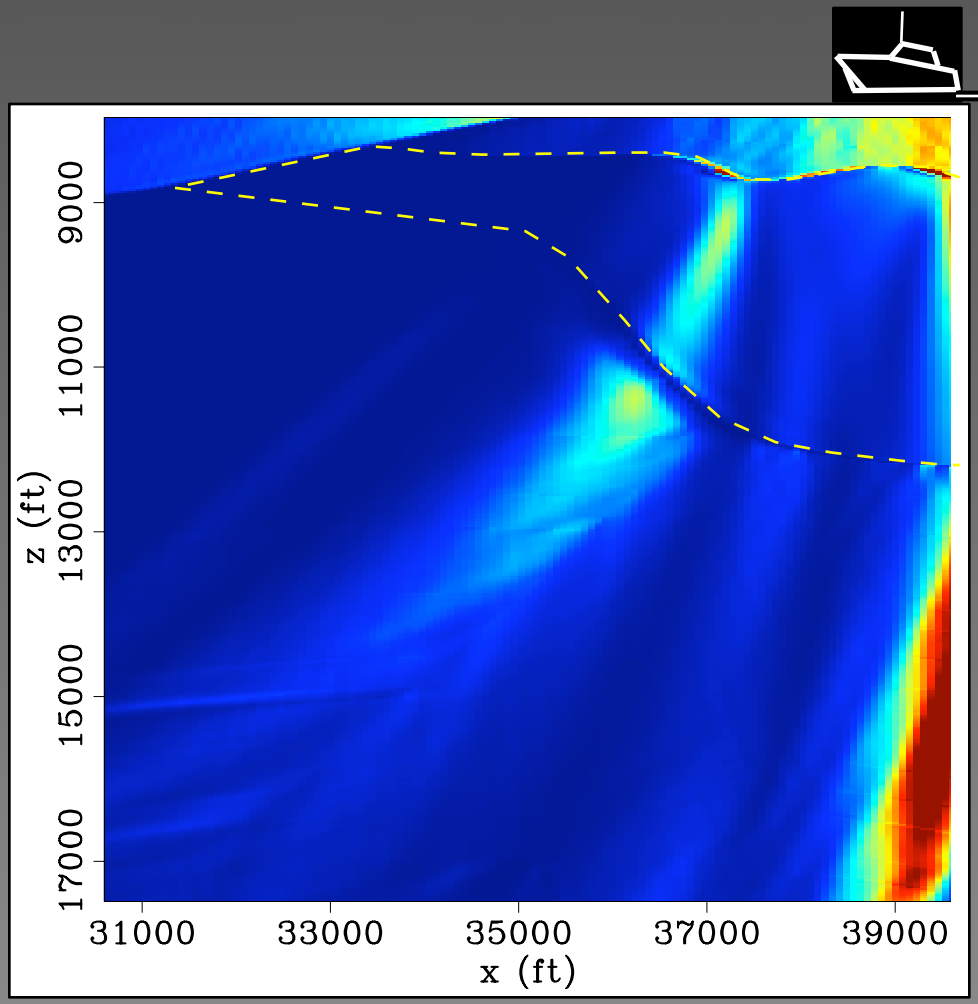

“illumination” from shot at x=38000 ft

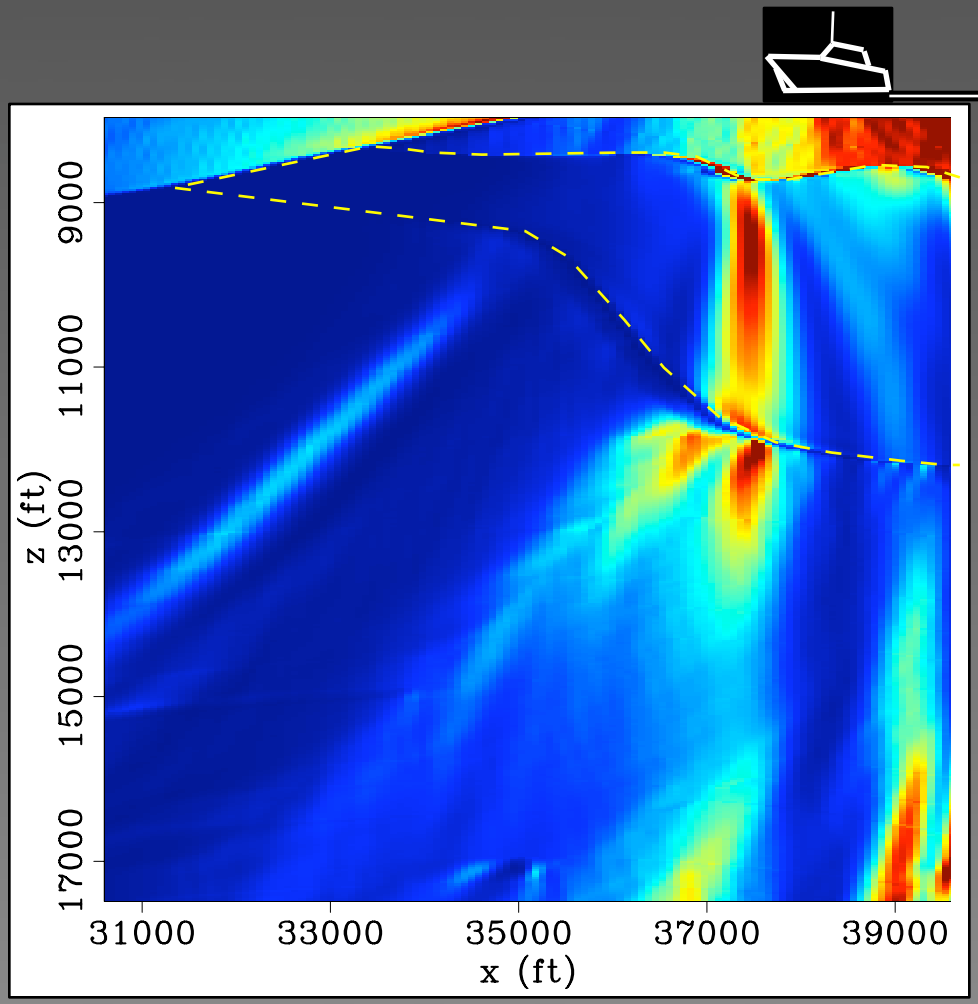

“illumination” from shot at x=37000 ft

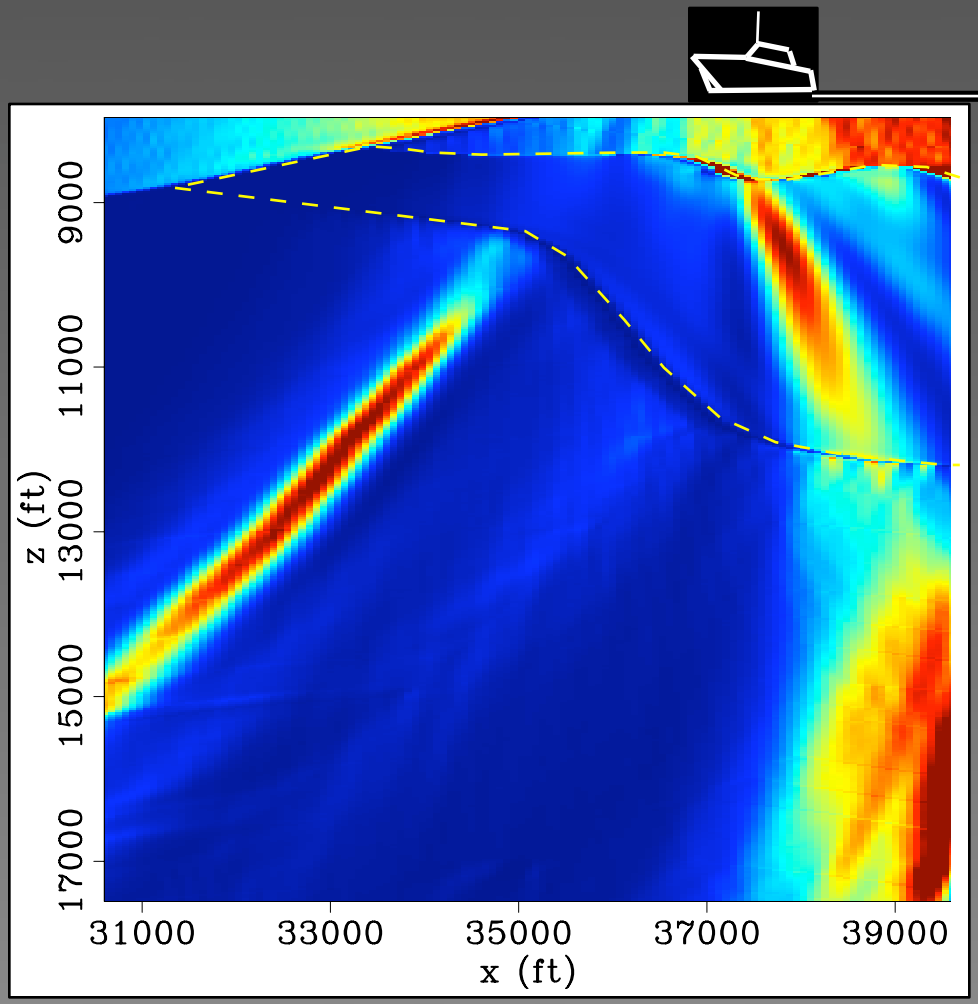

“illumination” from shot at x=36000 ft

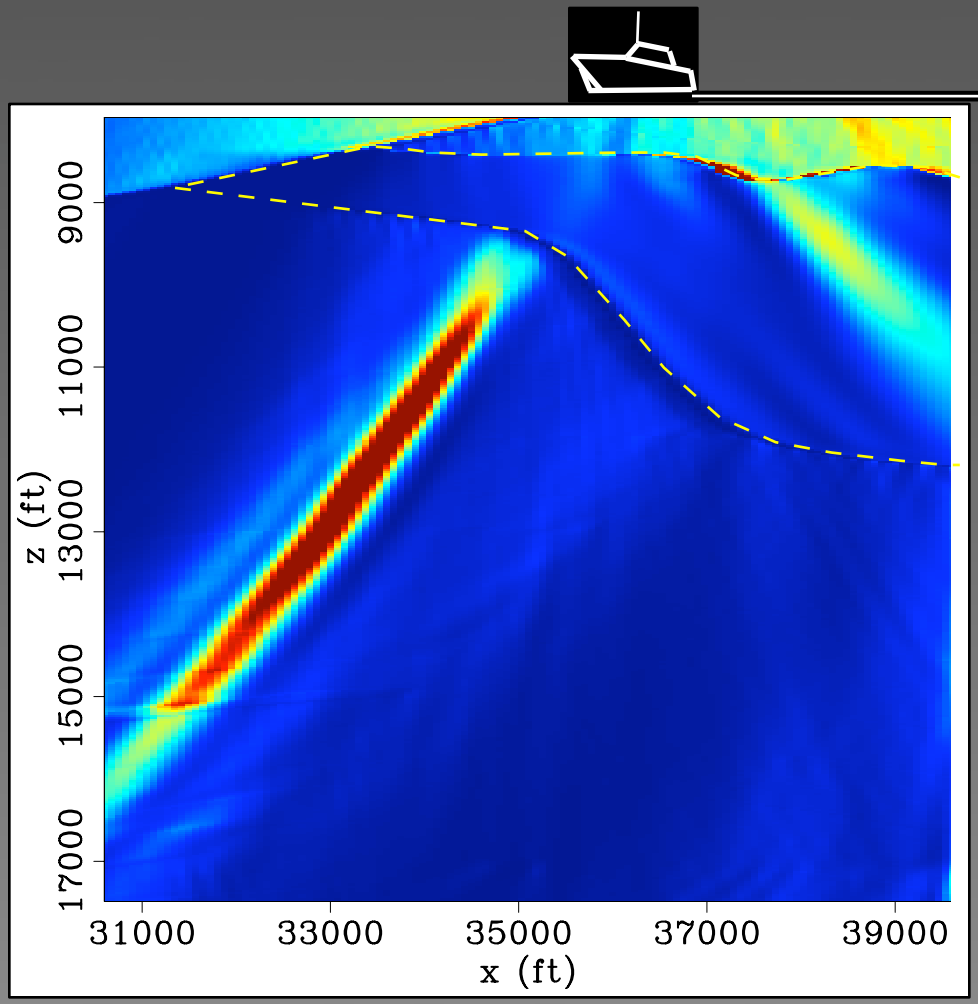

“illumination” from shot at x=35000 ft

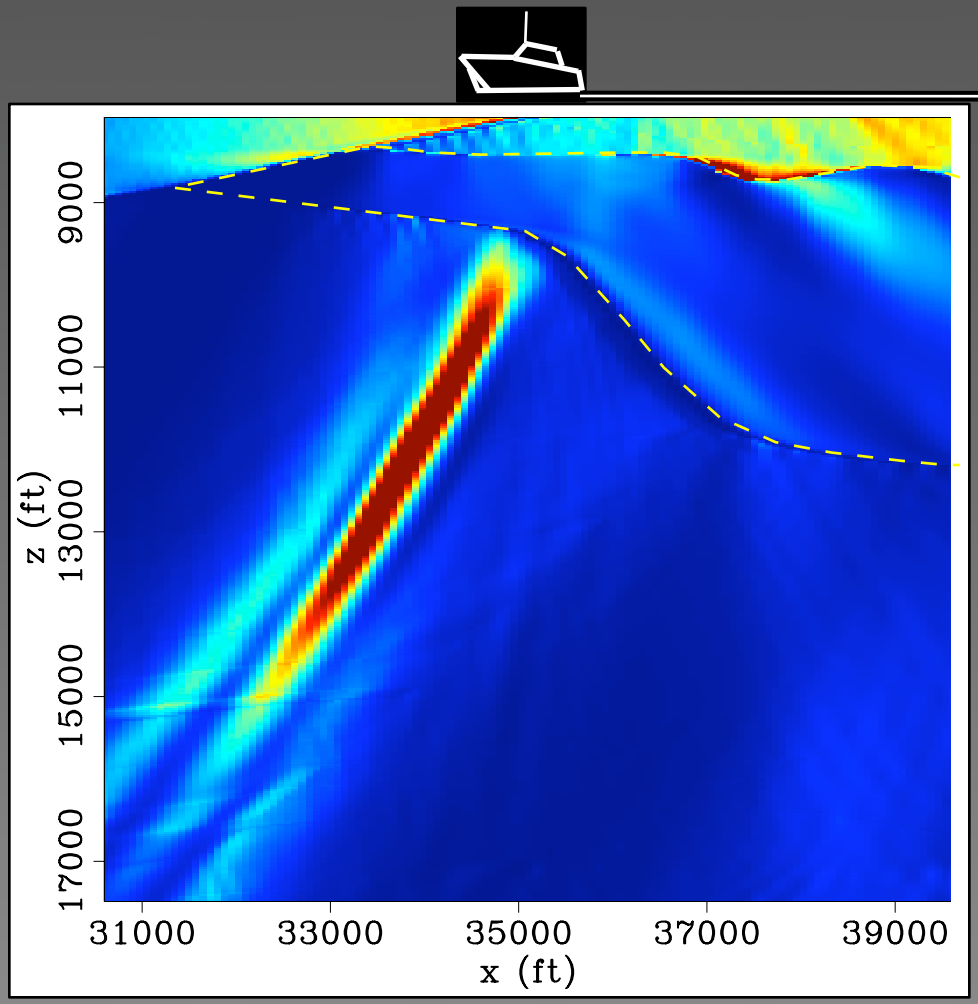

“illumination” from shot at x=34000 ft

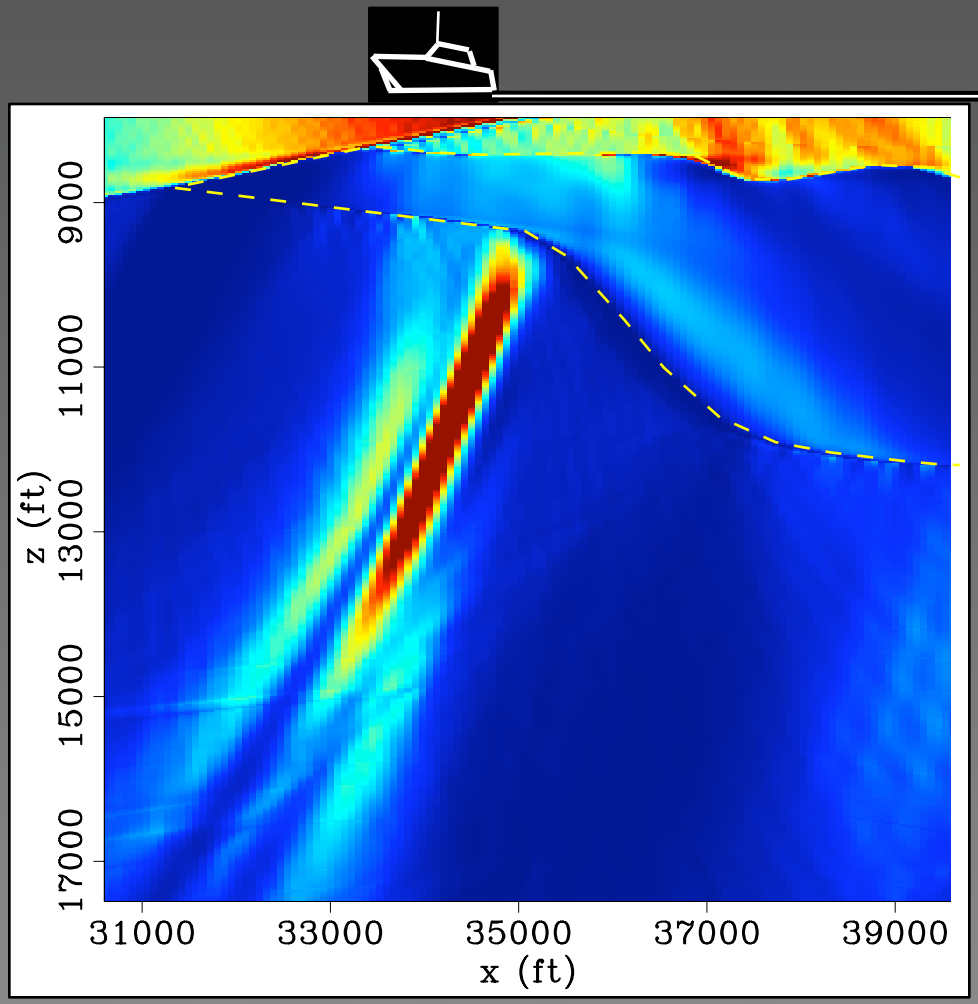

“illumination” from shot at x=33000 ft

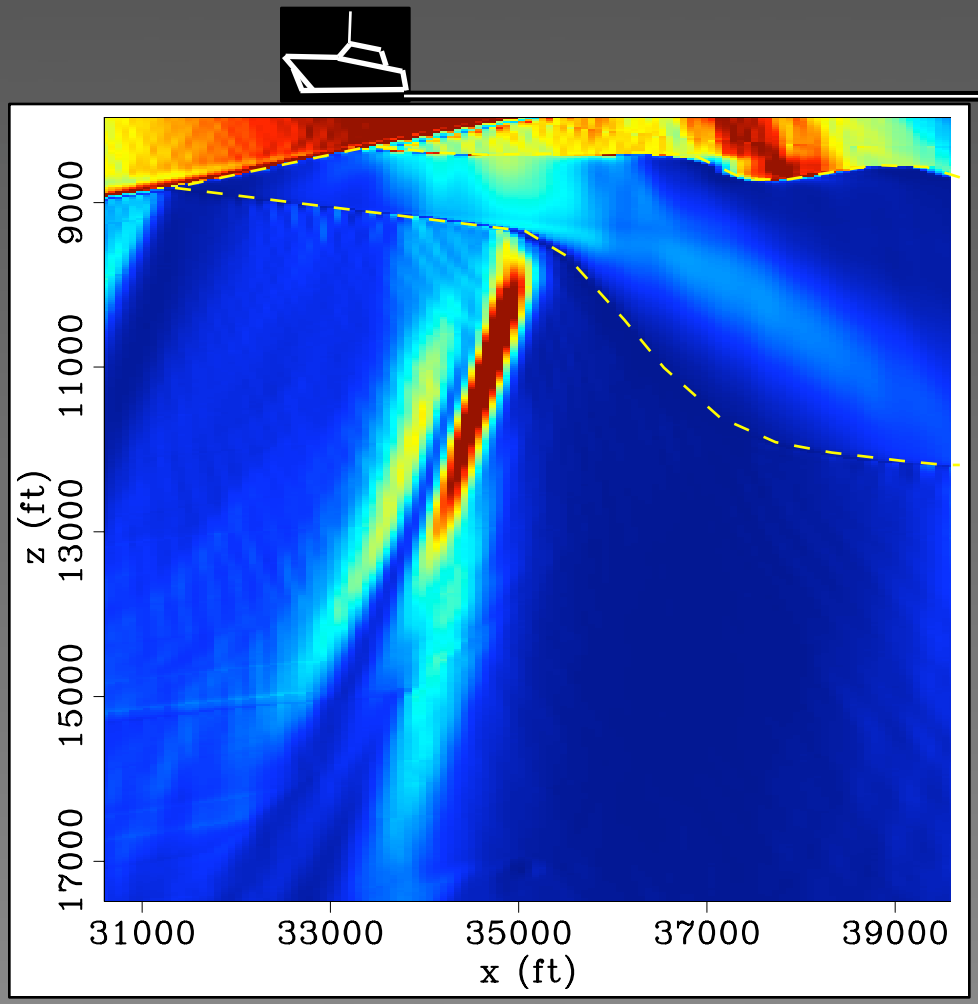

“illumination” from shot at x=32000 ft

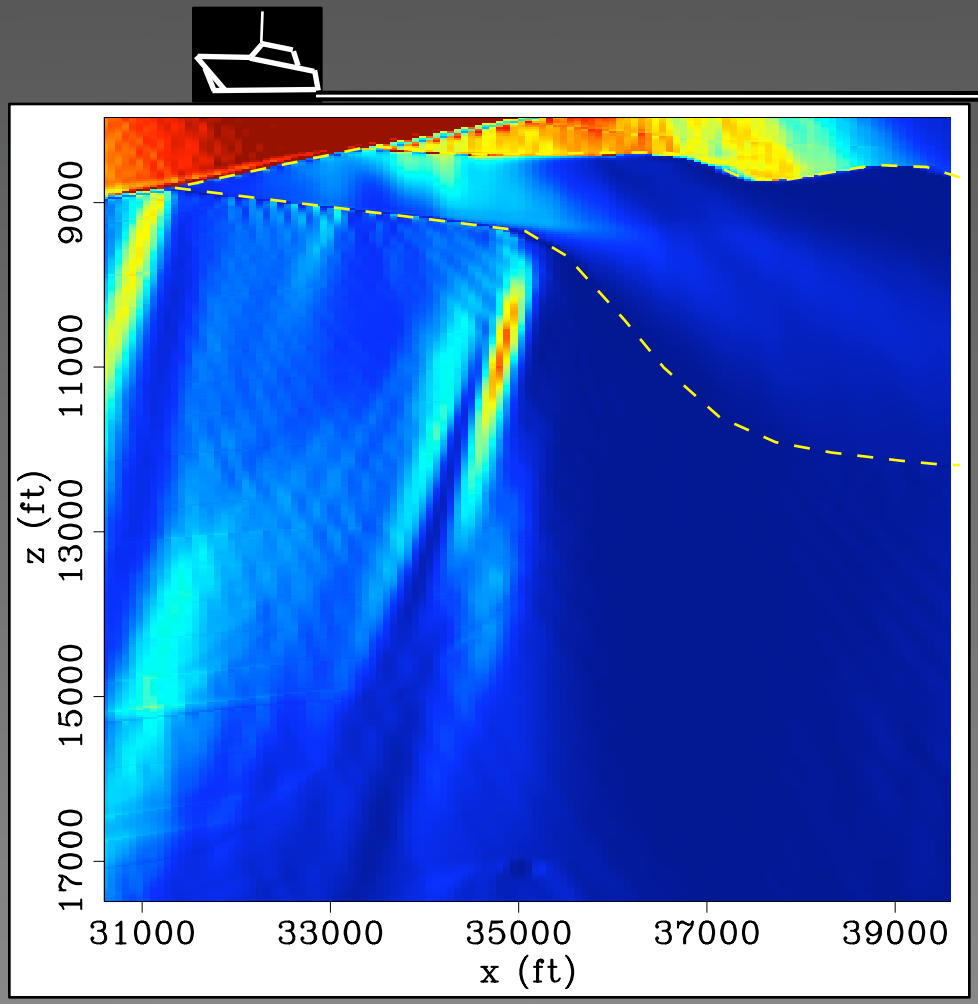

“illumination” from shot at x=31000 ft

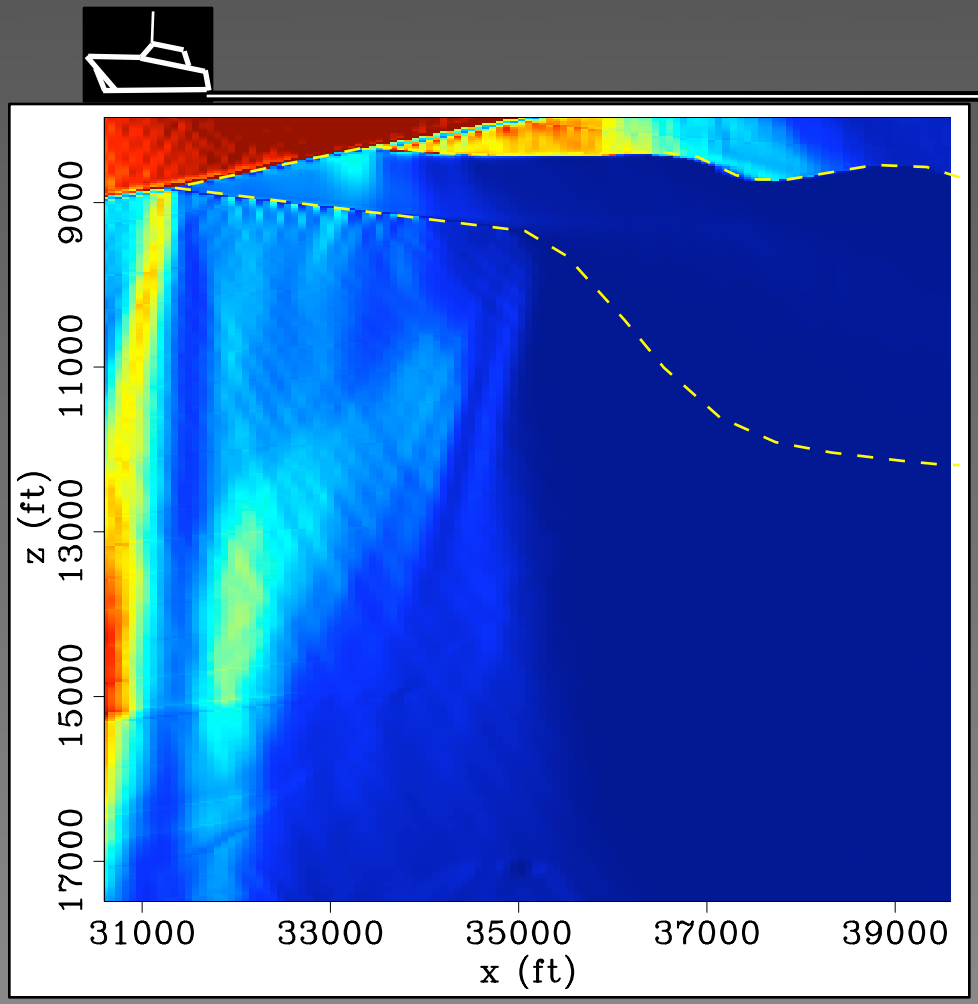

“illumination” from shot at x=30000 ft

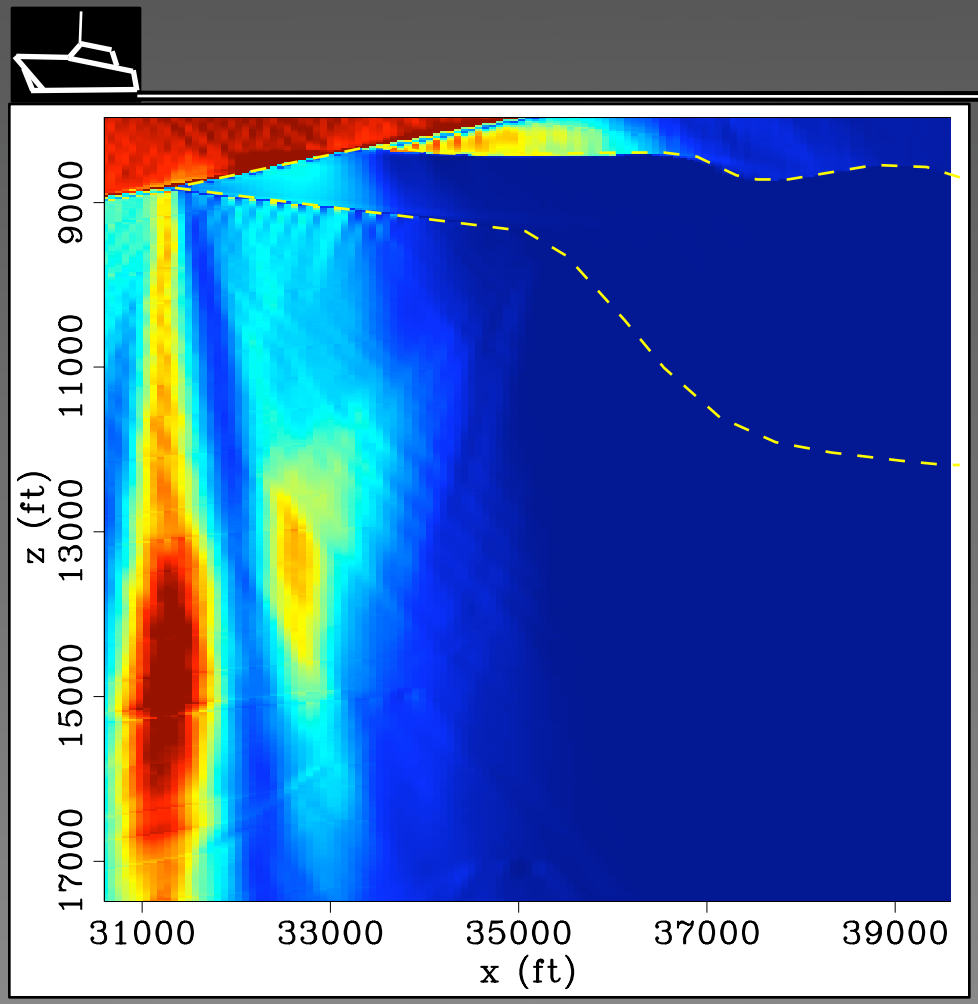

“illumination” from all shots

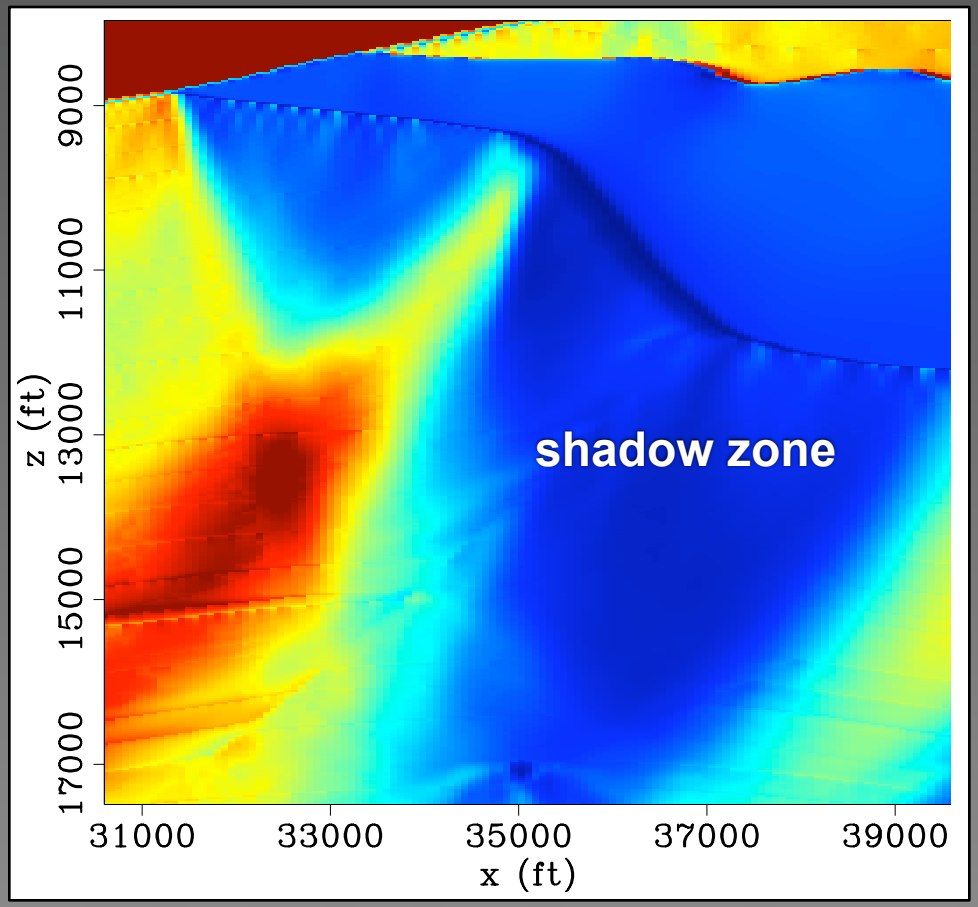

Migrated image

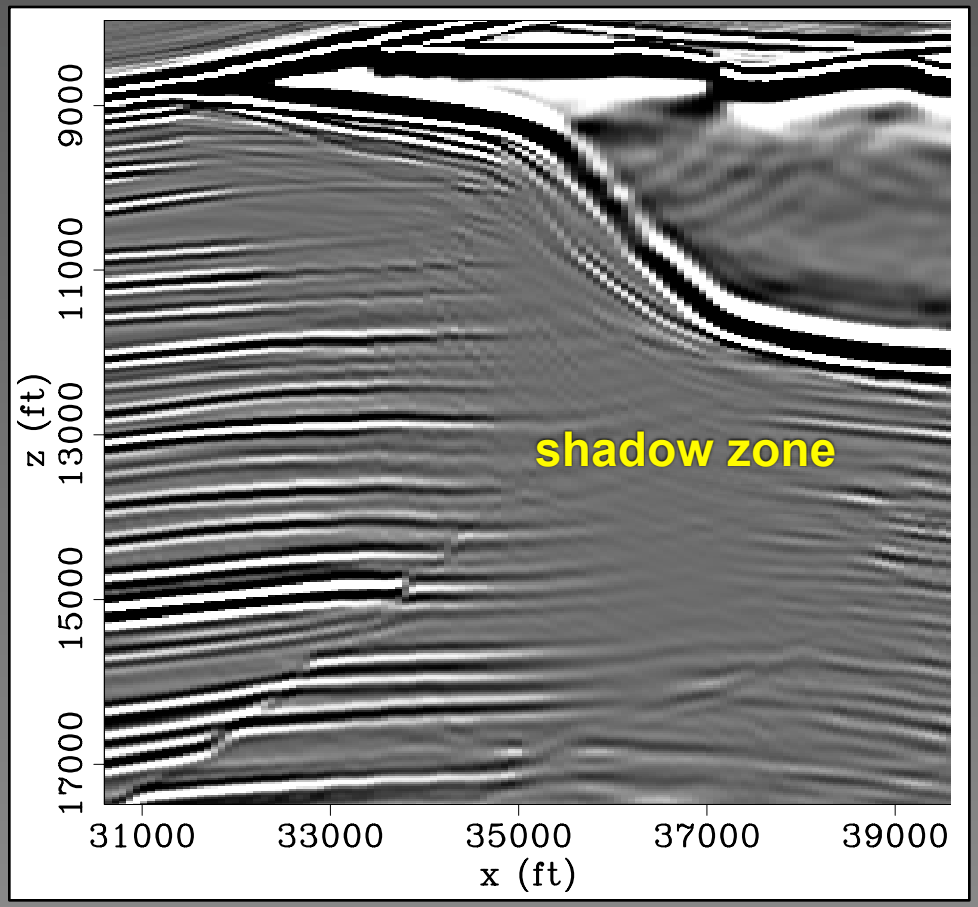

Migration = Imaging with an adjoint operator

$$\mathbf{m}_{mig} = \mathbf{L}'\mathbf{d}_{obs}$$

$\mathbf{d}_{obs}$ recorded seismic data

$\mathbf{L}'$ migration operator

$\mathbf{m}_{mig}$ migrated image

migration ≠ inversion

Non-unitary seismic imaging operators:

- Irregular acquisition geometry
- Complex velocity model
- Bandlimited seismic data

Thesis content

- Chapter 2: Theory of imaging by wave-equation inversion

Thesis content

- Chapter 2: Theory of imaging by wave-equation inversion
- Chapter 3: Structure and computation of the Hessian

Thesis content

- Chapter 2: Theory of imaging by wave-equation inversion
- Chapter 3: Structure and computation of the Hessian
- Chapter 4: Wave-equation inversion in practice

Thesis content

- Chapter 2: Theory of imaging by wave-equation inversion
- Chapter 3: Structure and computation of the Hessian
- Chapter 4: Wave-equation inversion in practice
- Chapter 5: Field data examples

Least-squares imaging

$$\mathbf{d} = \mathbf{L}\mathbf{m}$$

Least-squares imaging

$$\mathbf{d} = \mathbf{L}\mathbf{m}$$

$$\hat{\mathbf{m}} = (\mathbf{L}'\mathbf{L})^{-1}\mathbf{L}'\mathbf{d}_{obs}$$

Clapp (2005), and Kuhl & Sacchi (2003)

Inversion in the image space

$$\hat{\mathbf{m}} = (\mathbf{L}'\mathbf{L})^{-1}\mathbf{L}'\mathbf{d}_{obs}$$

$$\hat{\mathbf{m}} = \mathbf{H}^{-1}\mathbf{m}_{mig}$$

L′L versus H

iterative solver	L′L	H
cost per iteration	two migrations	one sparse matrix vector multiplication
cost upfront	none	approximately two migrations

Inversion in the image space and the PSF

$$\mathbf{H}\hat{\mathbf{m}} = \mathbf{m}_{mig}$$

Inversion in the image space and the PSF

$$\mathbf{H}\hat{\mathbf{m}} = \mathbf{m}_{mig}$$

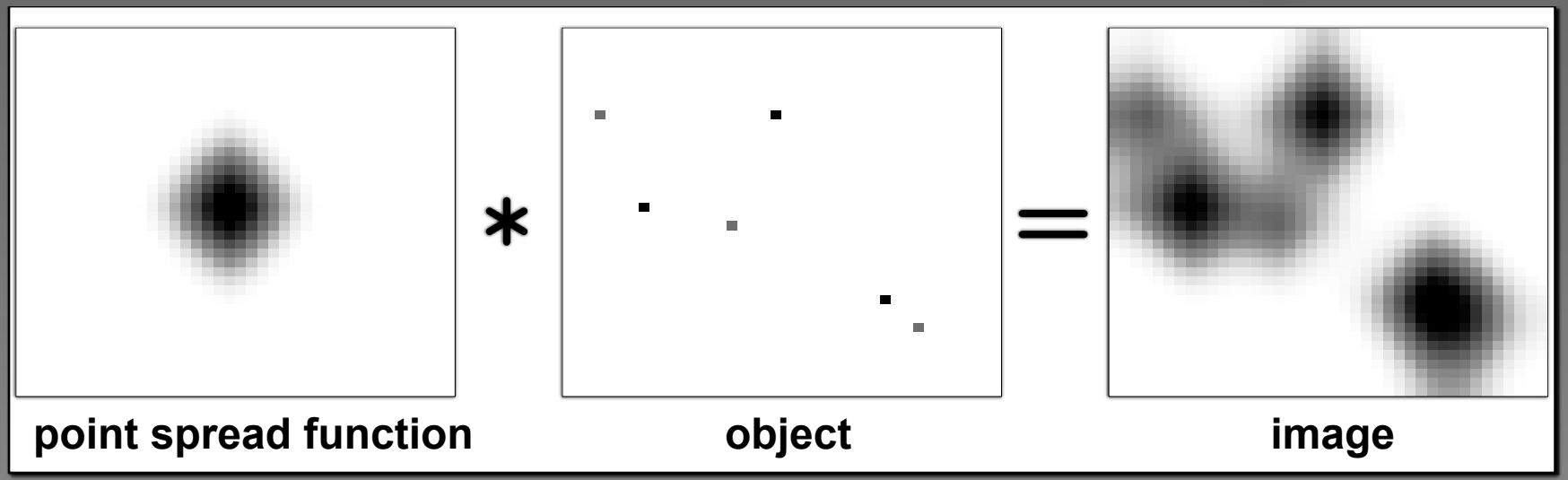

Inversion in the image space and the PSF

$$\mathbf{H}\hat{\mathbf{m}} = \mathbf{m}_{mig}$$

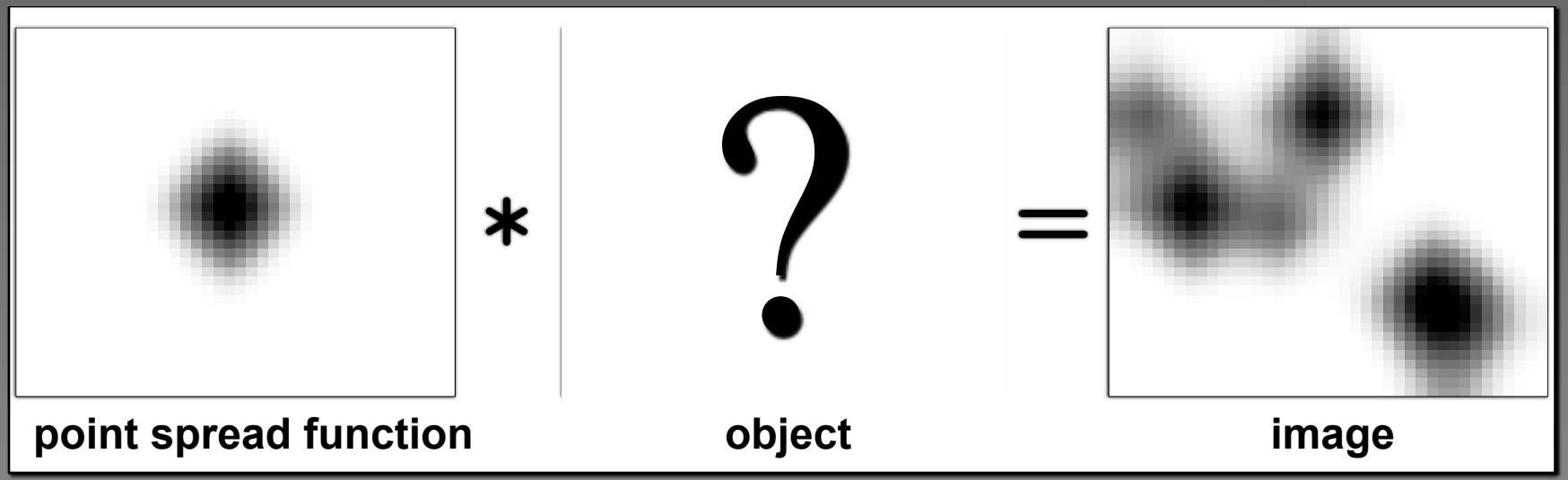

iterative solver

Diagonal Hessian approximations

Cross correlation imaging condition

$$\mathbf{H}_{appr} = \mathbf{I}$$

Diagonal Hessian approximations

Cross correlation imaging condition

$$\mathbf{H}_{appr} = \mathbf{I}$$

Division by shot illumination imaging condition

$$\mathbf{H}_{appr} = diag\left(\mathbf{H}\right)$$

Diagonal Hessian approximations

Cross correlation imaging condition

$$\mathbf{H}_{appr} = \mathbf{I}$$

Division by shot illumination imaging condition

$$\mathbf{H}_{appr} = diag\left(\mathbf{H}\right)$$

Rickett (2003), weighting functions from reference images

Non-diagonal Hessian approximations

Non-diagonal Hessian approximations

- Hu et al. (2001), horizontally invariant deconvolution operator

Non-diagonal Hessian approximations

- Hu et al. (2001), horizontally invariant deconvolution operator
- Guitton (2004), bank of matching filters

Point Spread Function in a complex model

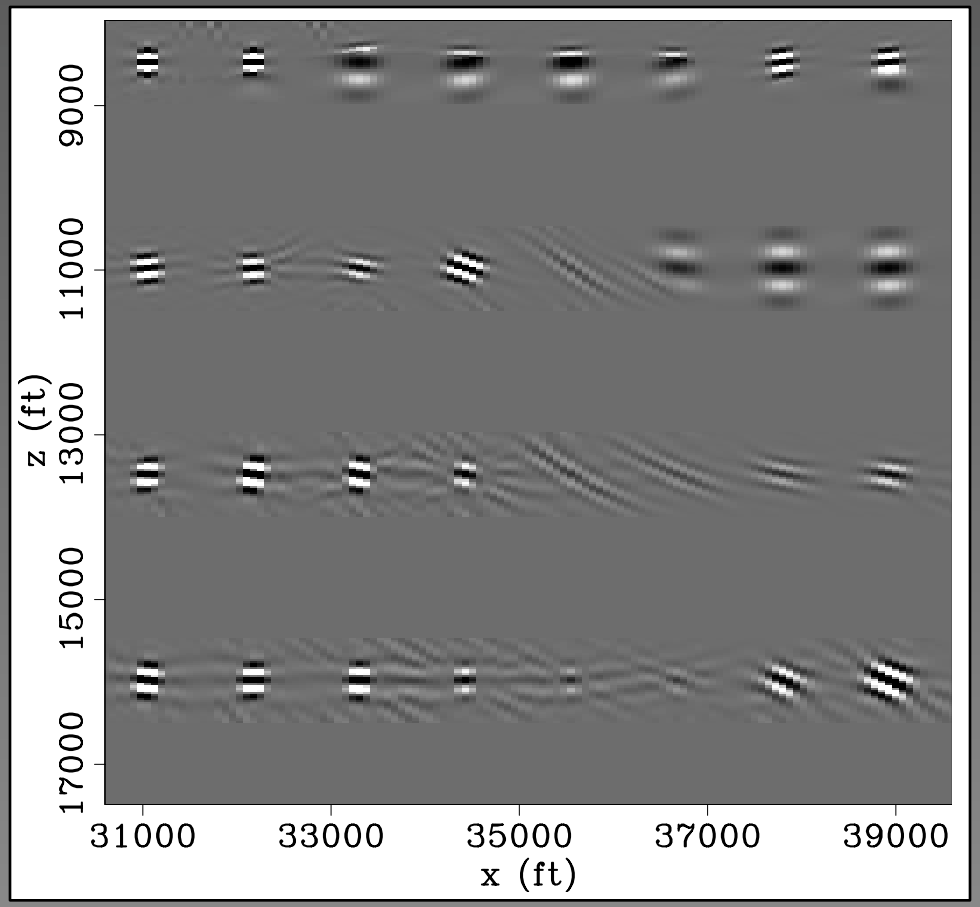

Point Spread Function in a complex model

diagonal of the Hessian

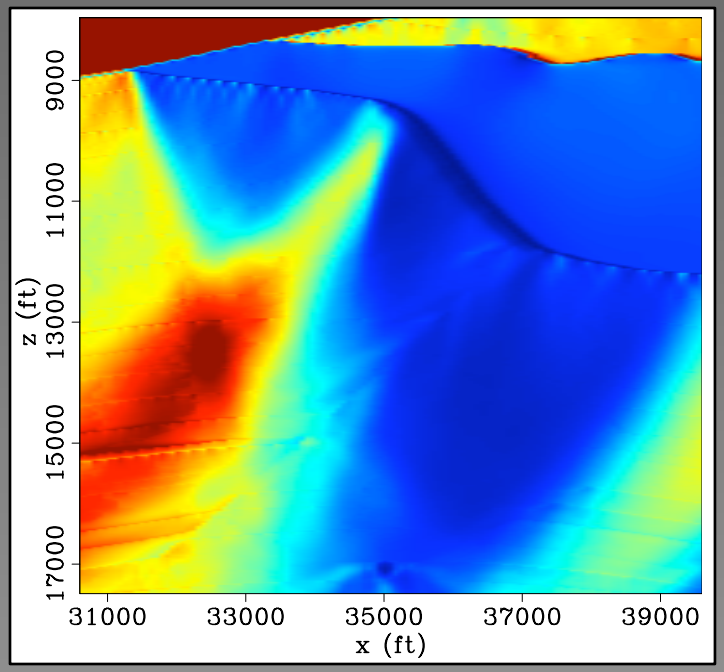

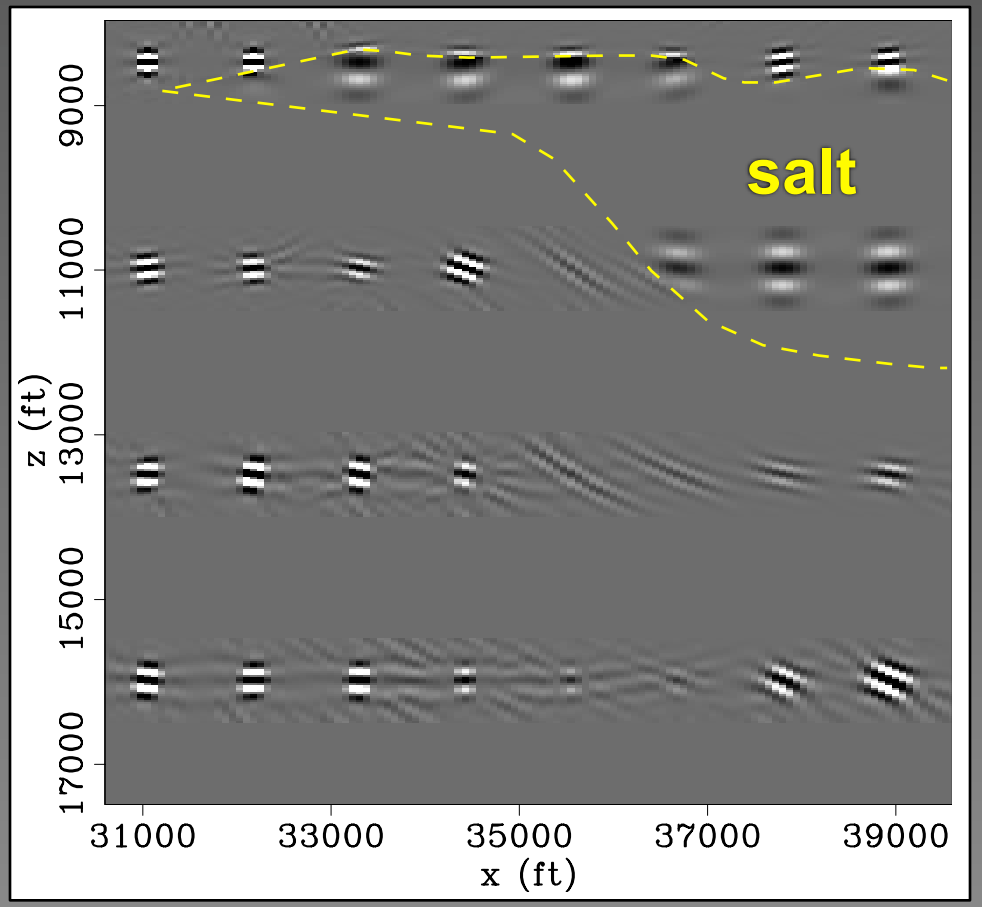

Migrated image

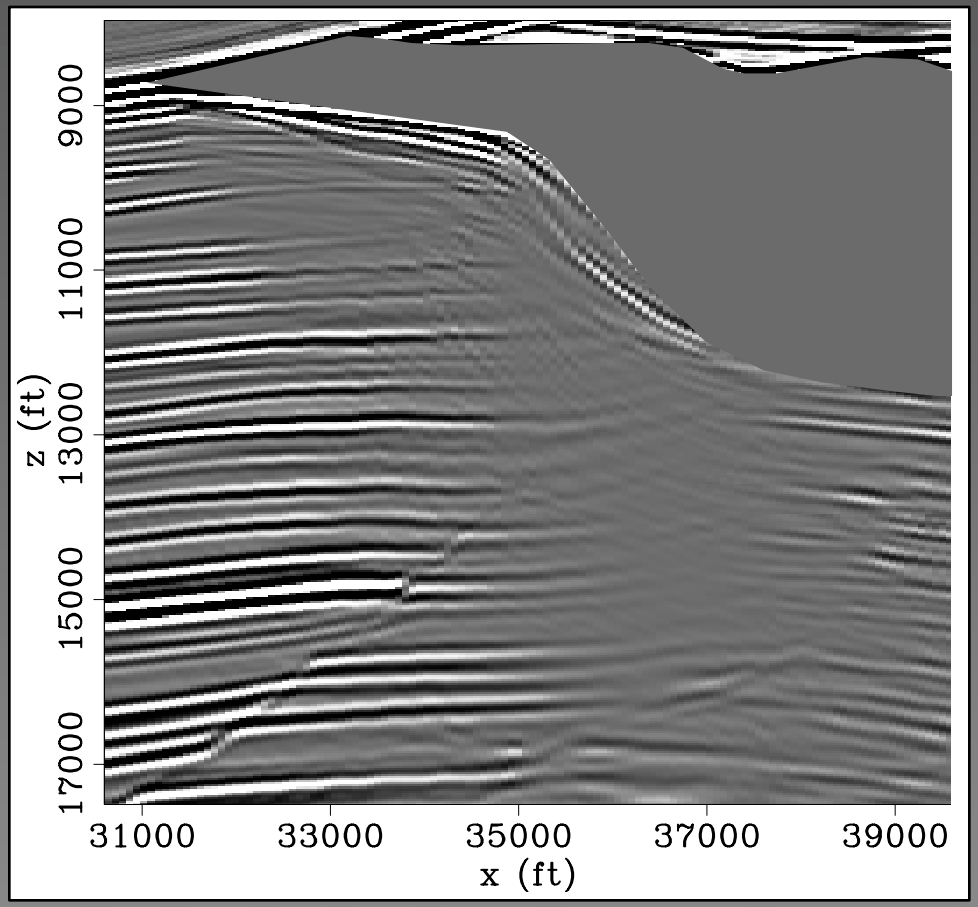

Image after inversion

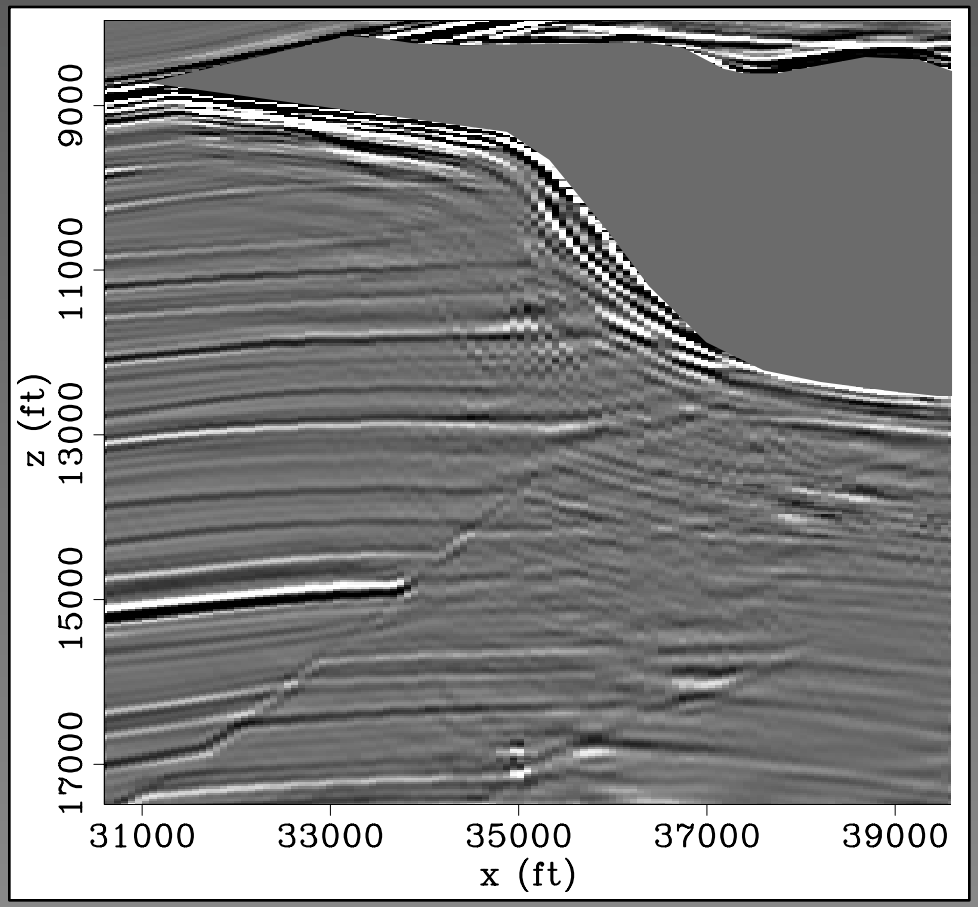

Migrated image

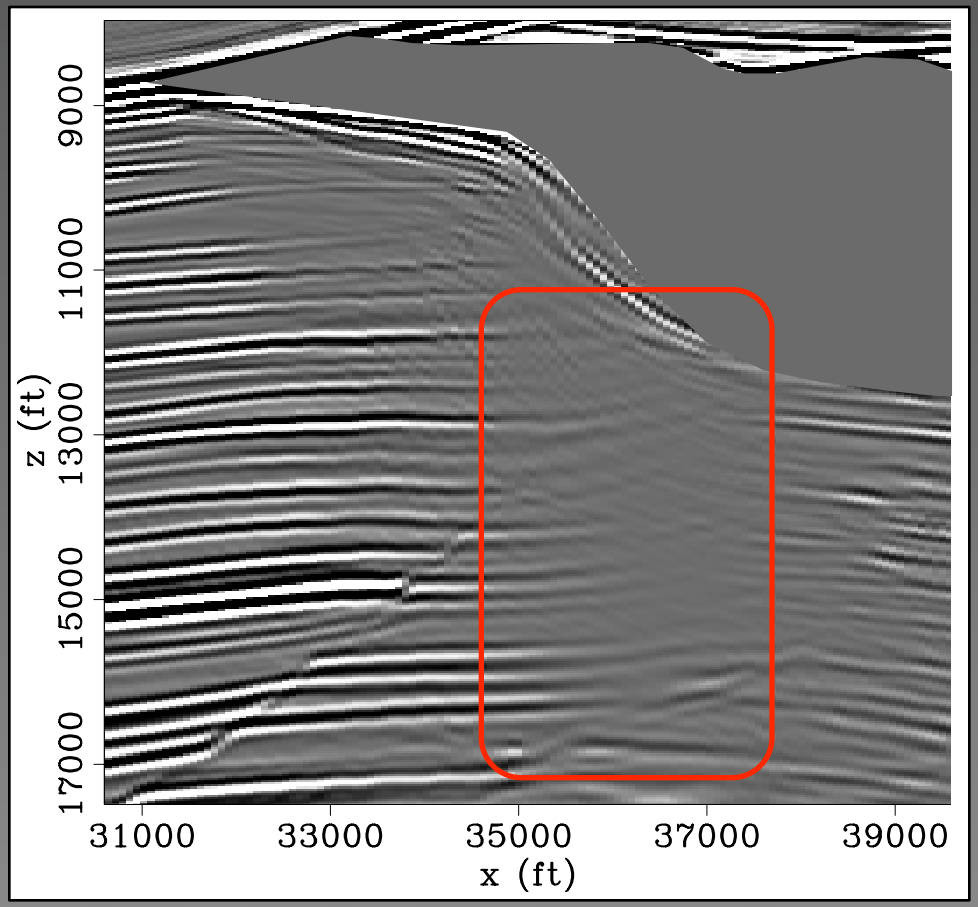

Image after inversion

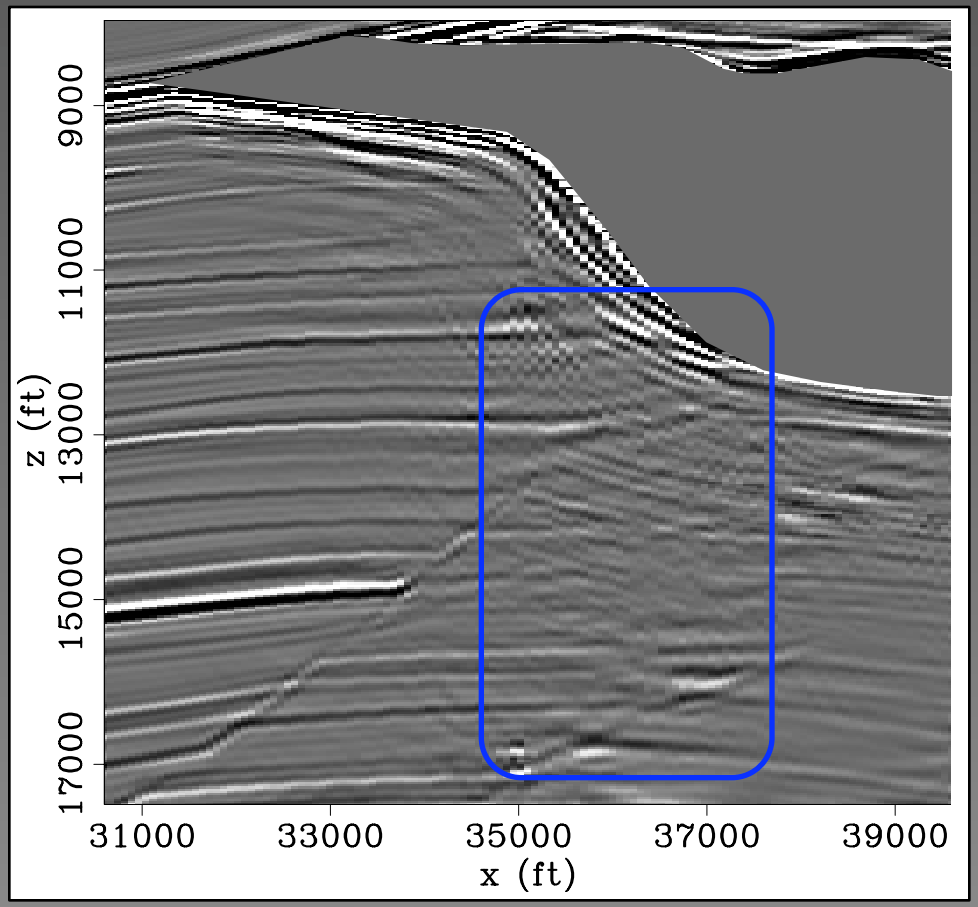

Thesis content

- Chapter 2: Theory of imaging by wave-equation inversion
- Chapter 3: Structure and computation of the Hessian
- Chapter 4: Wave-equation inversion in practice
- Chapter 5: Field data examples

Linear modeling operator

$$\mathbf{d}(\mathbf{x}_s, \mathbf{x}_r; \omega) = \mathbf{Lm}(\mathbf{x}, \mathbf{h})$$

$\mathbf{G}(\mathbf{x}, \mathbf{x}_s; \omega)$
$\mathbf{G}(\mathbf{x}, \mathbf{x}_r; \omega)$

one way wave equation Green's functions

$\mathbf{x} = (x, y, z)$ $\quad \mathbf{h} = (h_x, h_y)$

$\mathbf{x}_s = (x_s, y_s)$ $\quad \mathbf{x}_r = (x_r, y_r)$

Linear modeling operator

$$\mathbf{d}(\mathbf{x}_s, \mathbf{x}_r; \omega) = \mathbf{L}\mathbf{m}(\mathbf{x}, \mathbf{h})$$

$$\mathbf{L} = \sum_{\mathbf{x}} \sum_{\mathbf{h}} \mathbf{G}(\mathbf{x} - \mathbf{h}, \mathbf{x}_r; \omega)\mathbf{G}(\mathbf{x} + \mathbf{h}, \mathbf{x}_s; \omega)$$

$\mathbf{G}(\mathbf{x}, \mathbf{x}_s; \omega)$
$\mathbf{G}(\mathbf{x}, \mathbf{x}_r; \omega)$

one way wave equation Green's functions

$\mathbf{x} = (x, y, z)$ $\quad \mathbf{h} = (h_x, h_y)$

$\mathbf{x}_s = (x_s, y_s)$ $\quad \mathbf{x}_r = (x_r, y_r)$

Shot profile prestack migration

$$\mathbf{m}_{mig}(\mathbf{x},\mathbf{h}) = \mathbf{L}'\mathbf{d}_{obs}(\mathbf{x}_s,\mathbf{x}_r;\omega)$$

$\mathbf{G}(\mathbf{x},\mathbf{x}_s;\omega)$
$\mathbf{G}(\mathbf{x},\mathbf{x}_r;\omega)$

one way wave equation Green's functions

$\mathbf{x} = (x, y, z)$ $\quad \mathbf{h} = (h_x, h_y)$

$\mathbf{x}_s = (x_s, y_s)$ $\quad \mathbf{x}_r = (x_r, y_r)$

Shot profile prestack migration

$$\mathbf{m}_{mig}(\mathbf{x},\mathbf{h}) = \mathbf{L}'\mathbf{d}_{obs}(\mathbf{x}_s,\mathbf{x}_r;\omega)$$

$$\mathbf{L}' = \sum_{\omega}\sum_{\mathbf{x}_s}\sum_{\mathbf{x}_r} \mathbf{G}'(\mathbf{x}-\mathbf{h},\mathbf{x}_s;\omega)\mathbf{G}'(\mathbf{x}+\mathbf{h},\mathbf{x}_r;\omega)$$

$\mathbf{G}(\mathbf{x},\mathbf{x}_s;\omega)$
$\mathbf{G}(\mathbf{x},\mathbf{x}_r;\omega)$

one way wave equation Green's functions

$\mathbf{x} = (x, y, z)$ $\quad \mathbf{h} = (h_x, h_y)$

$\mathbf{x}_s = (x_s, y_s)$ $\quad \mathbf{x}_r = (x_r, y_r)$

Hessian matrix

$$\mathbf{H}(\mathbf{x},\mathbf{h};\mathbf{x}',\mathbf{h}') = \mathbf{L}'\mathbf{L}$$

$\mathbf{G}(\mathbf{x},\mathbf{x}_s;\omega)$
$\mathbf{G}(\mathbf{x},\mathbf{x}_r;\omega)$

one way wave equation Green's functions

$\mathbf{x} = (x, y, z)$ $\quad \mathbf{h} = (h_x, h_y)$

$\mathbf{x}_s = (x_s, y_s)$ $\quad \mathbf{x}_r = (x_r, y_r)$

Hessian matrix

$$\mathbf{H}(\mathbf{x},\mathbf{h};\mathbf{x}',\mathbf{h}') = \mathbf{L}'\mathbf{L}$$

$$\mathbf{L}'\mathbf{L} = \sum_{\omega}\sum_{\mathbf{x}_s} \mathbf{G}'(\mathbf{x}+\mathbf{h},\mathbf{x}_s;\omega)\mathbf{G}(\mathbf{x}'+\mathbf{h}',\mathbf{x}_s;\omega)$$

$$\sum_{\mathbf{x}_r} \mathbf{G}'(\mathbf{x}-\mathbf{h},\mathbf{x}_r;\omega)\mathbf{G}(\mathbf{x}'-\mathbf{h}',\mathbf{x}_r;\omega)$$

$\mathbf{G}(\mathbf{x},\mathbf{x}_s;\omega)$
$\mathbf{G}(\mathbf{x},\mathbf{x}_r;\omega)$

one way wave equation Green's functions

$\mathbf{x} = (x, y, z)$ $\quad \mathbf{h} = (h_x, h_y)$

$\mathbf{x}_s = (x_s, y_s)$ $\quad \mathbf{x}_r = (x_r, y_r)$

Hessian matrix

$$\mathbf{H}(\mathbf{x},\mathbf{h};\mathbf{x}',\mathbf{h}') = \mathbf{L}'\mathbf{L}$$

source term

$$\mathbf{L}'\mathbf{L} = \sum_{\omega} \sum_{\mathbf{x}_s} \mathbf{G}'(\mathbf{x}+\mathbf{h},\mathbf{x}_s;\omega)\mathbf{G}(\mathbf{x}'+\mathbf{h}',\mathbf{x}_s;\omega)$$

$$\sum_{\mathbf{x}_r} \mathbf{G}'(\mathbf{x}-\mathbf{h},\mathbf{x}_r;\omega)\mathbf{G}(\mathbf{x}'-\mathbf{h}',\mathbf{x}_r;\omega)$$

receiver term

$\mathbf{G}(\mathbf{x},\mathbf{x}_s;\omega)$
$\mathbf{G}(\mathbf{x},\mathbf{x}_r;\omega)$

one way wave equation
Green's functions

$\mathbf{x} = (x, y, z)$ $\quad \mathbf{h} = (h_x, h_y)$

$\mathbf{x}_s = (x_s, y_s)$ $\quad \mathbf{x}_r = (x_r, y_r)$

Tikhonov regularization

$$(\mathbf{H} + \varepsilon\mathbf{R})\,\hat{\mathbf{m}} - \mathbf{m}_{mig} = \mathbf{r} \approx 0$$

Tikhonov regularization

$$(\mathbf{H} + \varepsilon\mathbf{R})\,\hat{\mathbf{m}} - \mathbf{m}_{mig} = \mathbf{r} \approx 0$$

$\mathbf{R} = \mathbf{I}$ **damping**

Expanding the dimensionality to the prestack image domain

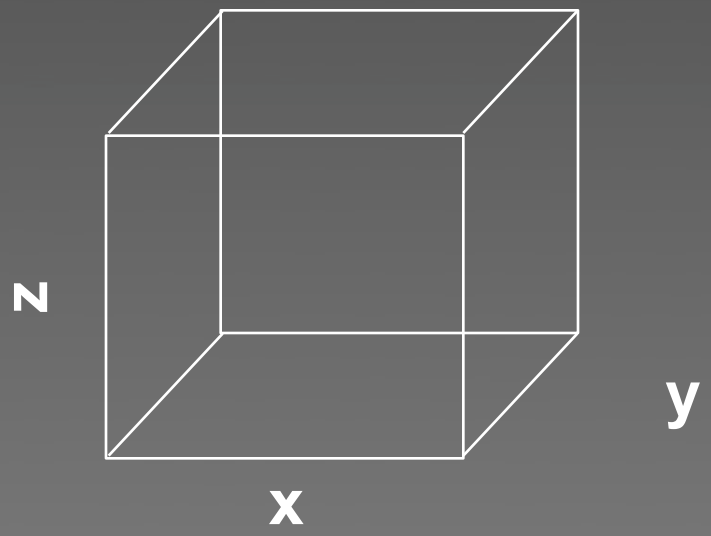

Expanding the dimensionality to the prestack image domain

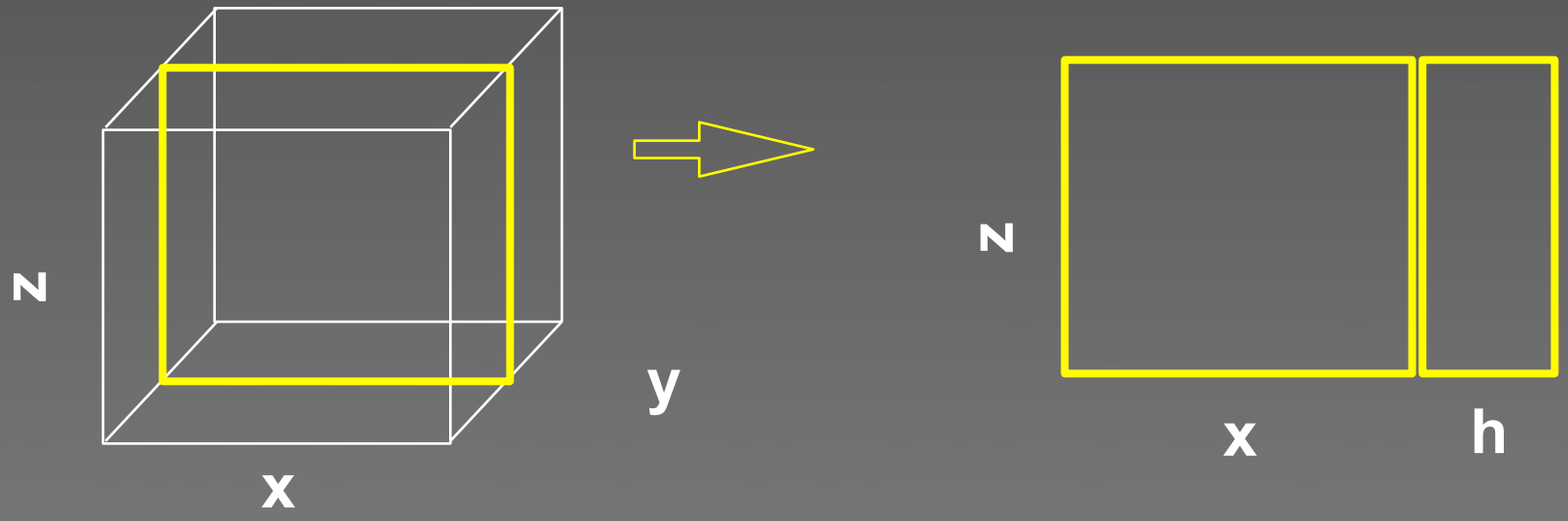

Expanding the dimensionality to the prestack image domain

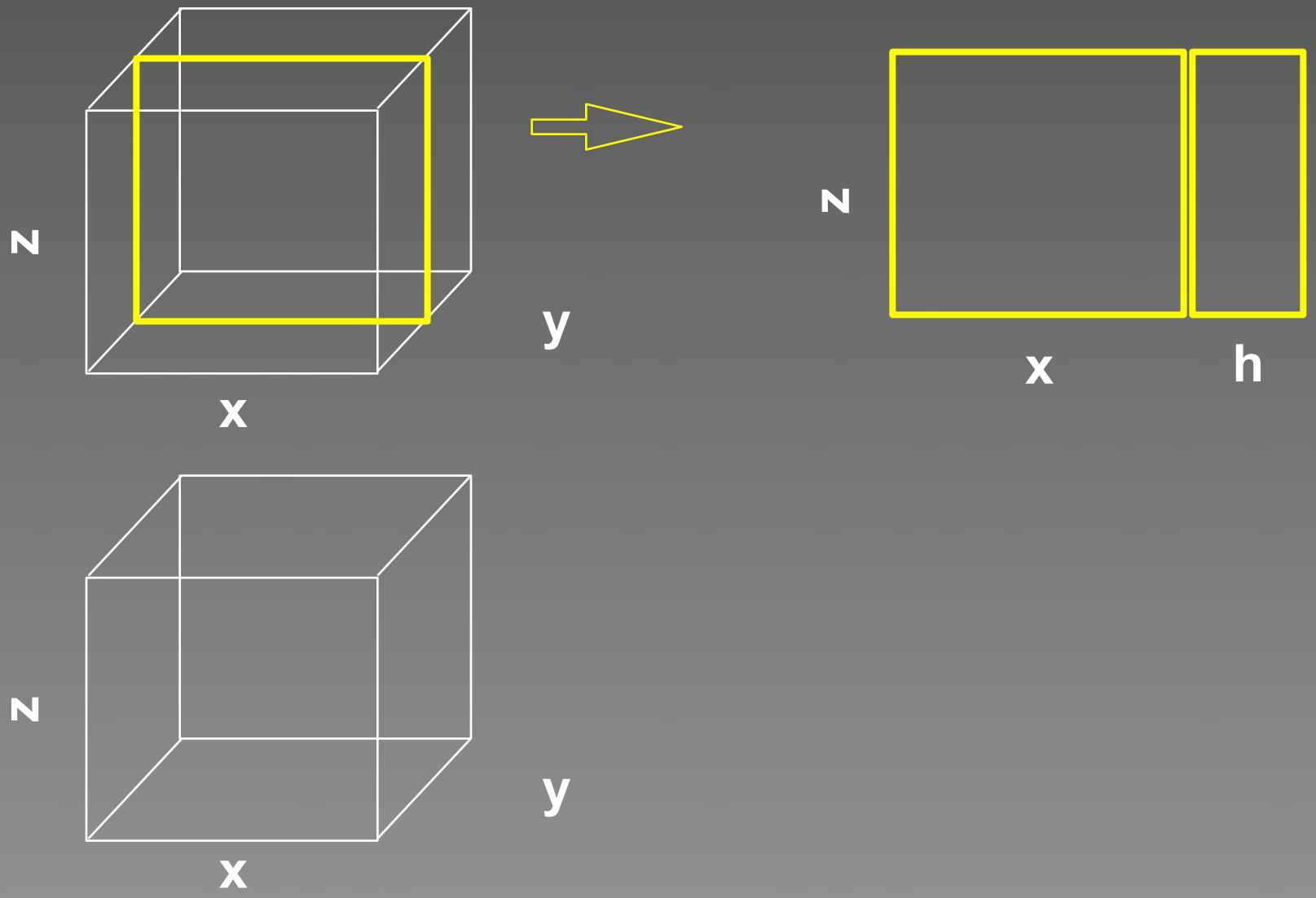

Expanding the dimensionality to the prestack image domain

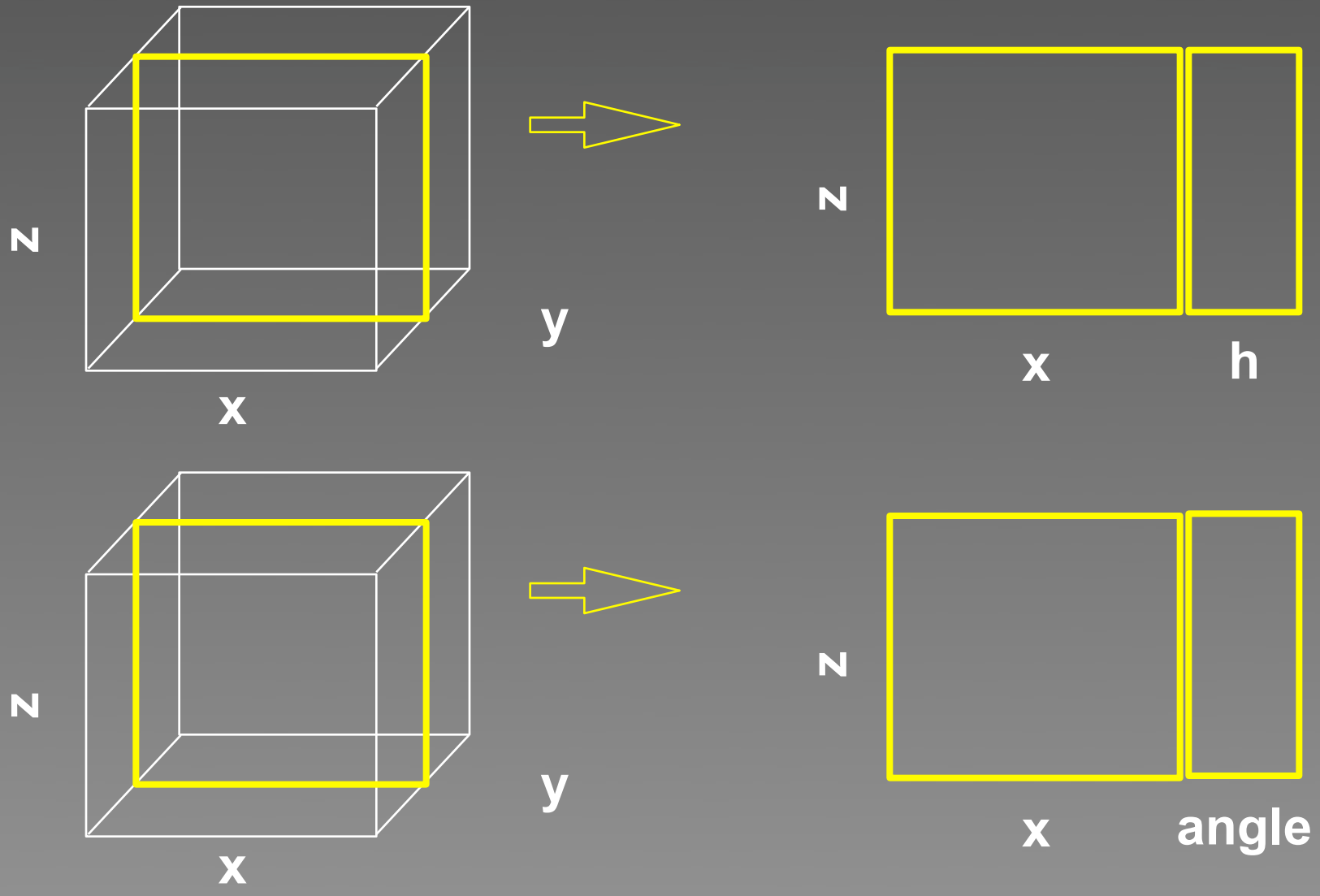

Why prestack image domain?

Why prestack image domain?

Wave-equation inversion regularization schemes

Why prestack image domain?

Wave-equation inversion regularization schemes

- Clapp (2005), and Kuhl & Sacchi (2003), regularization in the offset-ray parameter

Why prestack image domain?

Wave-equation inversion regularization schemes

- **Clapp (2005), and Kuhl & Sacchi (2003), regularization in the offset-ray parameter**
- **Shen et al. (2003), subsurface-offset differential semblance operators**

Tikhonov regularization

$$(\mathbf{H} + \varepsilon\mathbf{R})\,\hat{\mathbf{m}} - \mathbf{m}_{mig} = \mathbf{r} \approx 0$$

$$\mathbf{R} = \mathbf{P}_{\mathbf{h}}^{\mathbf{2}}$$

weighting subsurface-offset gathers

Reflection-angle gathers

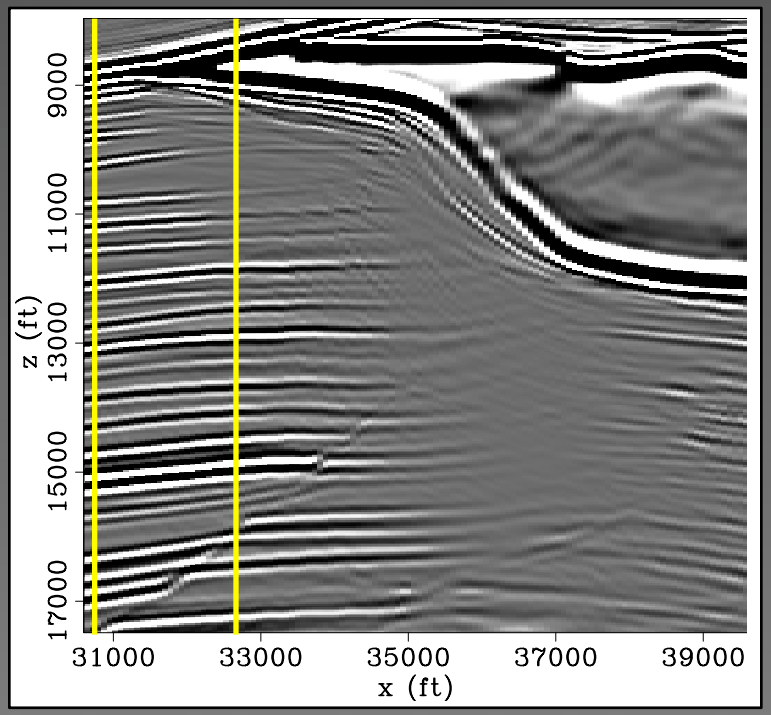

regular illumination

irregular illumination

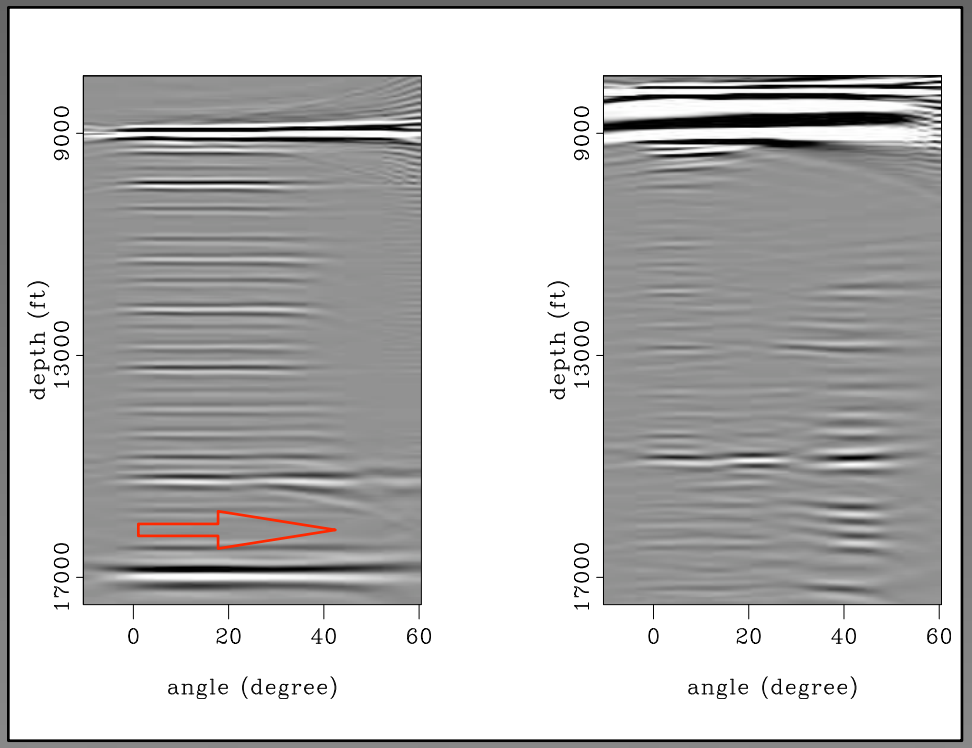

Subsurface-offset to reflection-angle

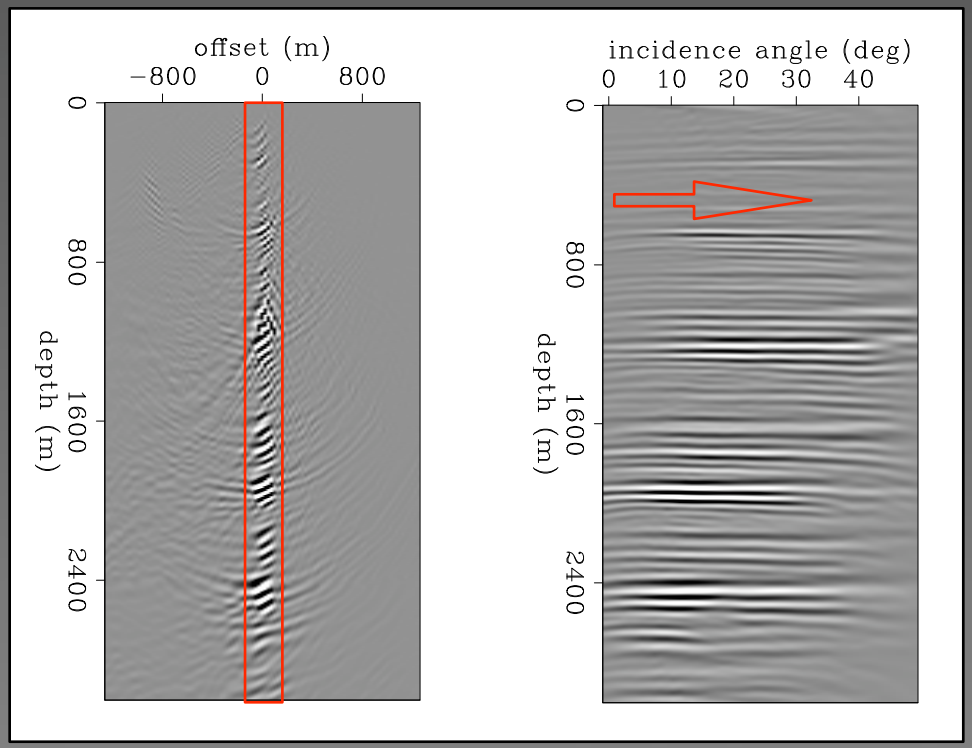

$$\mathbf{S}_{\Theta\rightarrow\mathbf{h}}\mathbf{m}(\mathbf{x},\Theta)=\mathbf{m}(\mathbf{x},\mathbf{h})$$

$\Theta=(\theta,\alpha)$ reflection and azimuth angles

$\mathbf{S}_{\Theta\rightarrow\mathbf{h}}$ slant stack

Subsurface-offset gathers

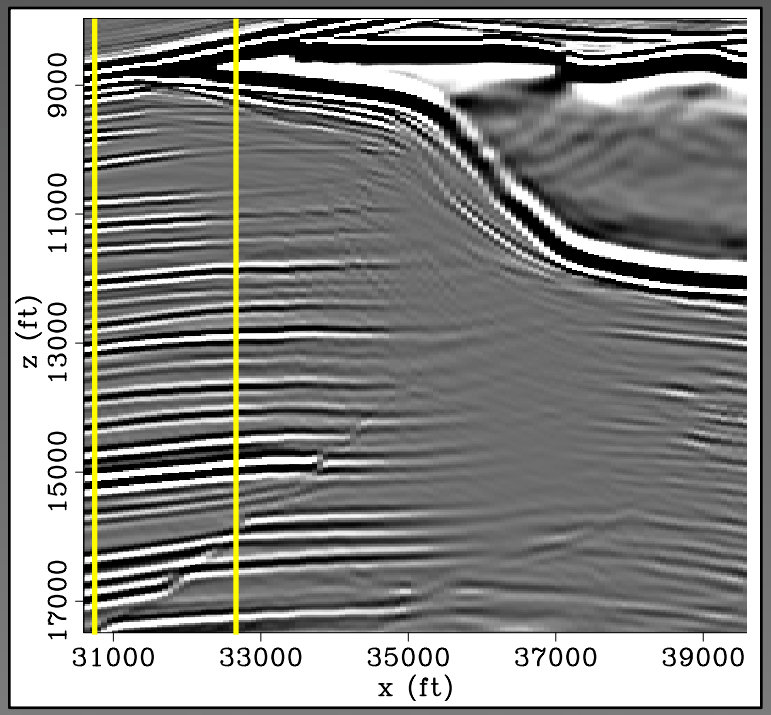

regular illumination

irregular illumination

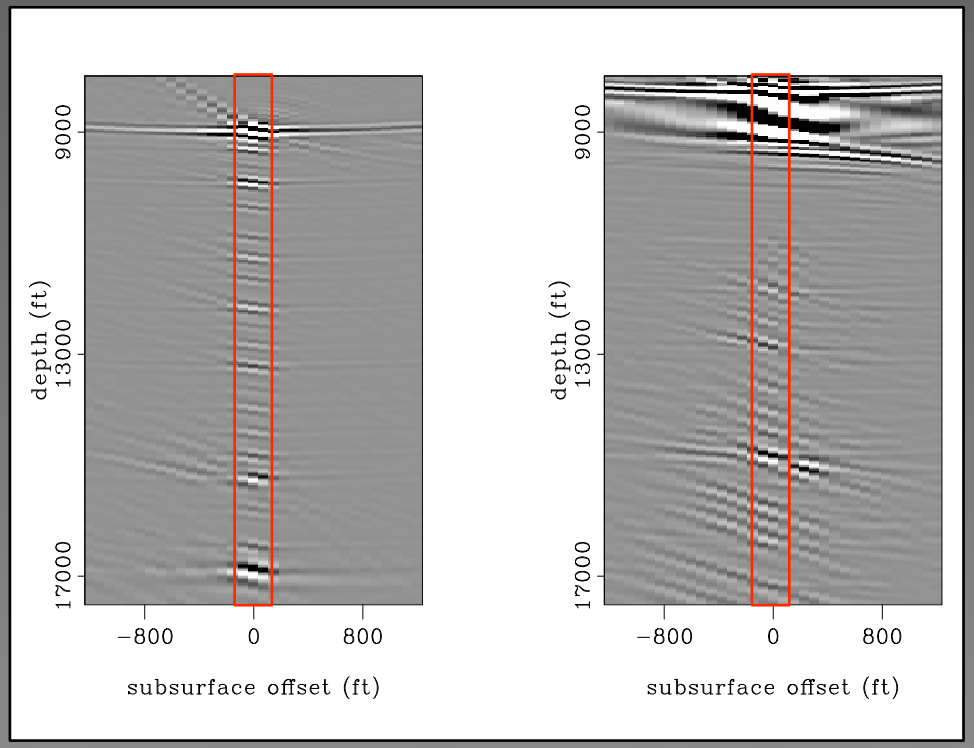

Thesis content

- Chapter 2: Theory of imaging by wave-equation inversion
- **Chapter 3: Structure and computation of the Hessian**
- Chapter 4: Wave-equation inversion in practice
- Chapter 5: Field data examples

Sparse Hessian matrix

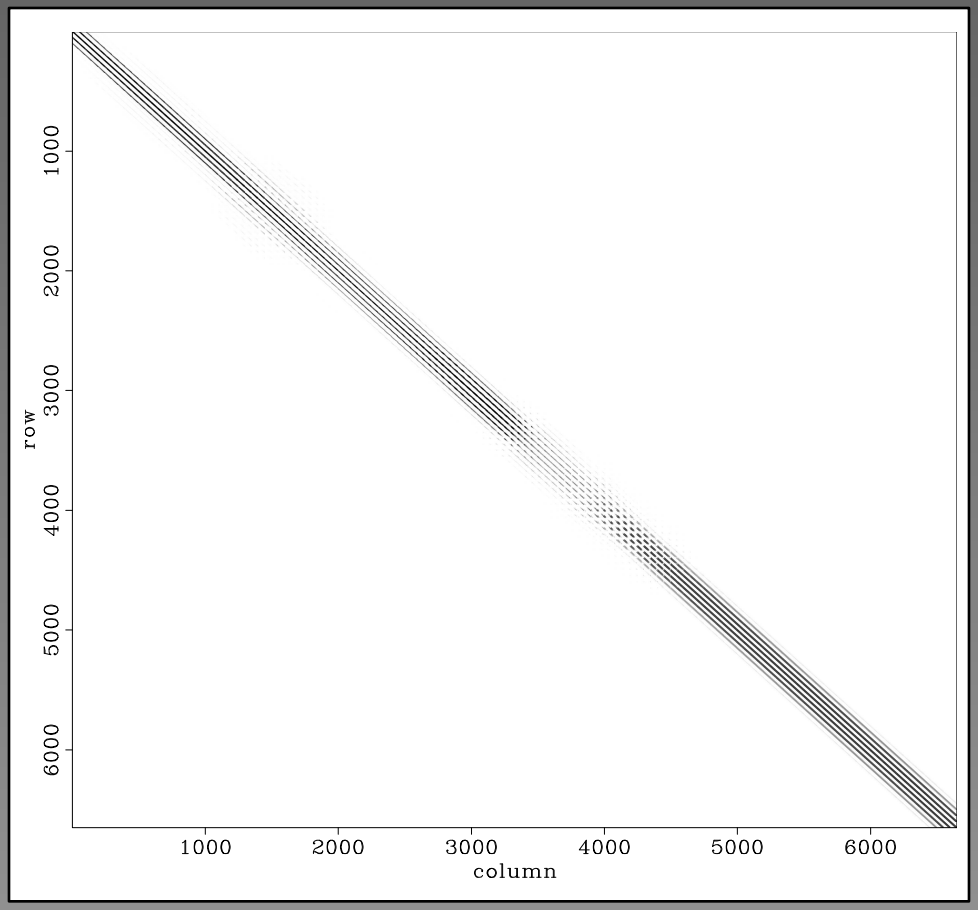

Sparse Hessian matrix

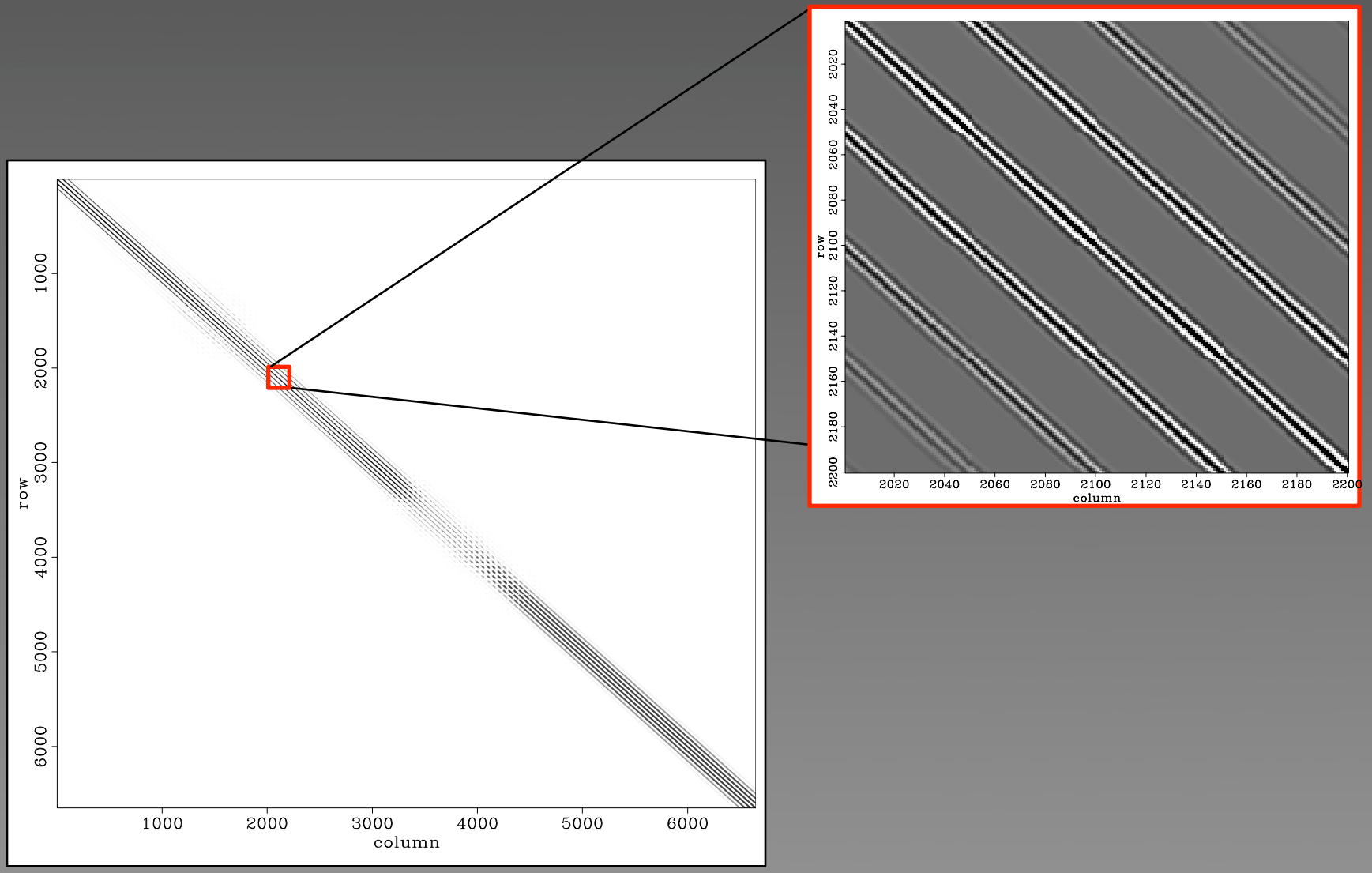

Total computational savings

Total computational savings

- Computational savings of five orders of magnitude or more compared to a direct implementation.

Total computational savings

- Computational savings of five orders of magnitude or more compared to a direct implementation.
- No velocity model or acquisition geometry approximations were made.

Total computational savings

- Computational savings of five orders of magnitude or more compared to a direct implementation.
- No velocity model or acquisition geometry approximations were made.
- Still, the 3D Hessian computation takes 1000 hours using 32 dual processor Opteron nodes in the CEES.

Thesis content

- Chapter 2: Theory of imaging by wave-equation inversion
- Chapter 3: Structure and computation of the Hessian
- **Chapter 4: Wave-equation inversion in practice**
- Chapter 5: Field data examples

Thesis content

- Chapter 2: Theory of imaging by wave-equation inversion
- Chapter 3: Structure and computation of the Hessian
- Chapter 4: Wave-equation inversion in practice
- Chapter 5: Field data examples

3D Gulf of Mexico data

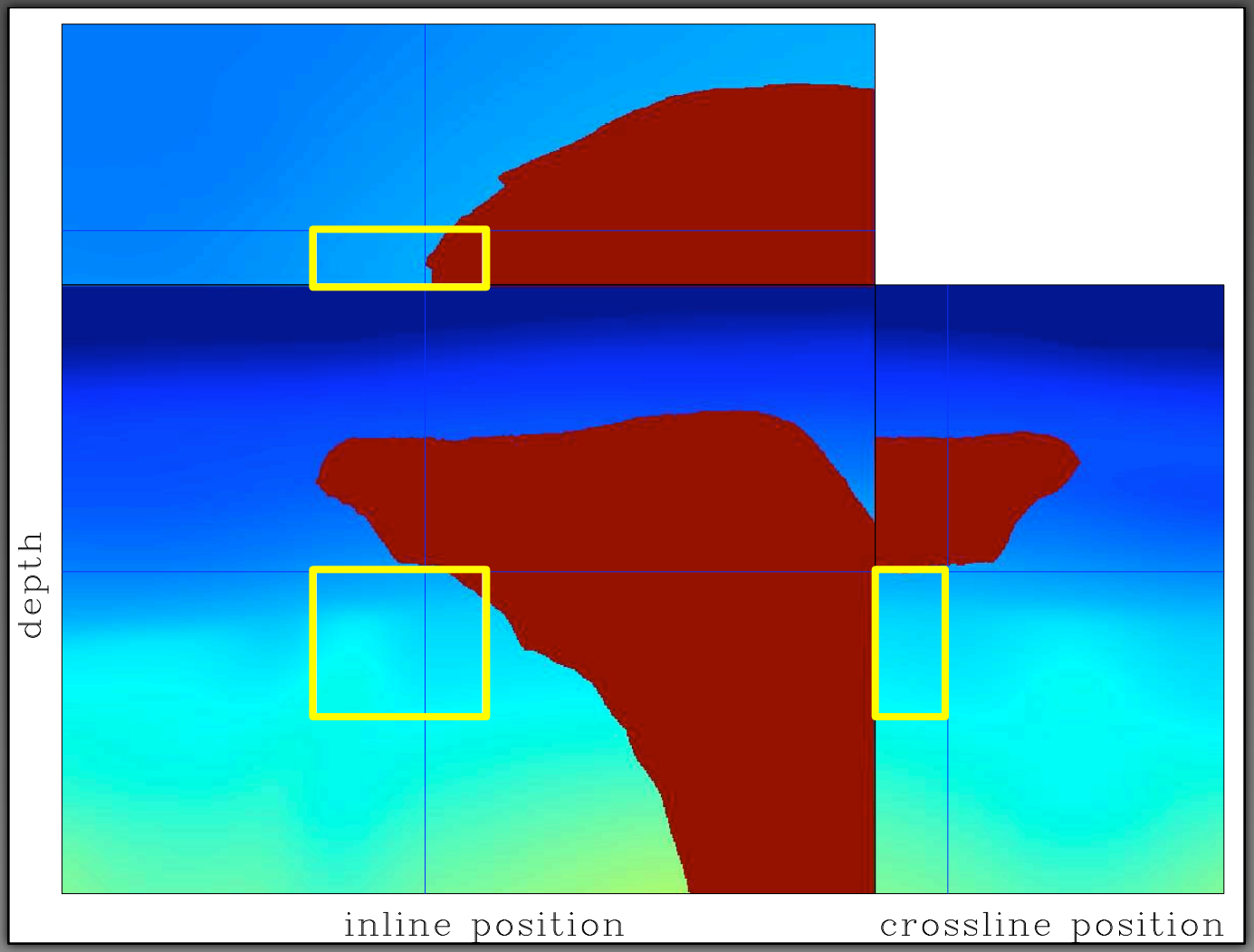

3D Gulf of Mexico data

3D Gulf of Mexico data

10000 shots (200 inline, 50 crossline)

3D Gulf of Mexico data

10000 shots (200 inline, 50 crossline)

maximum offset 30839 ft

3D Gulf of Mexico data

10000 shots (200 inline, 50 crossline)

maximum offset 30839 ft

frequency band 5 Hz to 35 Hz

3D Gulf of Mexico data

10000 shots (200 inline, 50 crossline)

maximum offset 30839 ft

frequency band 5 Hz to 35 Hz

target 726000 points

3D Gulf of Mexico data

10000 shots (200 inline, 50 crossline)

maximum offset 30839 ft

frequency band 5 Hz to 35 Hz

target	726000 points
Hessian matrix	7 billion nonzero elements

3D Gulf of Mexico data

10000 shots (200 inline, 50 crossline)

maximum offset 30839 ft

frequency band 5 Hz to 35 Hz

target	726000 points
Hessian matrix	7 billion nonzero elements
Green's functions	3 Terabytes

3D illumination

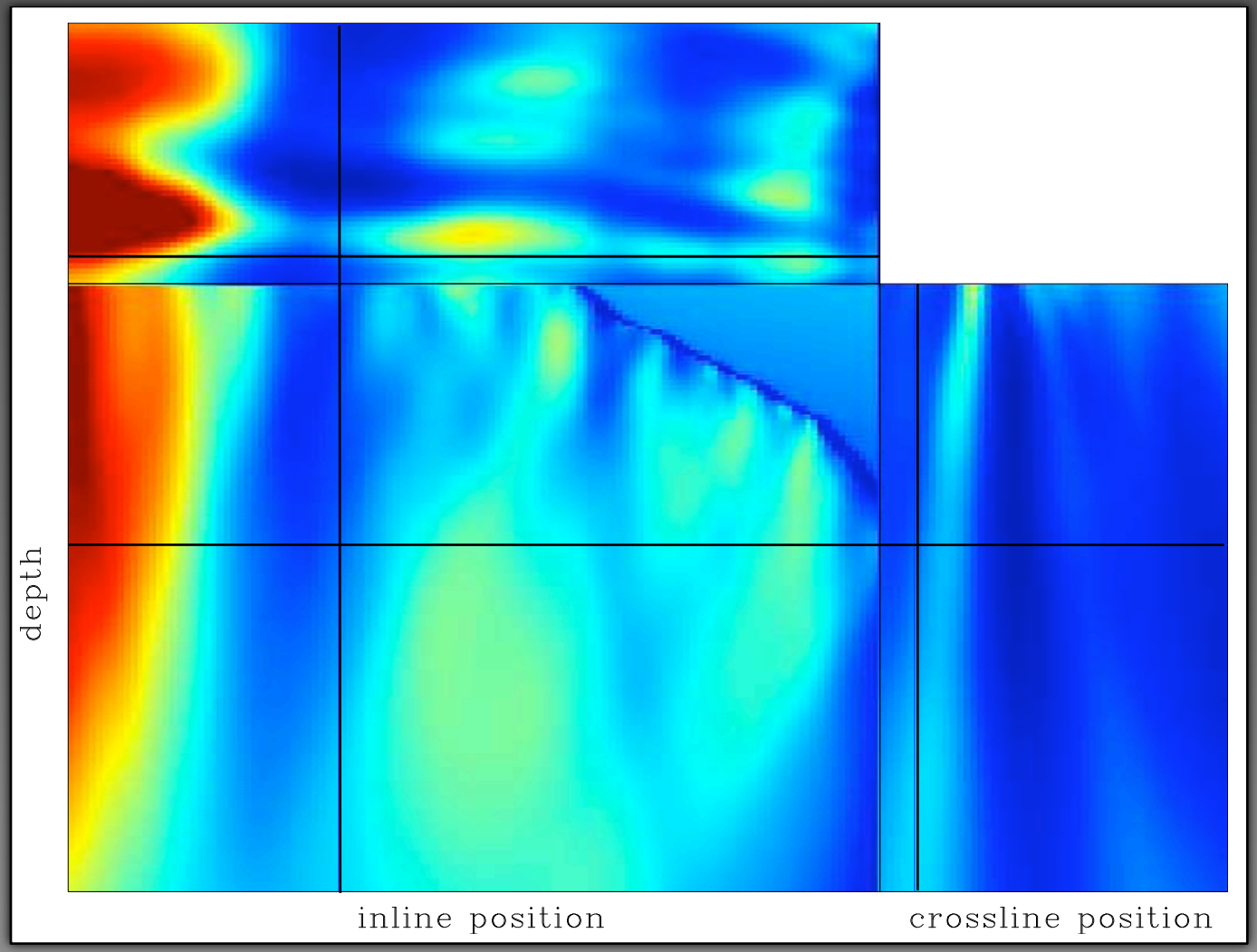

3D illumination

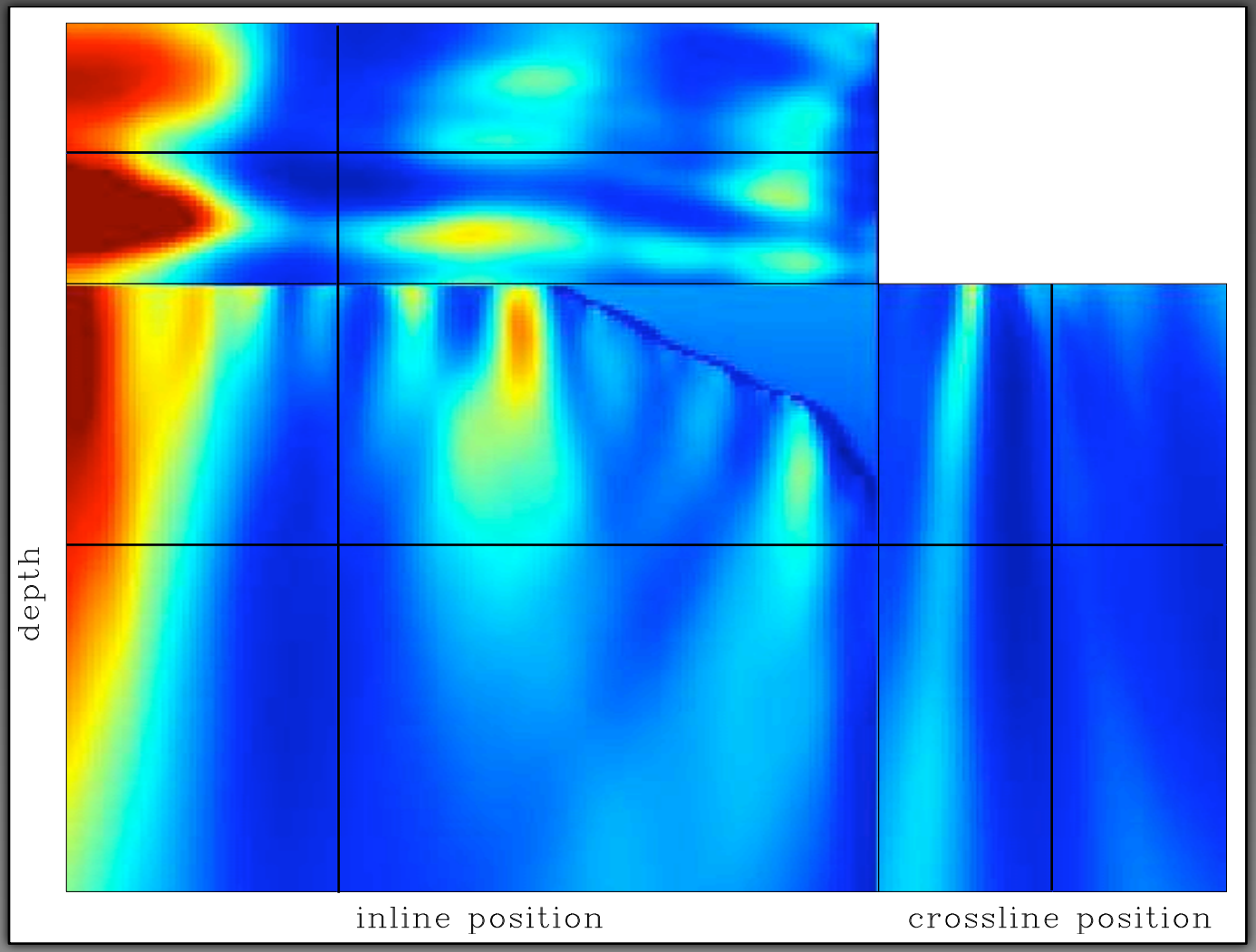

3D illumination

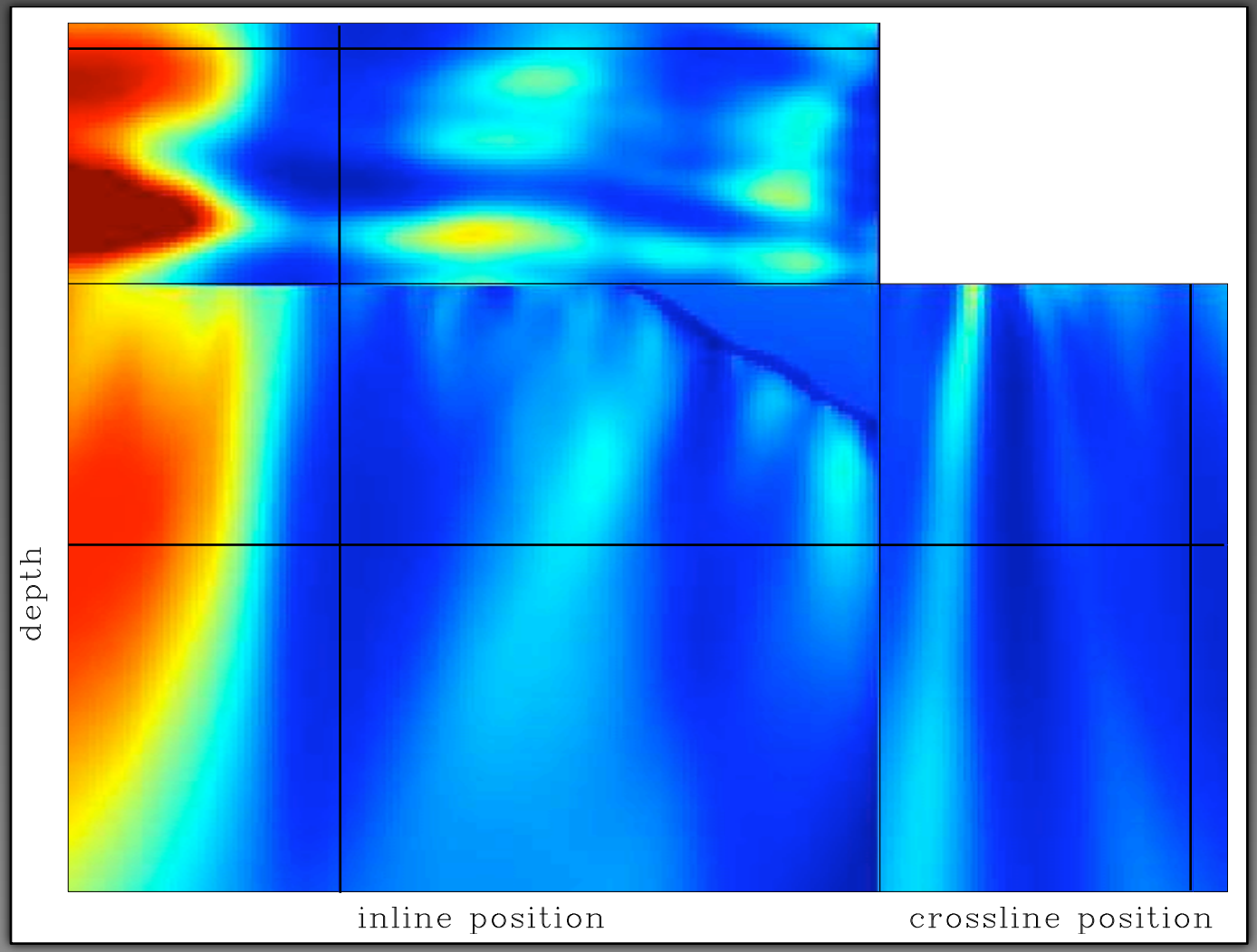

3D point spread function

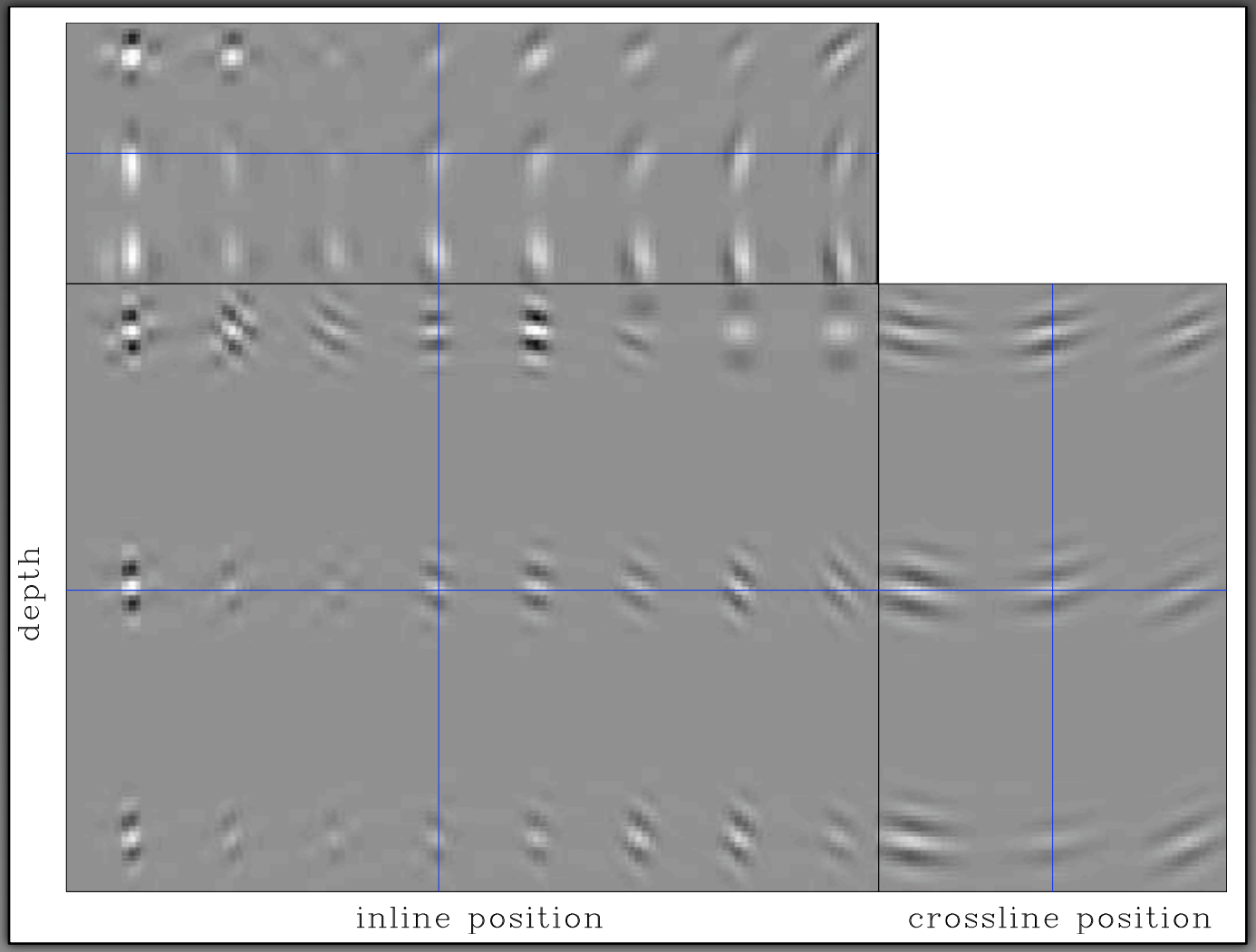

Regularization in the poststack image domain

$$(\mathbf{H} + \varepsilon\mathbf{R})\,\hat{\mathbf{m}} - \mathbf{m}_{mig} = \mathbf{r} \approx 0$$

Regularization in the poststack image domain

$$(\mathbf{H} + \varepsilon\mathbf{R})\,\hat{\mathbf{m}} - \mathbf{m}_{mig} = \mathbf{r} \approx 0$$

$\mathbf{R} = \mathbf{I}$ damping

3D point spread function

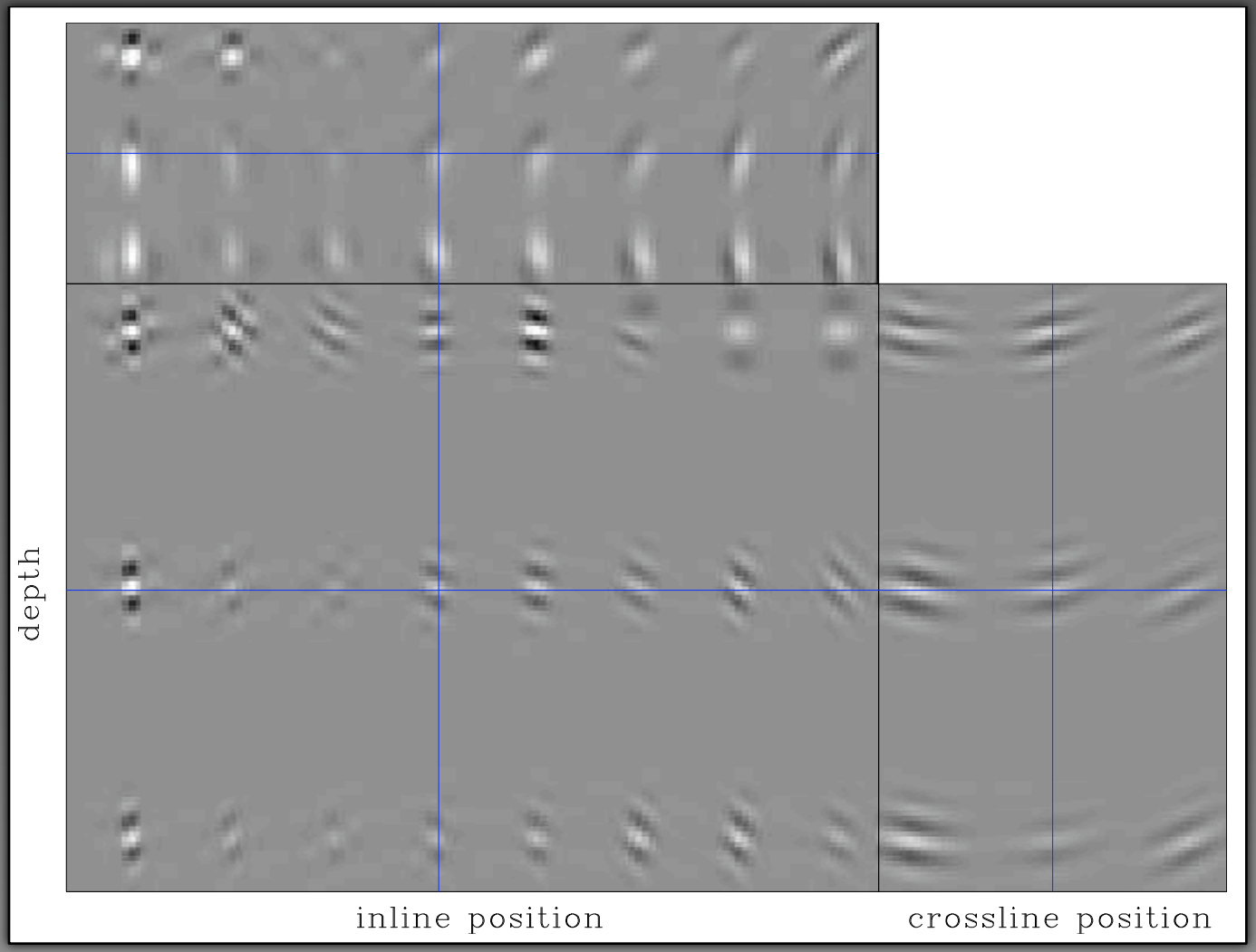

3D Inversion with 2D PSF

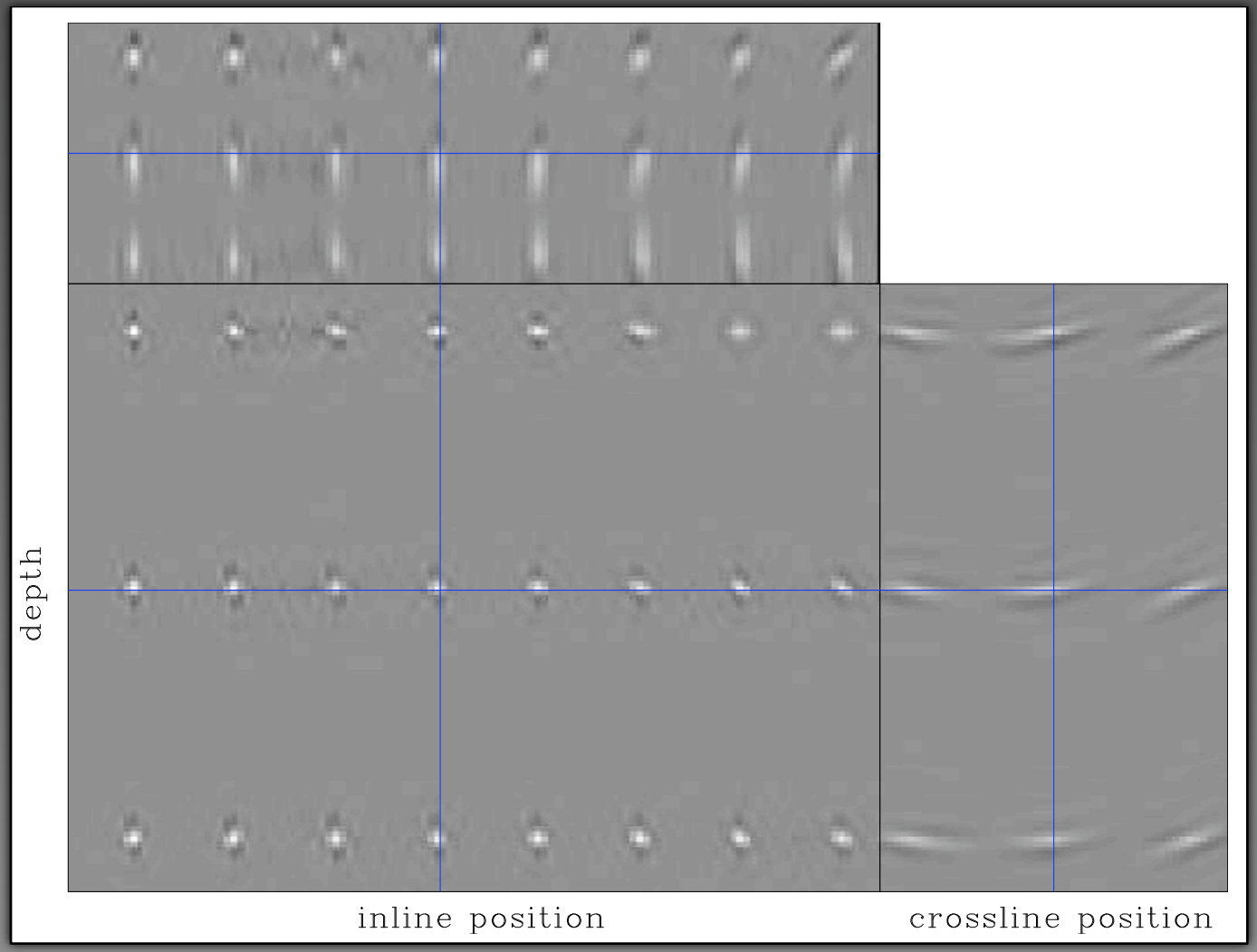

3D Inversion with 3D PSF

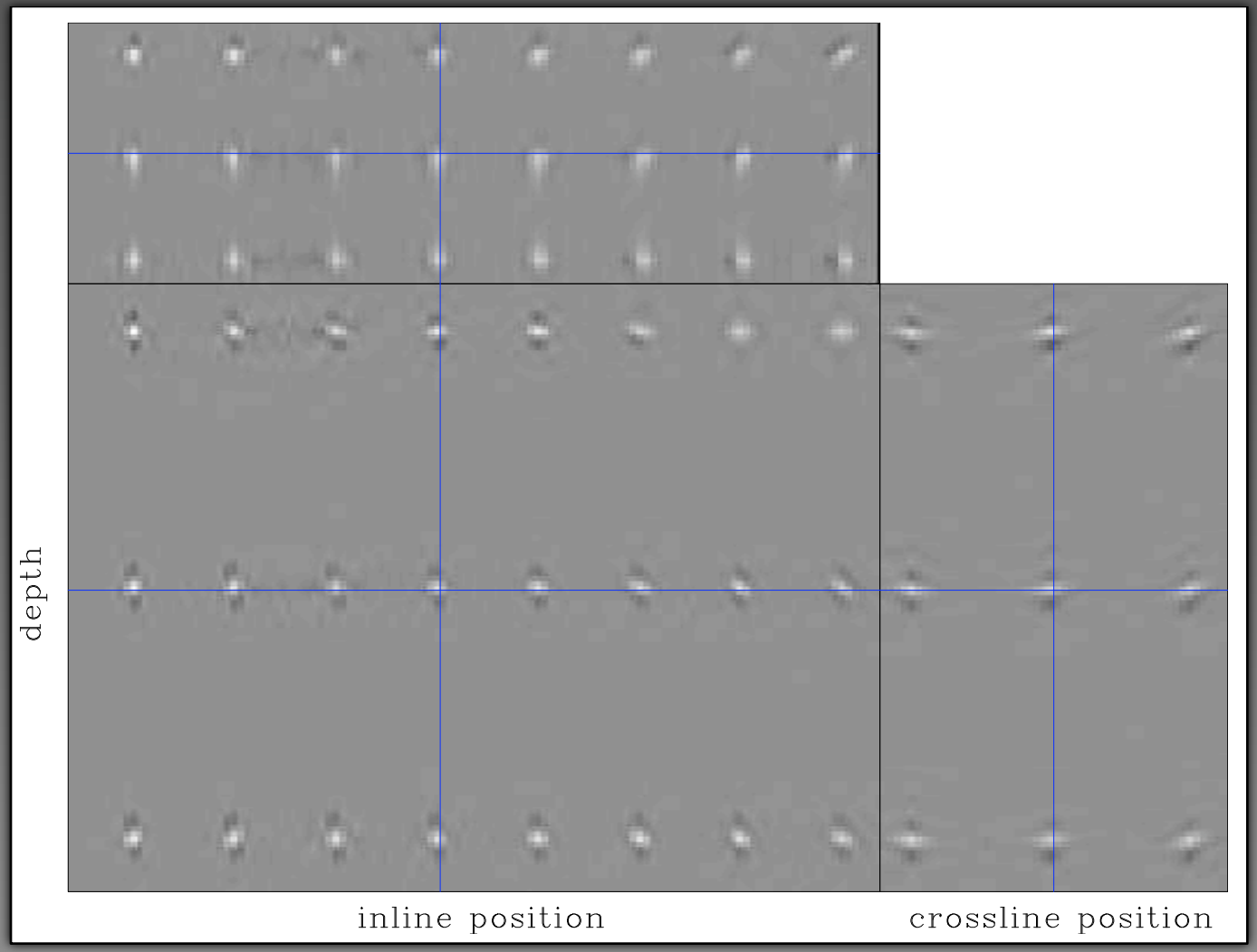

3D Migration

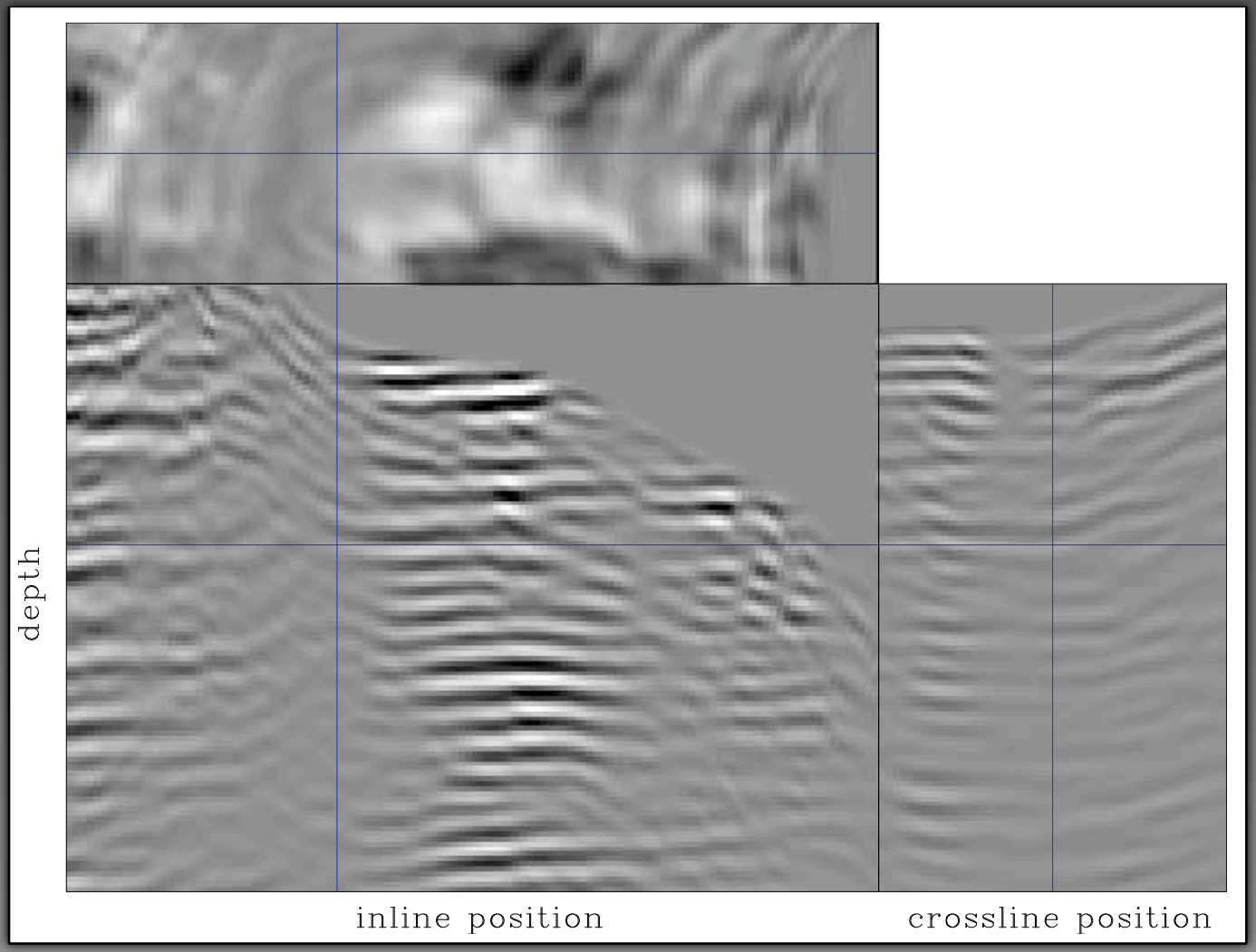

3D Inversion with 2D PSF

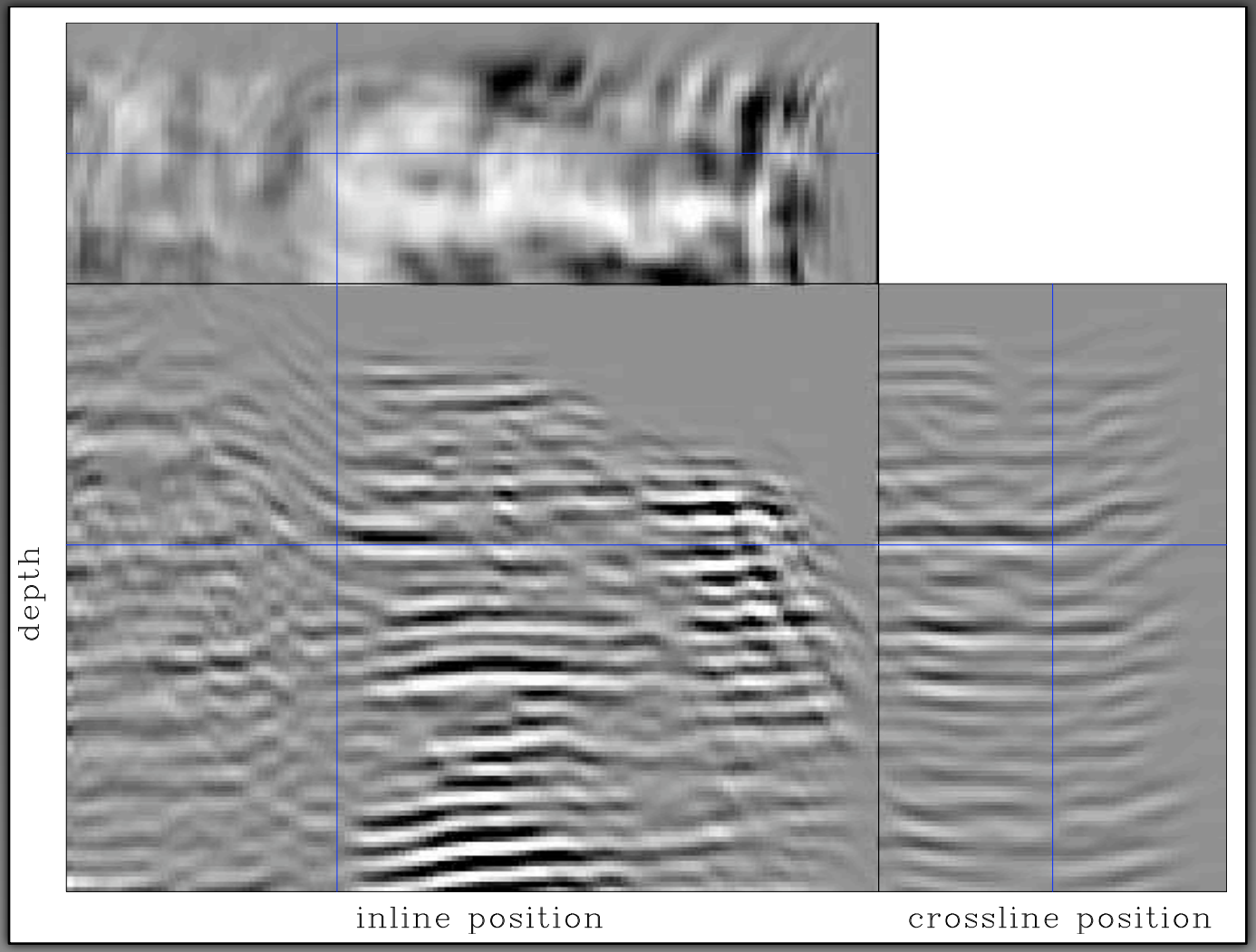

3D Migration

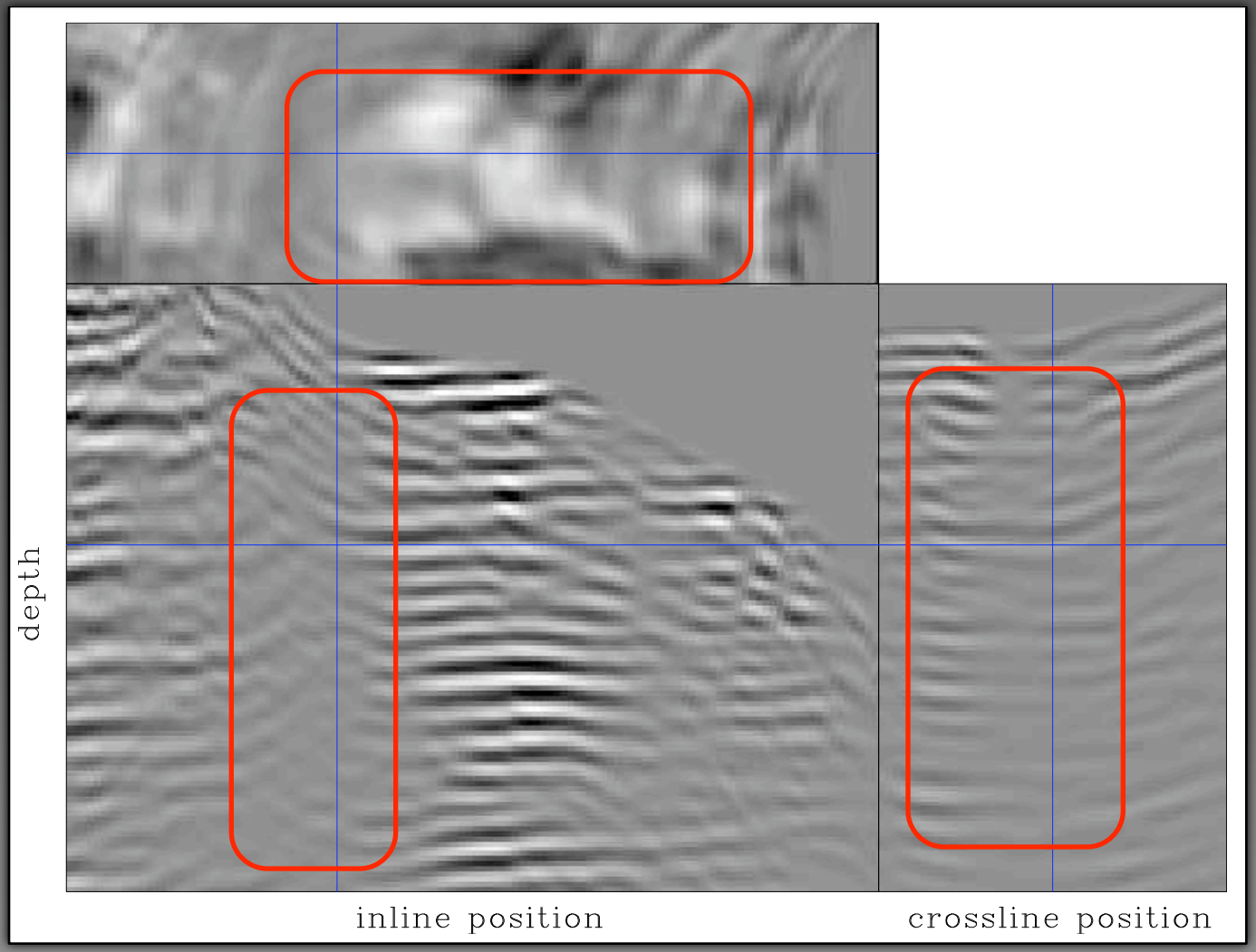

3D Inversion with 2D PSF

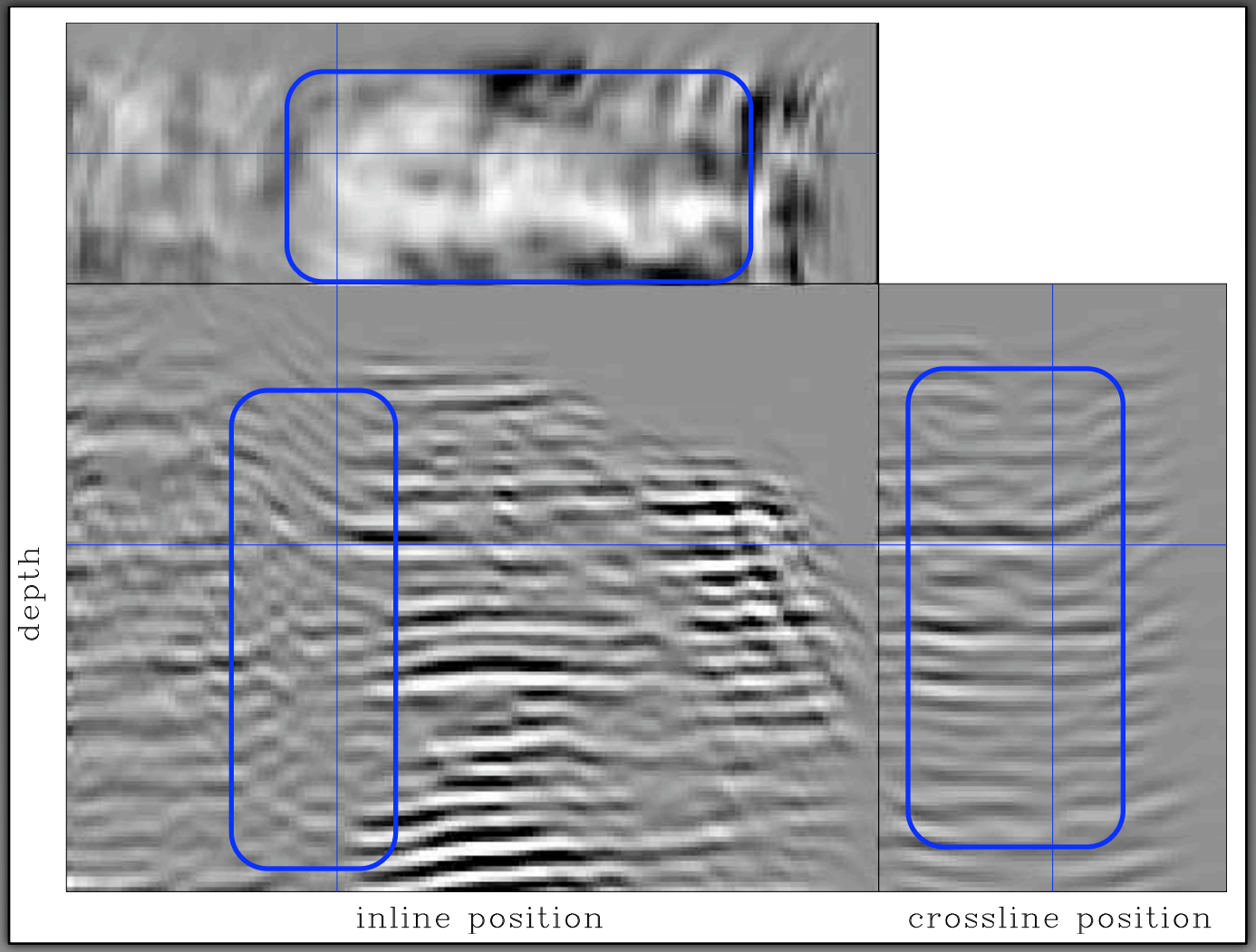

Regularization in the prestack image domain

$$(\mathbf{H} + \varepsilon\mathbf{R})\,\hat{\mathbf{m}} - \mathbf{m}_{mig} = \mathbf{r} \approx 0$$

Regularization in the prestack image domain

$$(\mathbf{H} + \varepsilon \mathbf{R})\, \hat{\mathbf{m}} - \mathbf{m}_{mig} = \mathbf{r} \approx 0$$

$$\mathbf{R} = \mathbf{P}_{\mathbf{h}}^{\mathbf{2}}$$

weighting subsurface-offset gathers

Expanding the dimensionality

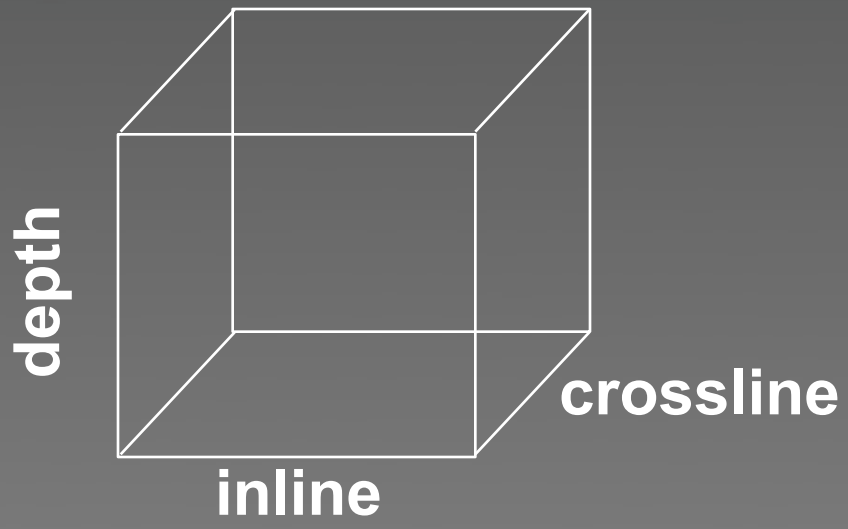

Expanding the dimensionality

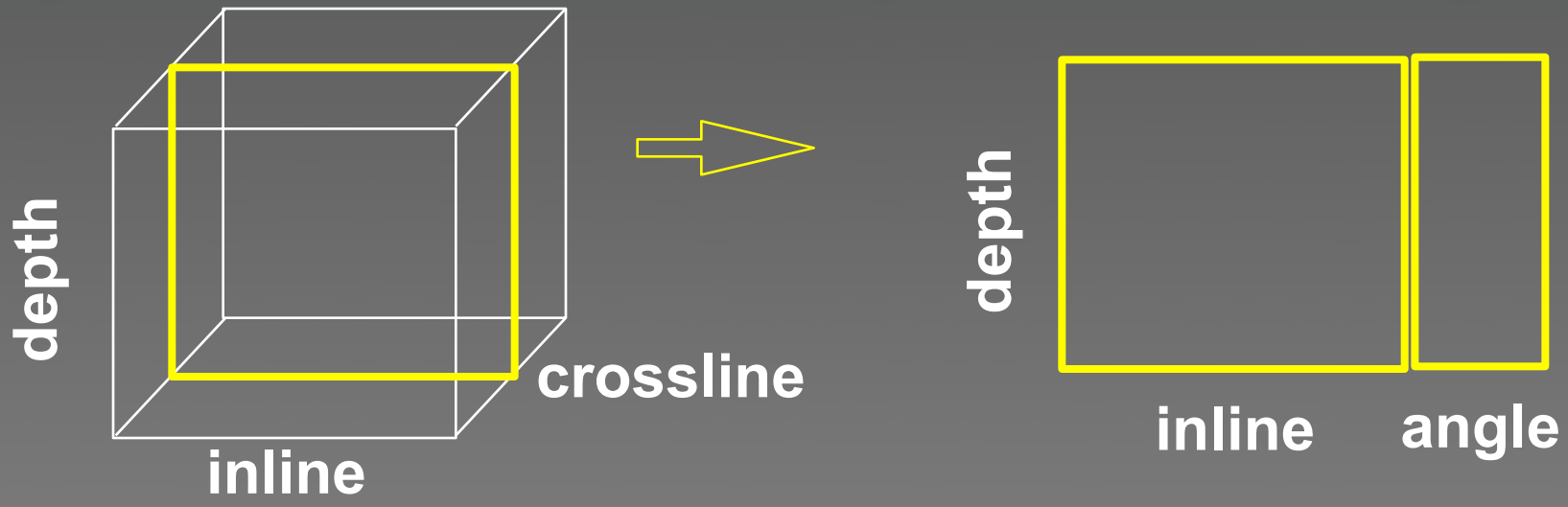

Slice of the 3D migration (x,y=const,z,angle): reflection angle

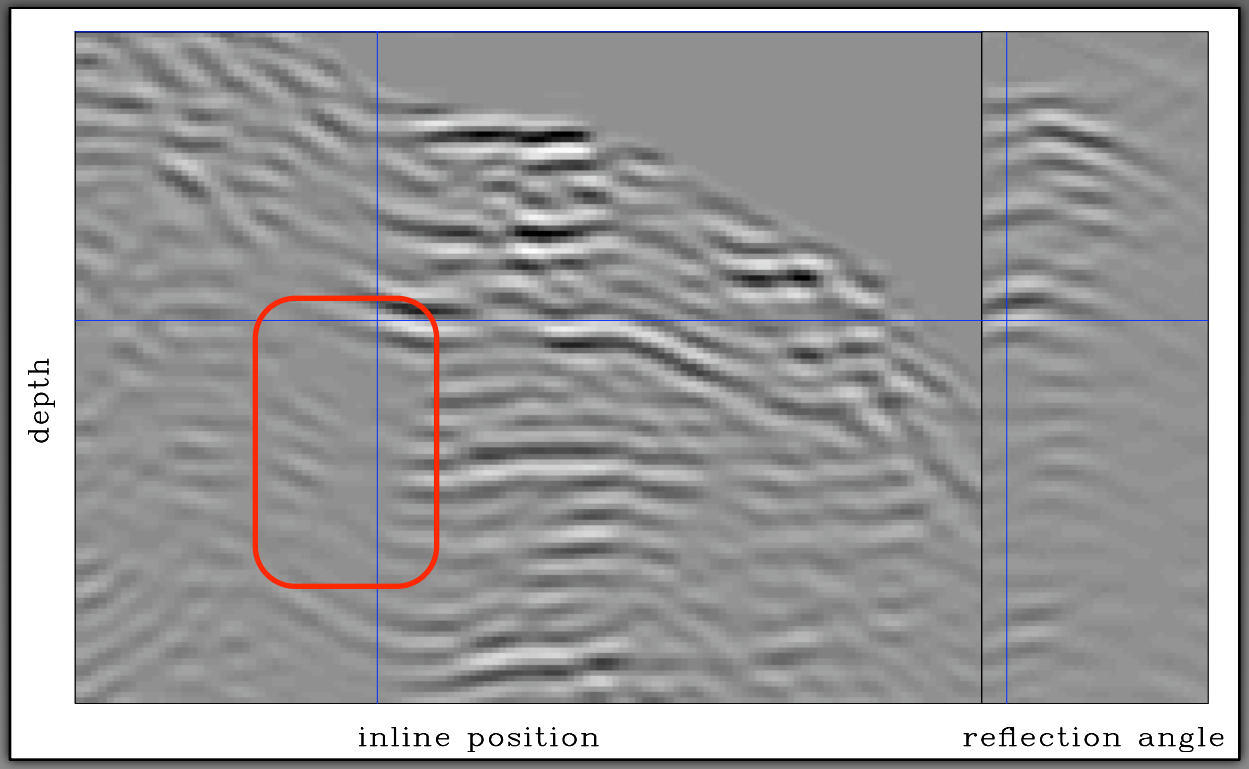

Slice of the 3D inversion (x,y=const,z,angle):reflection angle

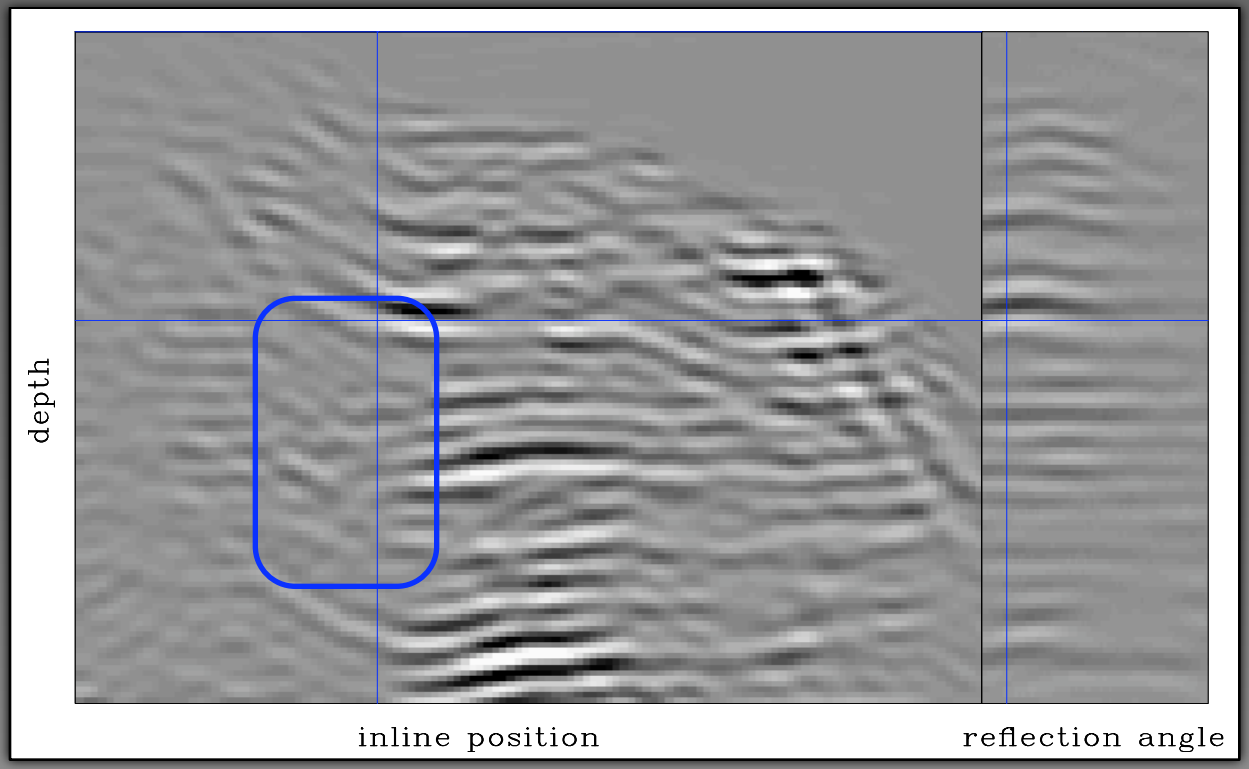

Migration versus inversion (x,y,z,0º)

migration

inversion

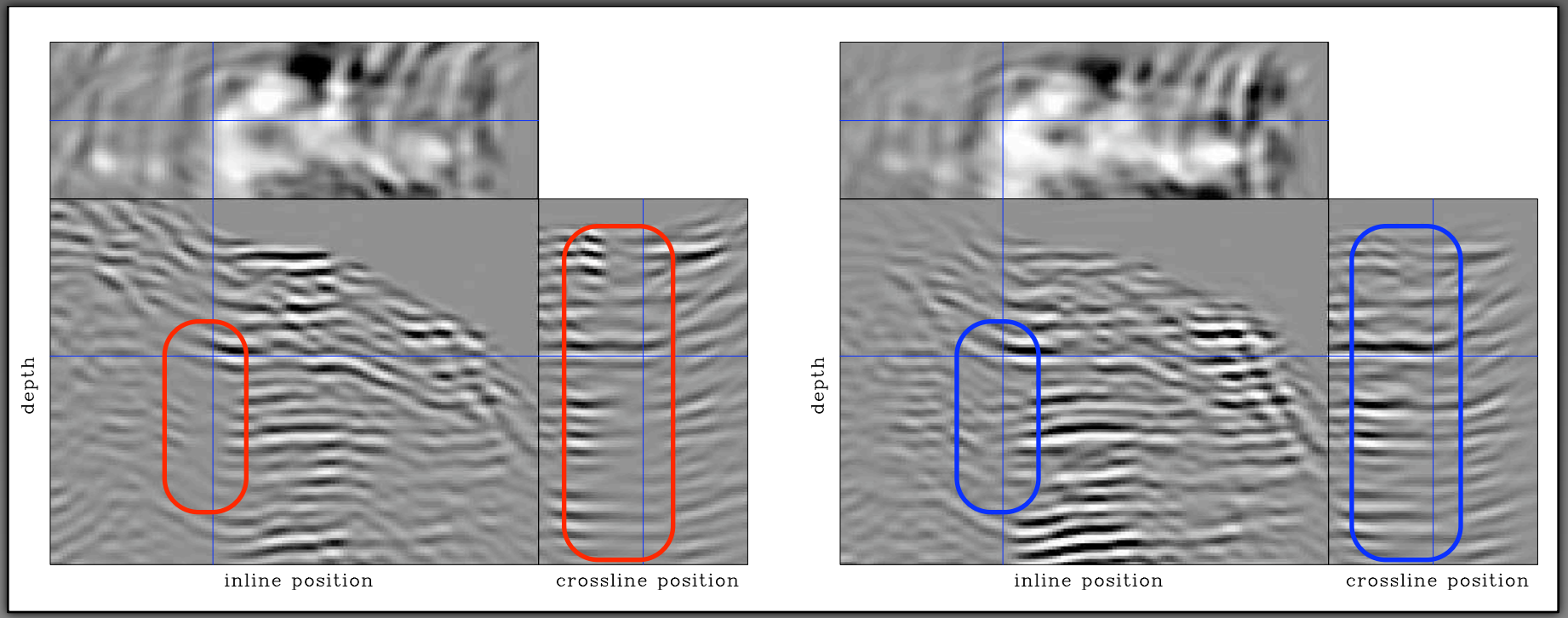

near angle cubes

Migration versus inversion (x,y,z,30º)

migration

inversion

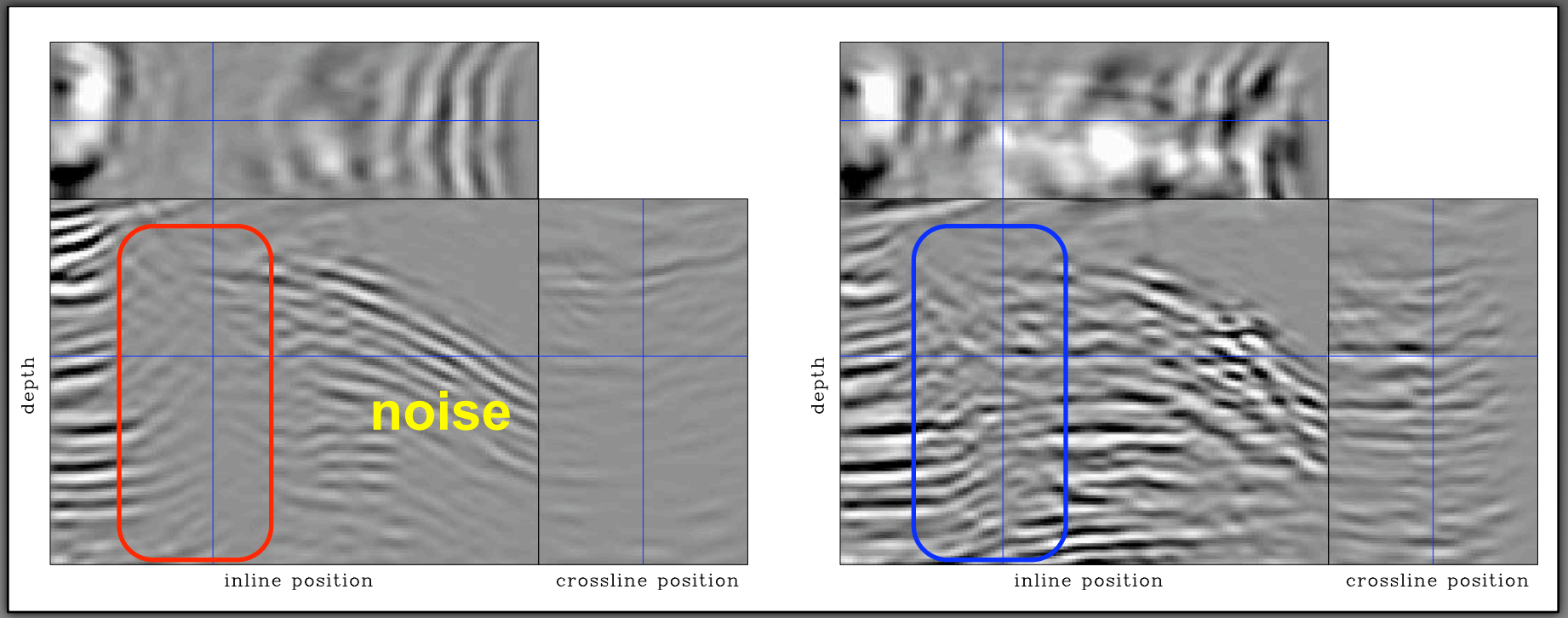

far angle cubes

3D Migration angle stack

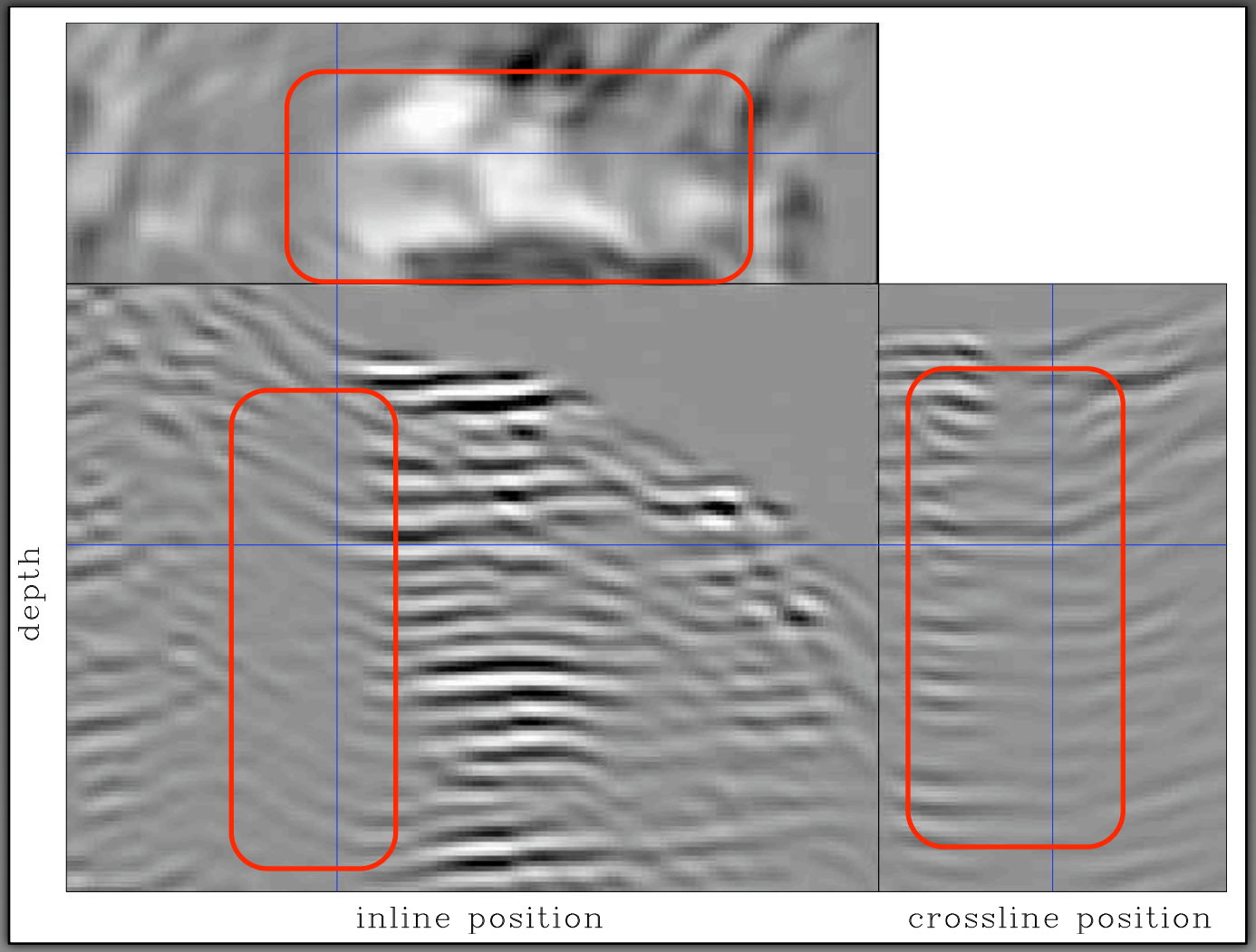

3D inversion angle stack $\varepsilon = 0.5$

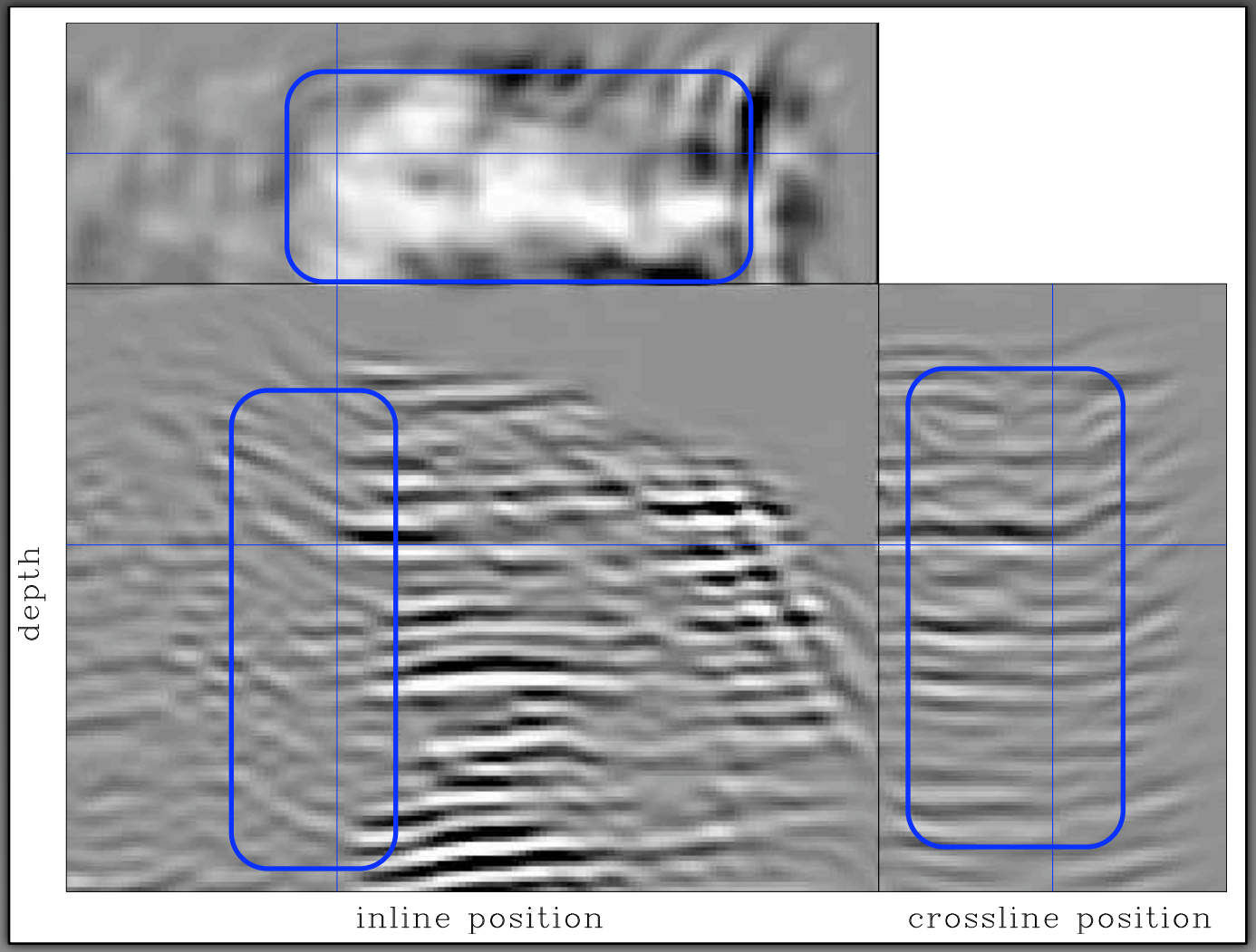

Conclusion

Imaging by wave-equation inversion can be done in practice

Acknowledgments

- BP, ExxonMobil, and SMAART JV for the data

3D Inversion with 3D PSF

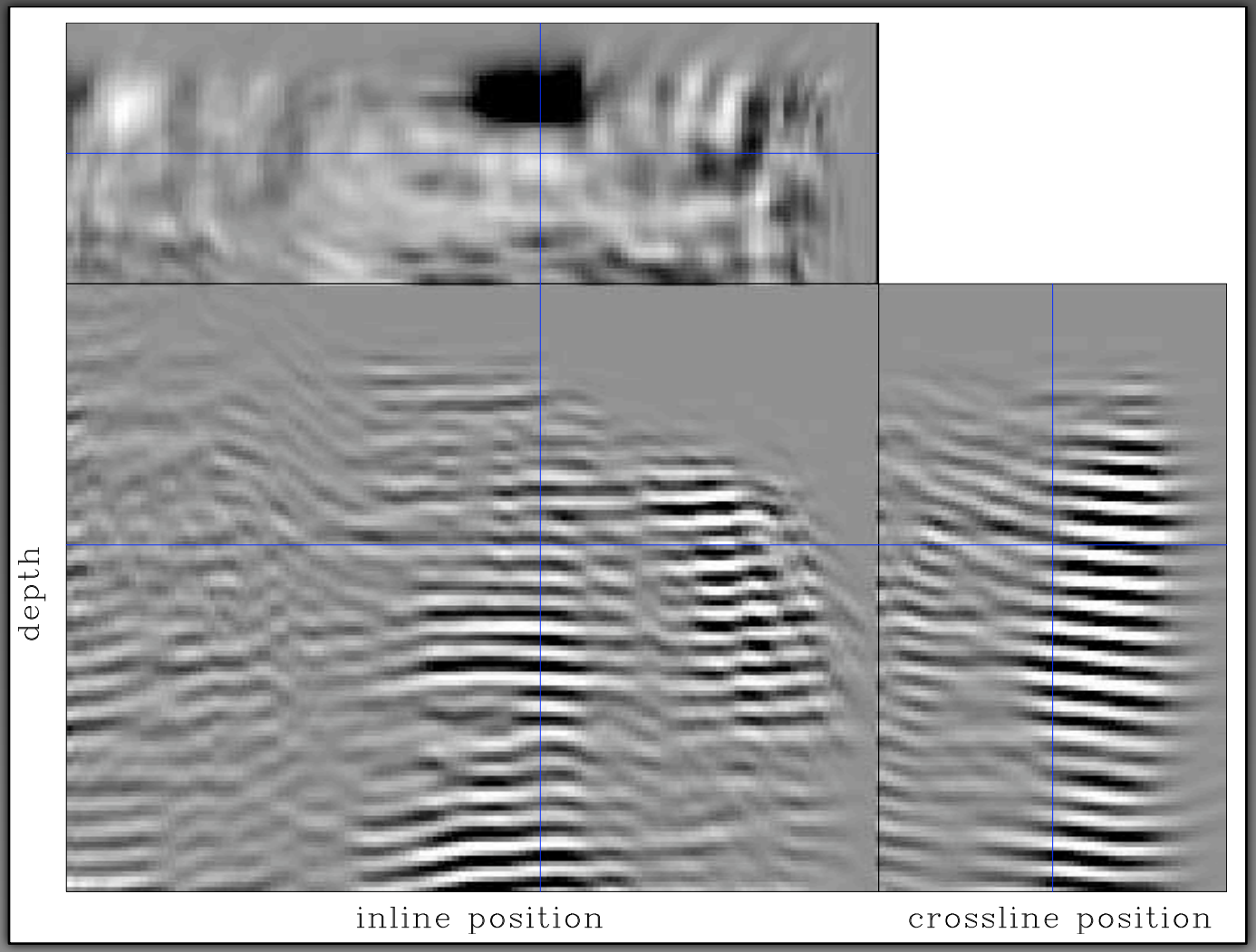

Slice of the 3D migration (x,y=const,z,hx): subsurface offset

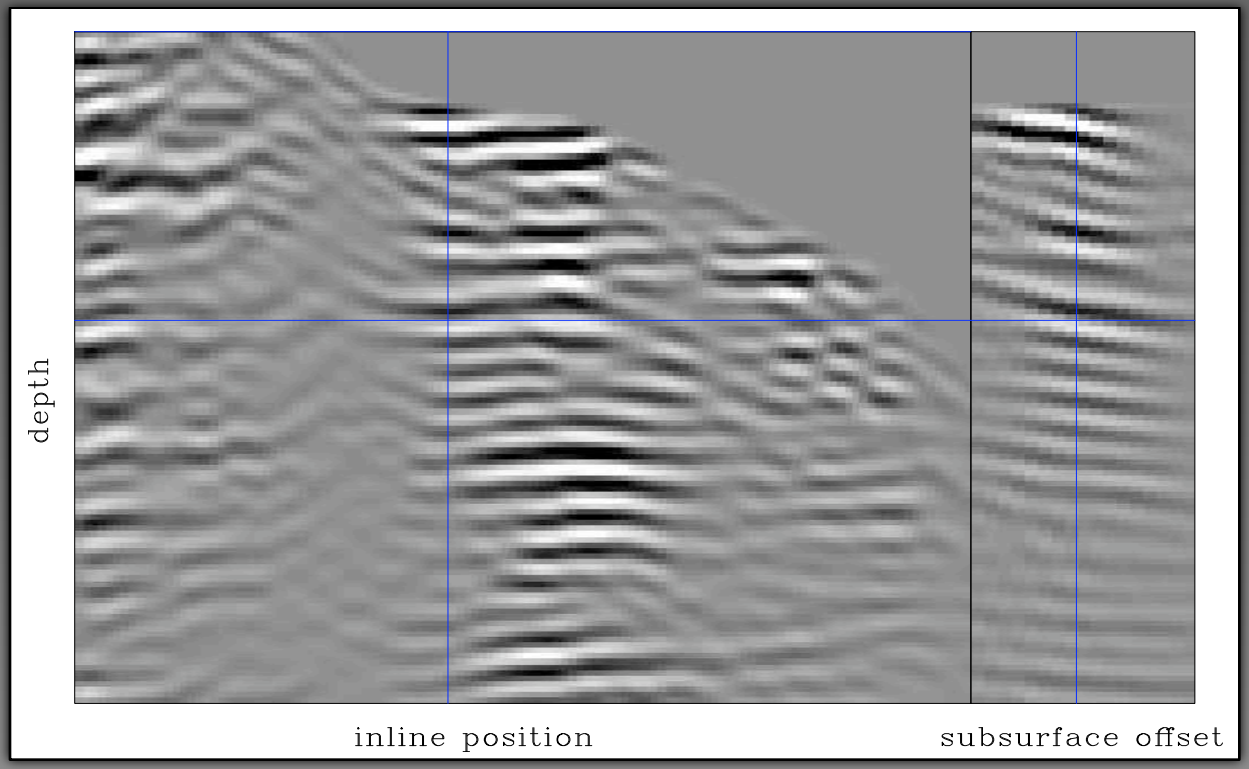

Slice of the 3D inversion (x,y=const,z,hx): subsurface offset

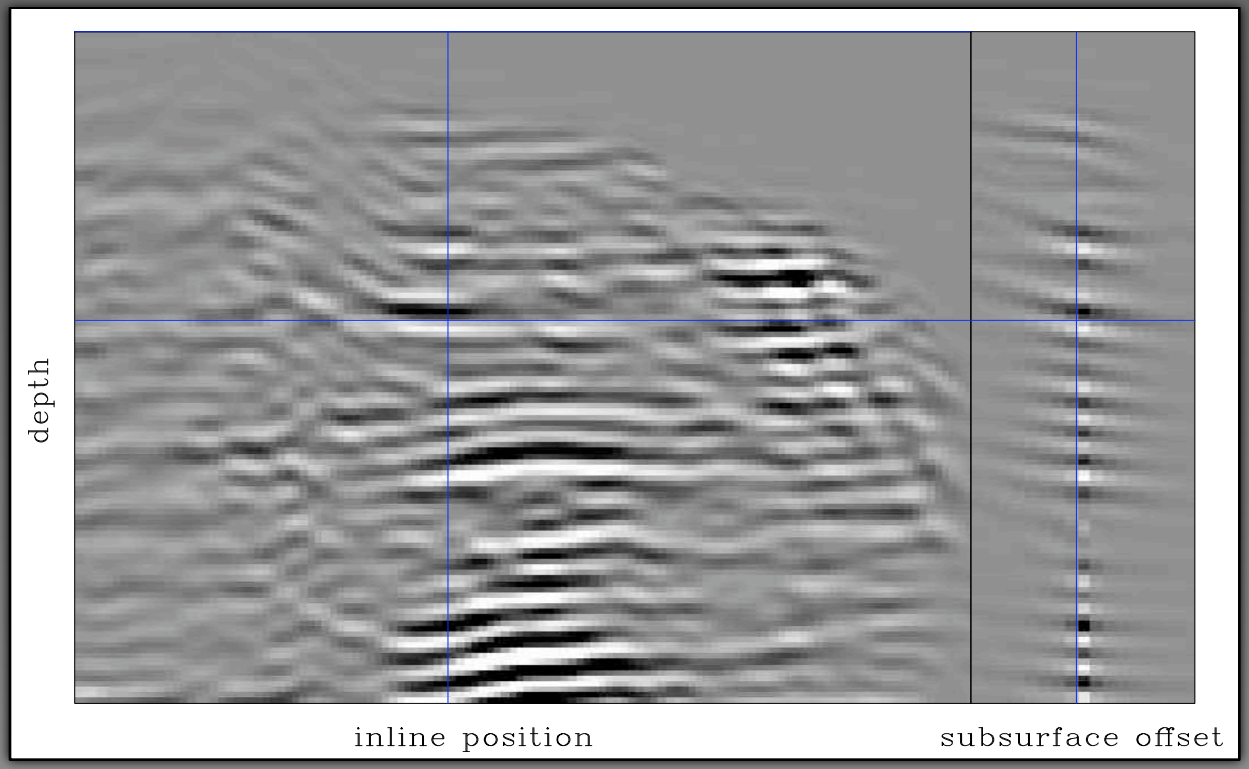

Reflectivity image

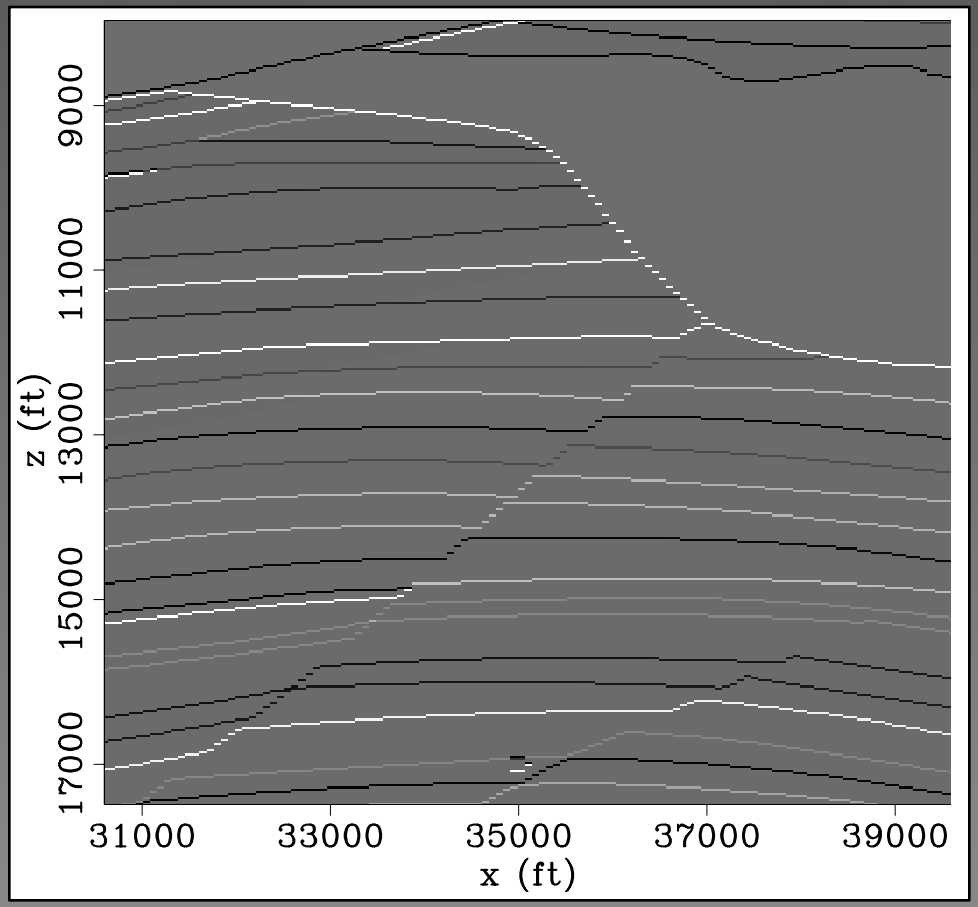

Convolution of the Hessian with the reflectivity (forward modeling)

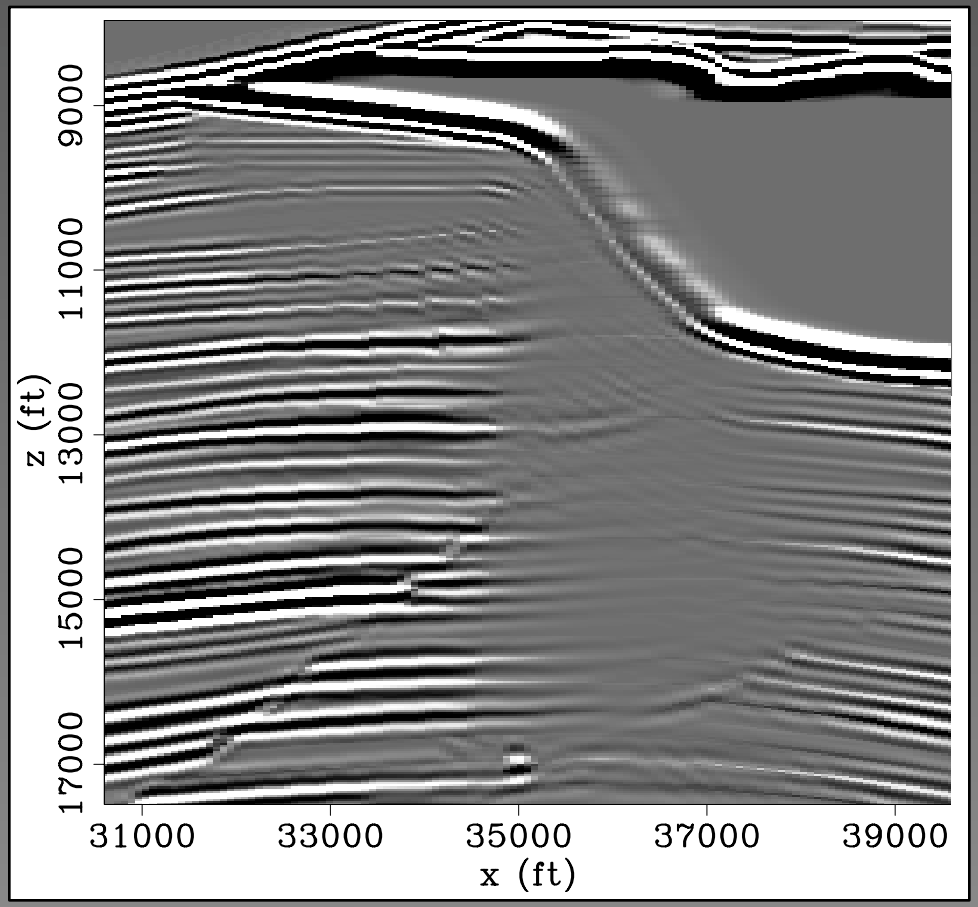

Migrated image

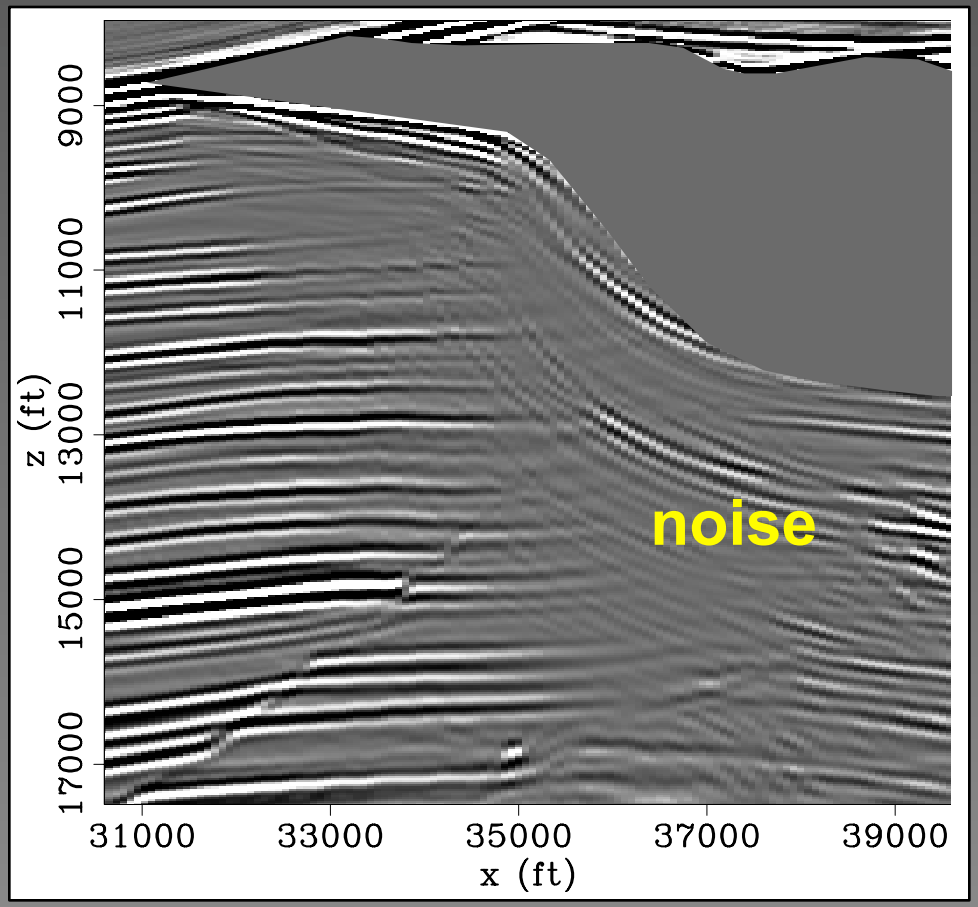

Migrated image after filtering

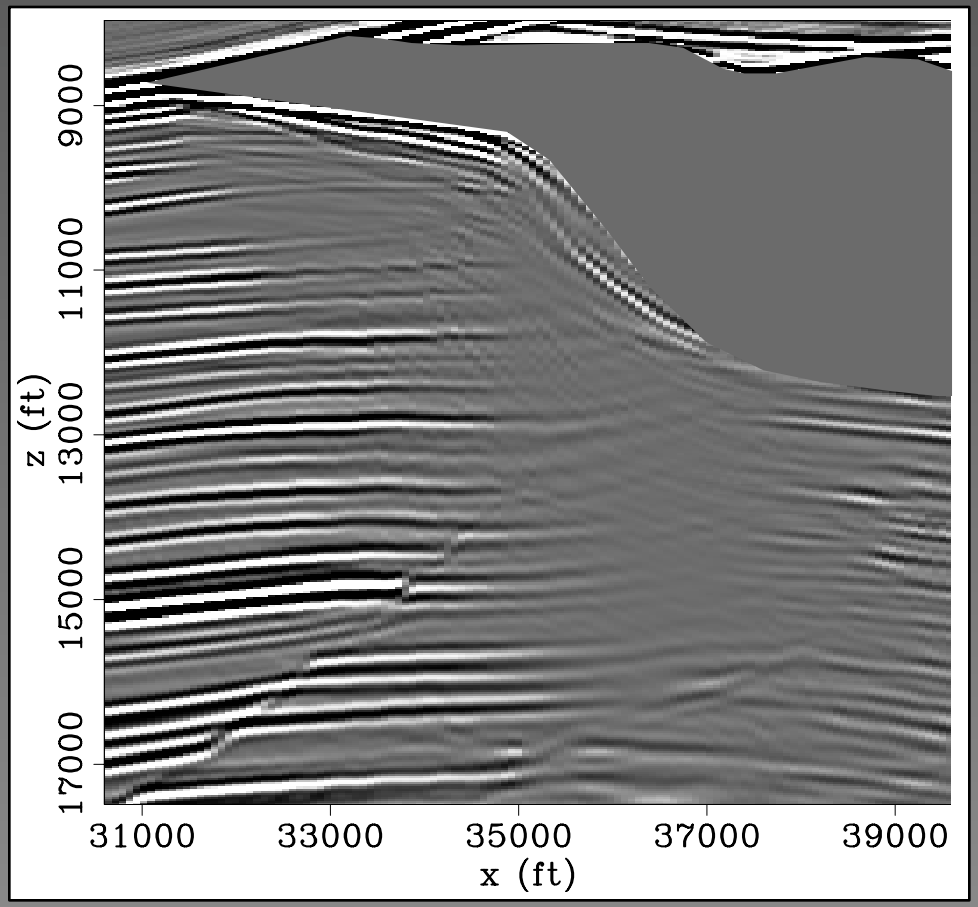

Image after inversion

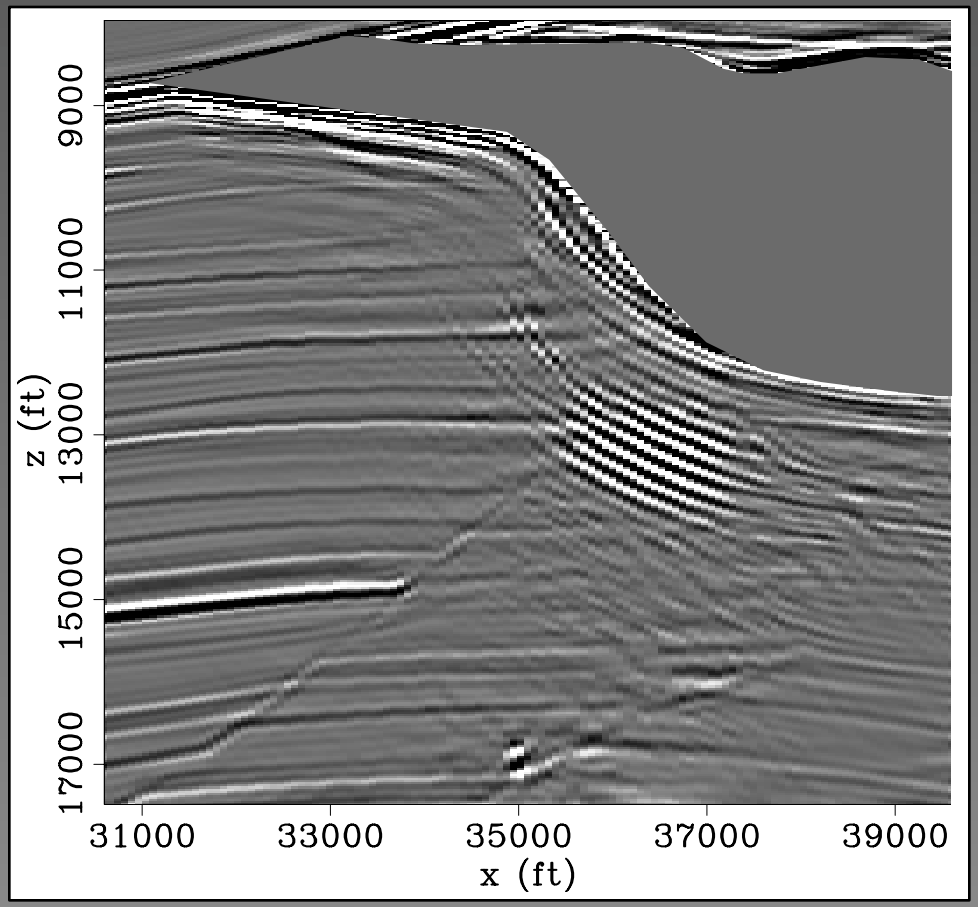

Image after inversion (filtered input)

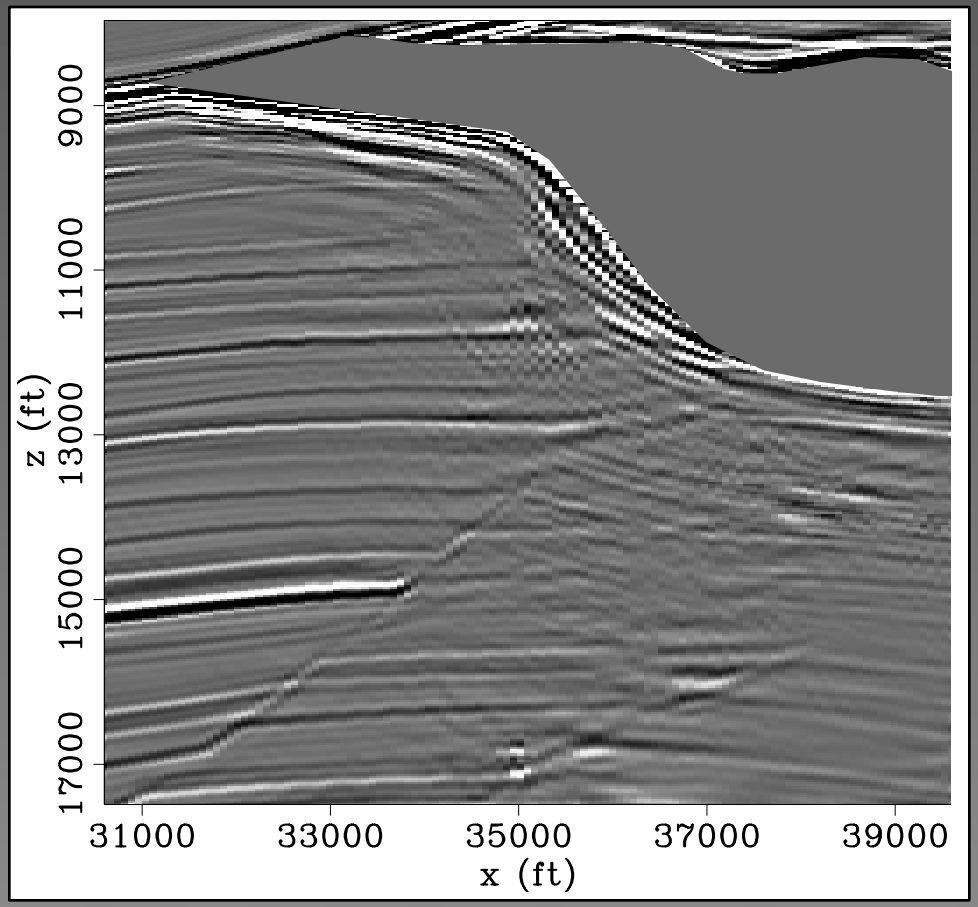

Residuals after 7 iterations

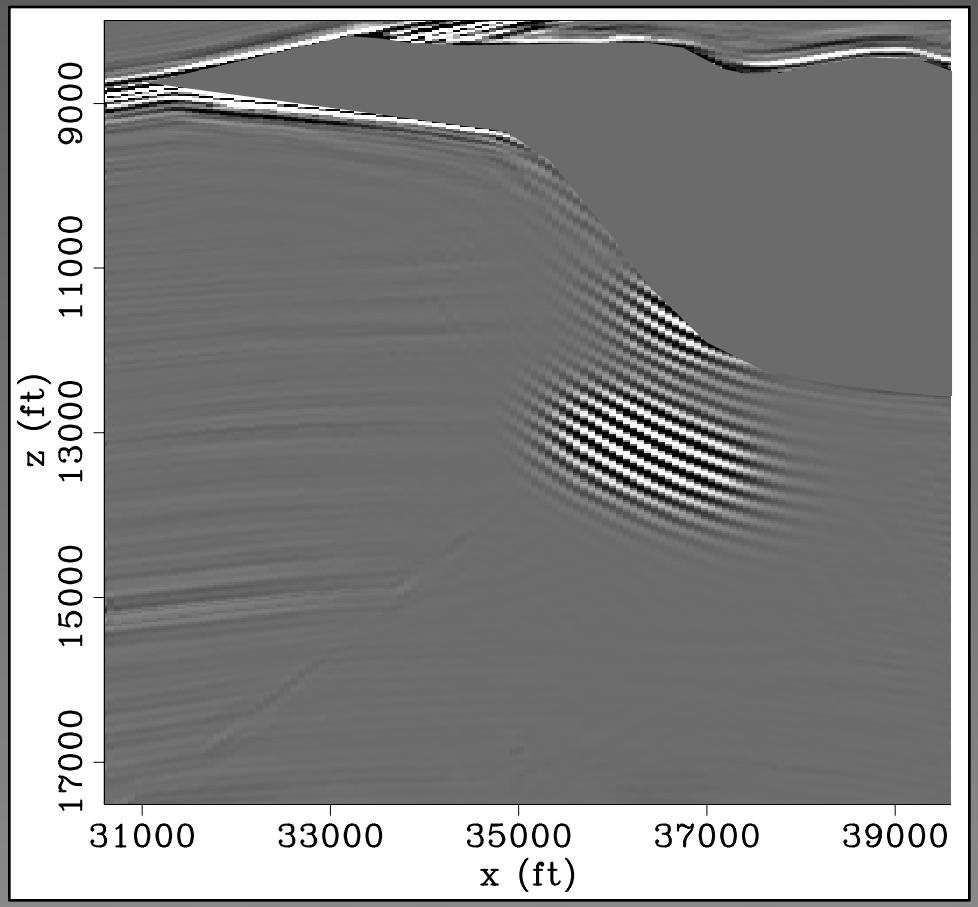

Residuals after 7 iterations (filtered input)

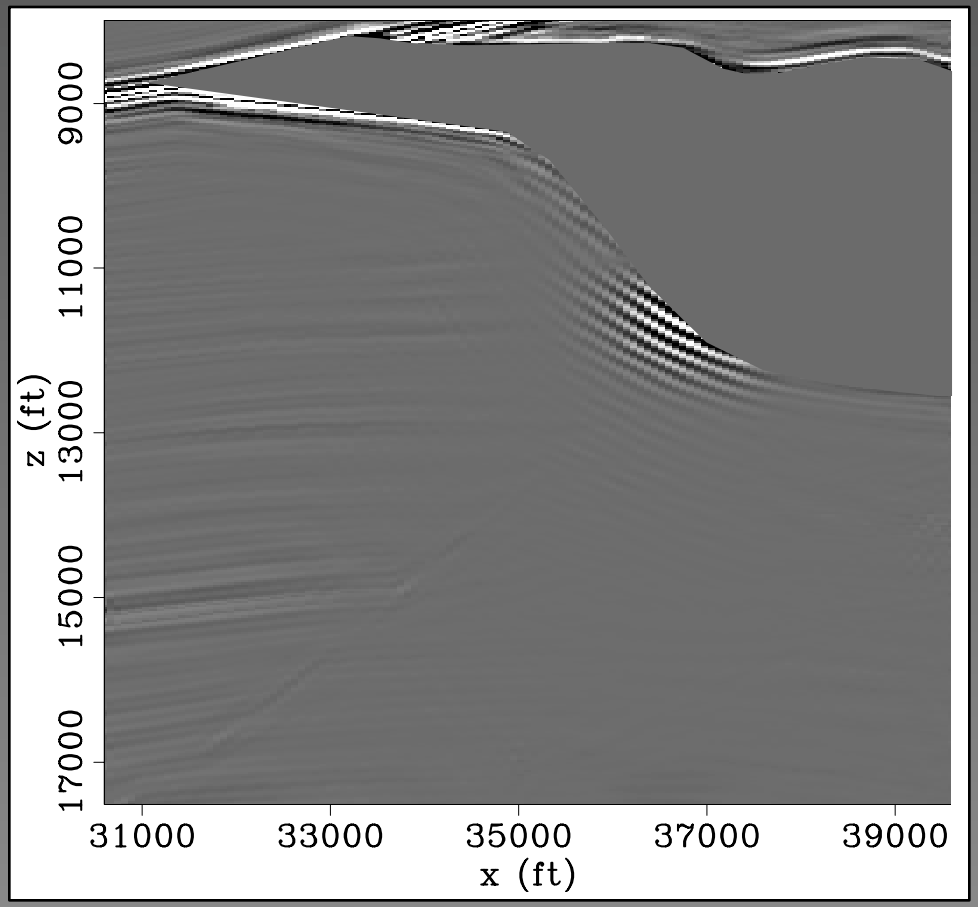

Improving “illumination” from the acquisition side

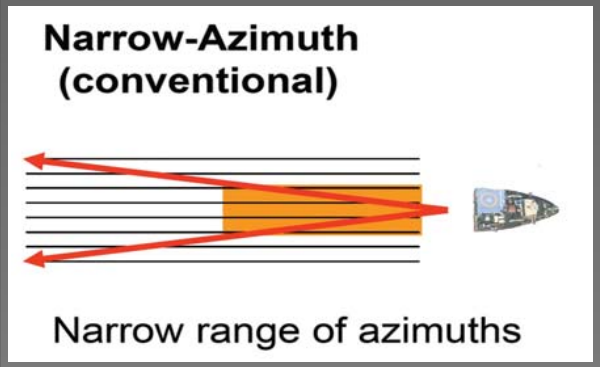

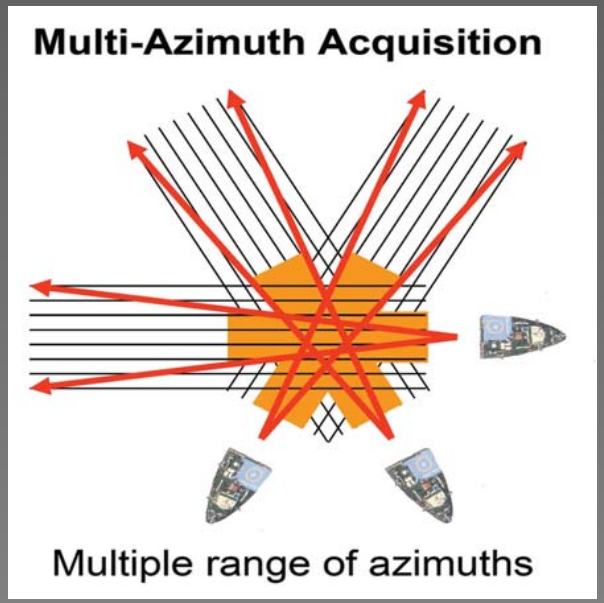

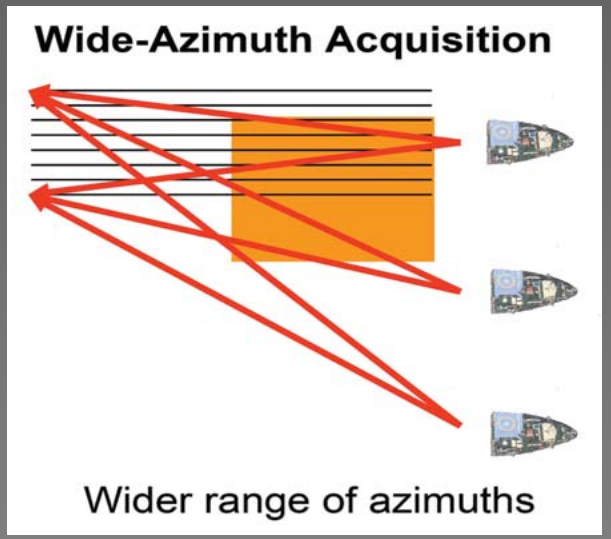

Inversion image

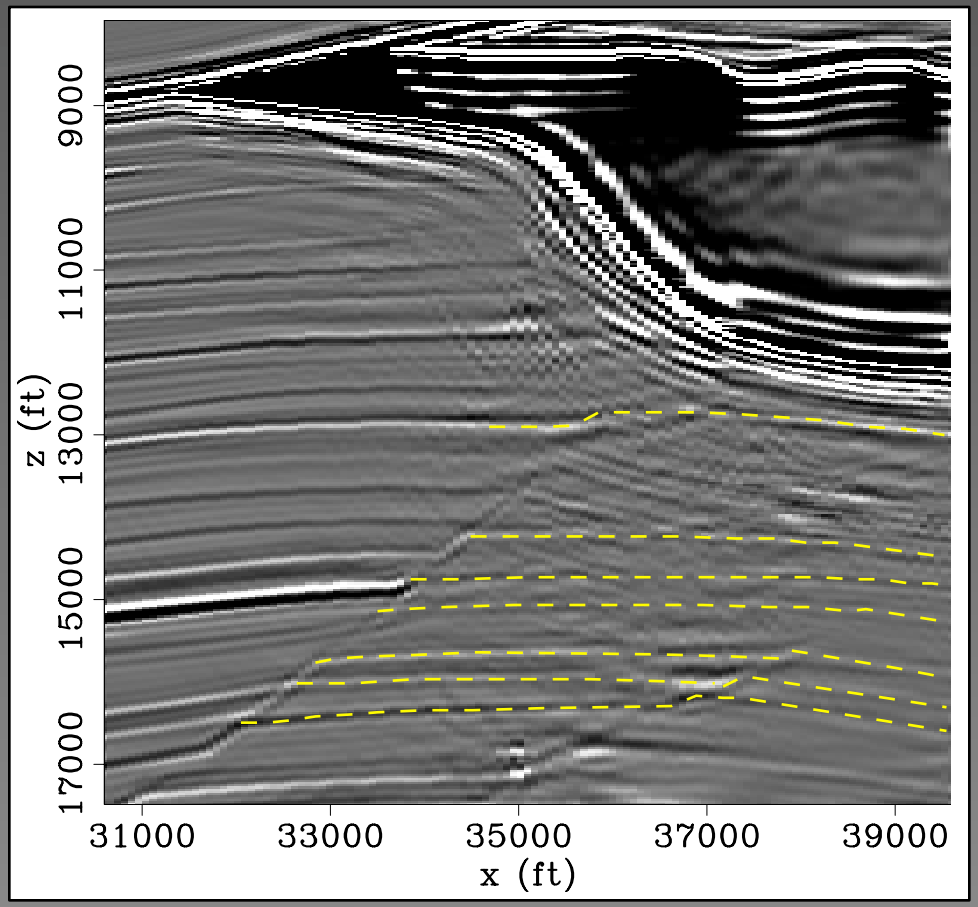

Green's function dimensions

$$\mathbf{G}(\mathbf{x}, \mathbf{x}_{surf}; \omega)$$

$$\mathbf{G}(x, y, z, x_{surf}, y_{surf}; \omega)$$

$$(n_x, n_y, n_z, n_{x_{surf}}, n_{y_{surf}}; n_\omega)$$

$$8 \times 4 \times 10^2 \times 2 \times 10^2 \times 2 \times 10^2 \times 4 \times 10^2 \times 2 \times 10^2 \times 2 \times 10^2 = 2 \times 10^{15}$$

(petabyte)

In parallel $\dfrac{2 \times 10^{15}}{2 \times 10^2} = 10^{13}$

(terabytes)

Hessian dimensions

$$\mathbf{H}(\mathbf{x}, \mathbf{y})$$

$$\mathbf{H}(x, y, z, x', y', z')$$

$$(n_x, n_y, n_z, n_x, n_y, n_z)$$

$$4 \times 4 \times 10^2 \times 2 \times 10^2 \times 2 \times 10^2 \times 4 \times 10^2 \times 2 \times 10^2 \times 2 \times 10^2 = 10^{15}$$

(petabyte)

Green's function dimensions

$$\mathbf{G}(\mathbf{x}_T, \mathbf{x}_s; \omega)$$

$$\mathbf{G}(x_T, y_T, z_T, x_{surf}, y_{surf}; \omega)$$

$$(n_{x_T}, n_{y_T}, n_{z_T}, n_{x_{surf}}, n_{y_{surf}}; n_\omega)$$

$$8 \times 4 \times 10 \times 2 \times 10 \times 2 \times 10 \times 4 \times 10^2 \times 2 \times 10^2 \times 2 \times 10^2 = 2 \times 10^{12}$$

(terabytes)

In parallel $\dfrac{2 \times 10^{12}}{2 \times 10^2} = 10^{10}$

(gigabytes)

Hessian dimensions

$$\mathbf{H}(x_T, y_T)$$

$$\mathbf{H}(x_T, y_T, z_T, x'_T, y'_T, z'_T)$$

$$(n_{x_T}, n_{y_T}, n_{z_T}, n_{x_T}, n_{y_T}, n_{z_T})$$

$$4 \times 4 \times 10 \times 2 \times 10 \times 2 \times 10 \times 4 \times 10 \times 2 \times 10 \times 2 \times 10 = 10^9$$

(gigabyte)

Hessian dimensions

$$\mathbf{H}(\mathbf{x}_T, \mathbf{x}_T + \mathbf{a_x})$$

$$\mathbf{H}(x_T, y_T, z_T, x_T + a_x, y_T + a_T, z_T + a_T)$$

$$(n_{x_T}, n_{y_T}, n_{z_T}, n_{a_x}, n_{a_y}, n_{a_z})$$

$$4 \times (4 \times 10) \times (2 \times 10) \times (2 \times 10) \times 10 \times 10 \times 10 = 6 \times 10^7$$

(megabytes)

Toy example

$n_x = 400$
$n_y = 200$
$n_z = 200$

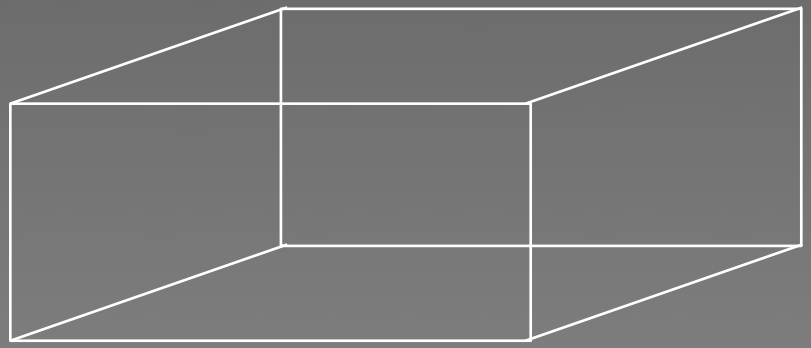

model space

$n_{sx} = 400$
$n_{sy} = 200$
$n_w = 200$

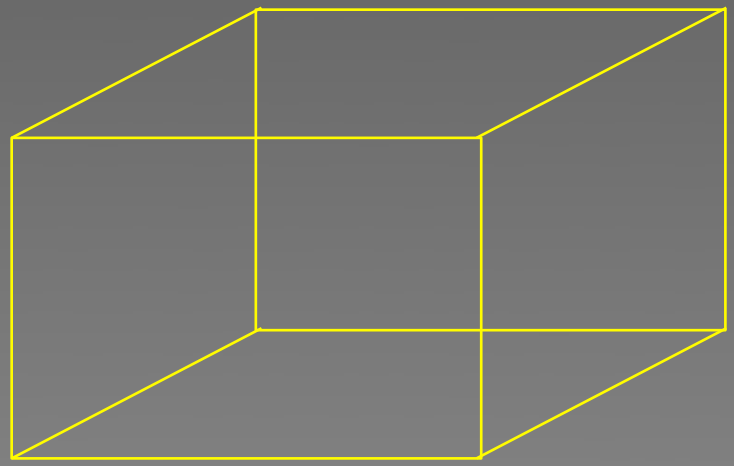

data space

Problem dimensions

Approximation	G		H
	Serial	Parallel	
NA	$2x10^{15}$ (petabytes)	10^{13} (terabytes)	10^{15} (petabyte)

Toy example

$n_{xT} = 40$
$n_{yT} = 20$
$n_{zT} = 20$

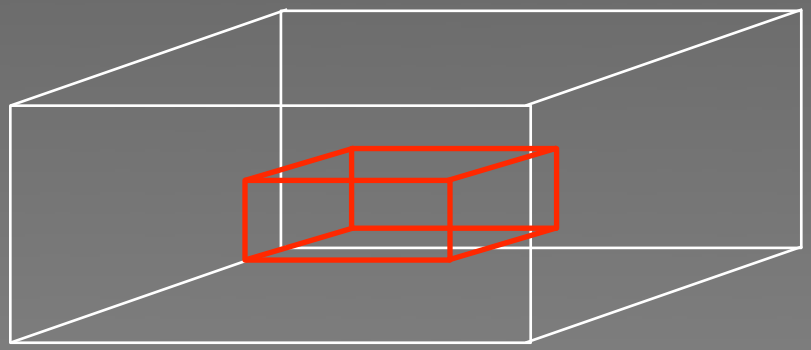

model space

$n_{sx} = 400$
$n_{sy} = 200$
$n_{w} = 200$

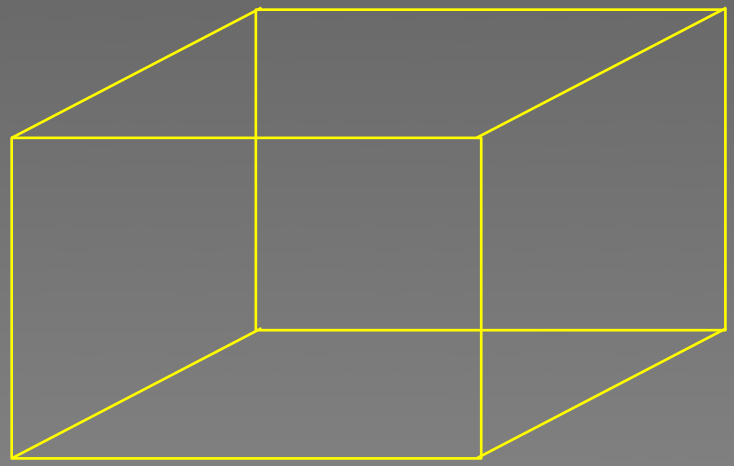

data space

Problem dimensions

Approximation	G		H
	Serial	Parallel	
NA	$2x10^{15}$ (petabytes)	10^{13} (terabytes)	10^{15} (petabyte)
target	$2x10^{12}$ (terabytes)	10^{10} (gigabytes)	10^{9} (gigabyte)

Hessian matrix

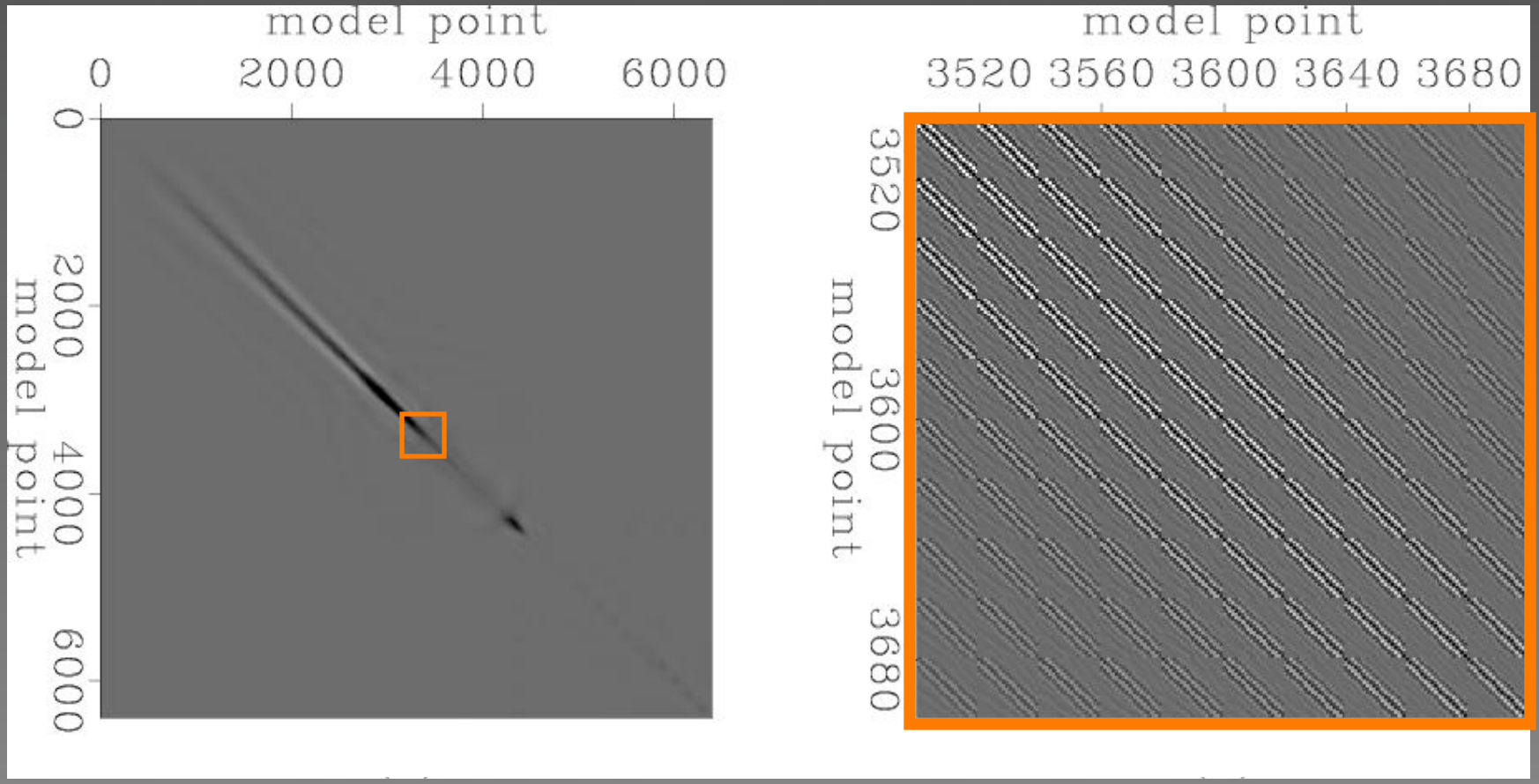

Sparse symmetric matrix

Problem dimensions

Approximation	G		H
	Serial	Parallel	
NA	$2x10^{15}$ (petabytes)	10^{13} (terabytes)	10^{15} (petabyte)
target	$2x10^{12}$ (terabytes)	10^{10} (gigabytes)	10^{9} (gigabyte)
structure	$2x10^{12}$ (terabytes)	10^{10} (gigabytes)	$6x10^{7}$(megabytes)

Outline

- Least-squares imaging (explicit Hessian)
- Prestack image-domain Hessian
- Hessian construction cost
- **Inversion with regularization in the subsurface-offset domain: Sigsbee model**

Non-diagonal Hessian approximations

Non-diagonal Hessian approximations

- Hu et al. (2001), horizontally invariant deconvolution operator

Non-diagonal Hessian approximations

- Hu et al. (2001), horizontally invariant deconvolution operator
- Guitton (2004), bank of matching filters

From offset to angle

$$\mathbf{S}_{\Theta \rightarrow \mathbf{h}} \mathbf{m}(\mathbf{x}, \Theta) = \mathbf{m}(\mathbf{x}, \mathbf{h})$$

$\Theta = (\theta, \alpha)$ **reflection and azimuth angles**

$\mathbf{S}_{\Theta \rightarrow \mathbf{h}}$ **slant stack operator**

Diagonal Hessian approximations

Cross correlation imaging condition

$$\mathbf{H}_{appr} = \mathbf{I}$$

Division by shot illumination imaging condition

$$\mathbf{H}_{appr} = \sum_{\omega} \sum_{\mathbf{x}_s} \mathbf{G}'(\mathbf{x}, \mathbf{x}_s; \omega) \mathbf{G}(\mathbf{x}, \mathbf{x}_s; \omega)$$

Inversion in the subsurface-offset (DSO)

$$\mathbf{H}(\mathbf{x},\mathbf{h};\mathbf{x}',\mathbf{h}')\hat{\mathbf{m}}(\mathbf{x},\mathbf{h}) - \mathbf{m}_{mig}(\mathbf{x},\mathbf{h}) \approx 0$$

$$\varepsilon \mathbf{P_h}\hat{\mathbf{m}}(\mathbf{x},\mathbf{h}) \approx 0$$

$\mathbf{P_h} = |\mathbf{h}|$ **differential semblance operator**

Iterative inversion algorithm

10 degree cube

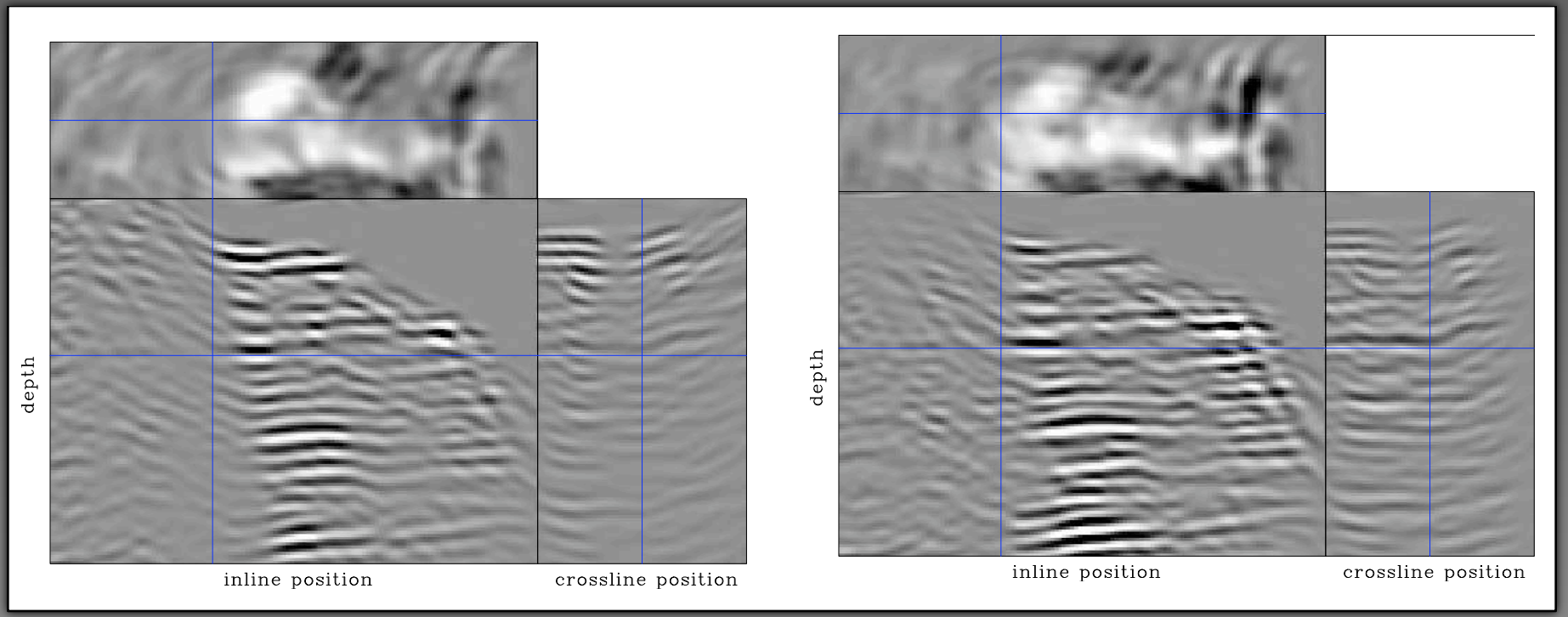

3D Narrow azimuth acquisition

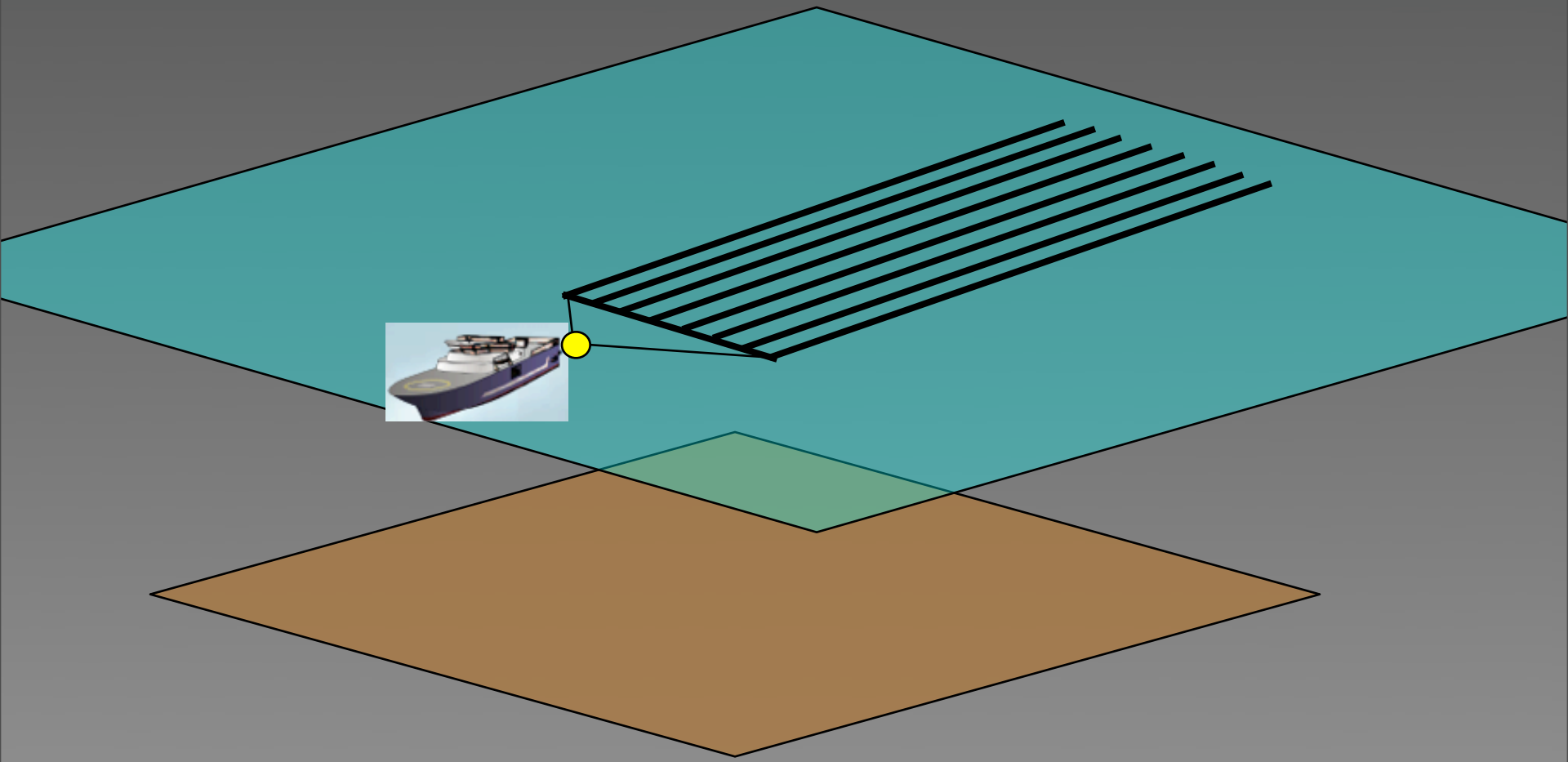

3D Narrow azimuth acquisition

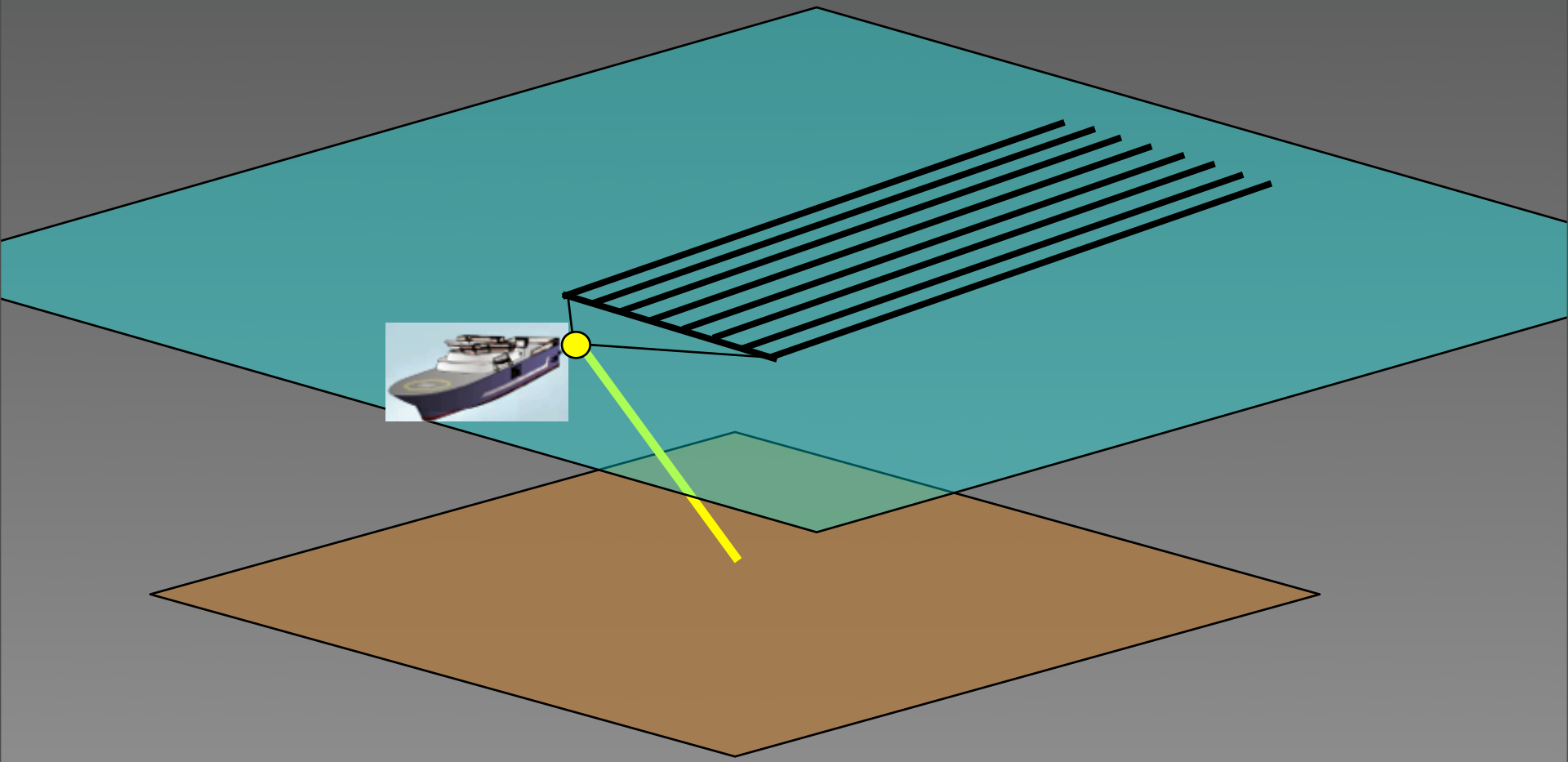

3D Narrow azimuth acquisition

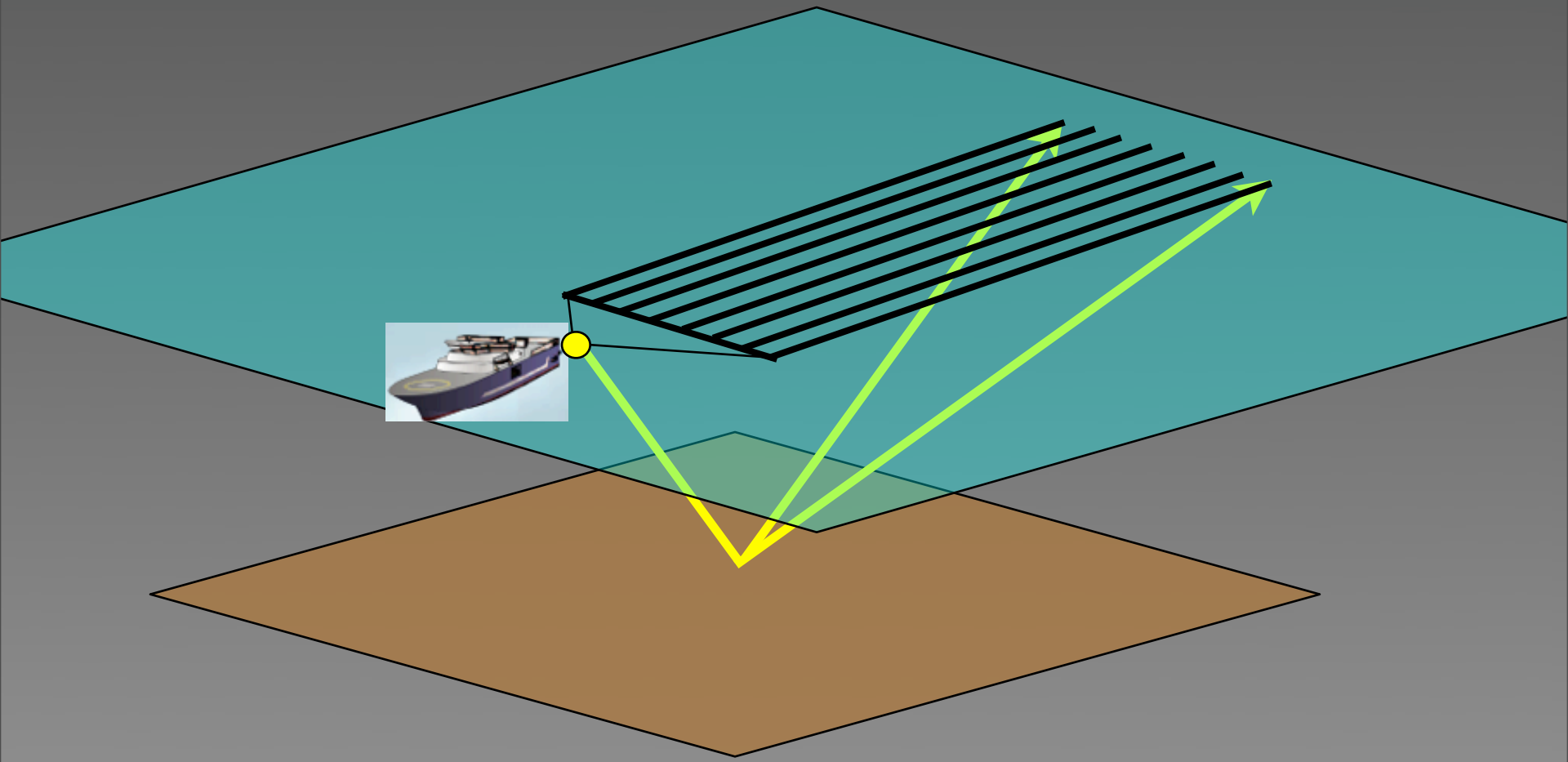

3D Narrow azimuth acquisition

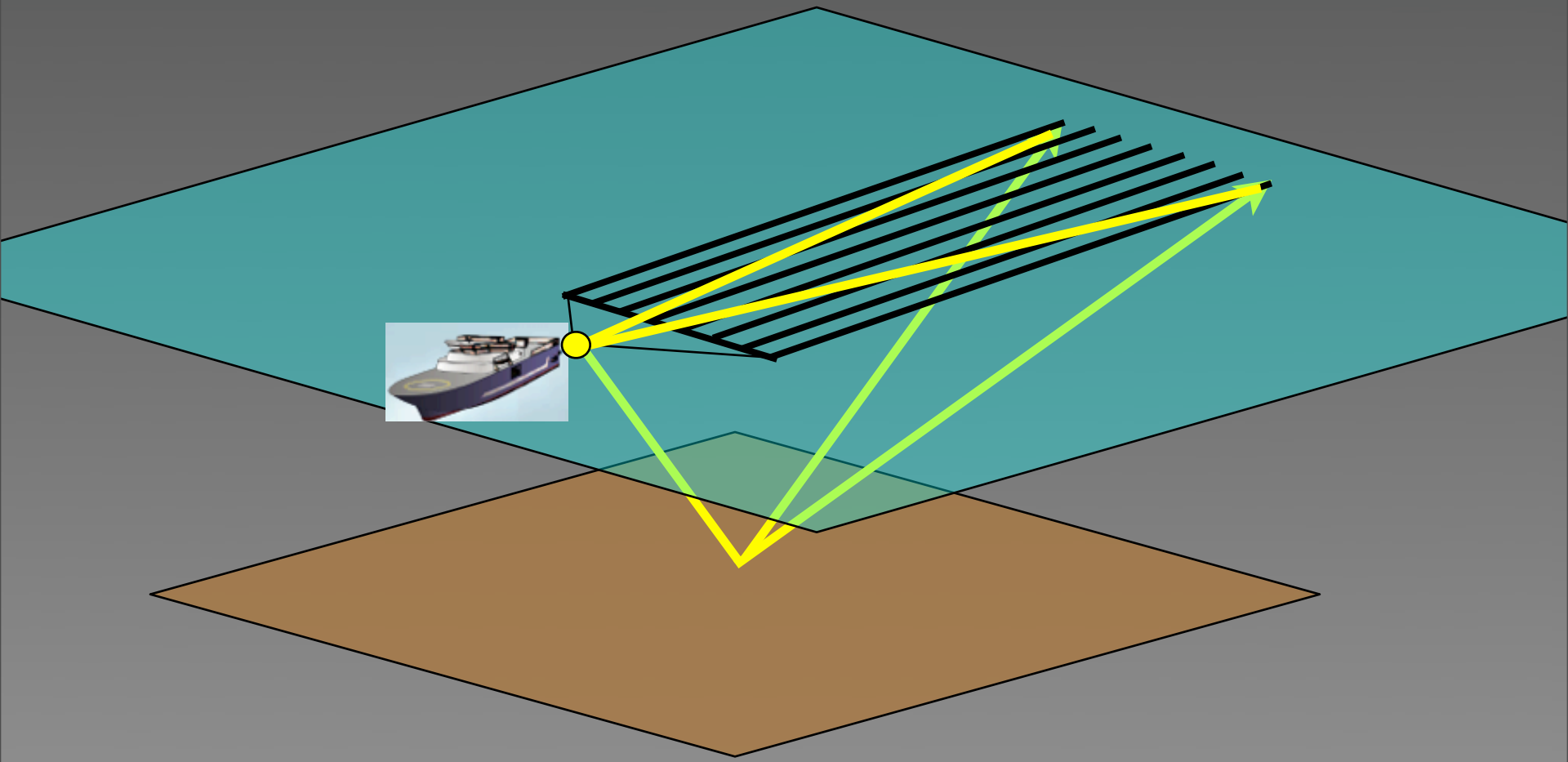

3D Wide azimuth acquisition

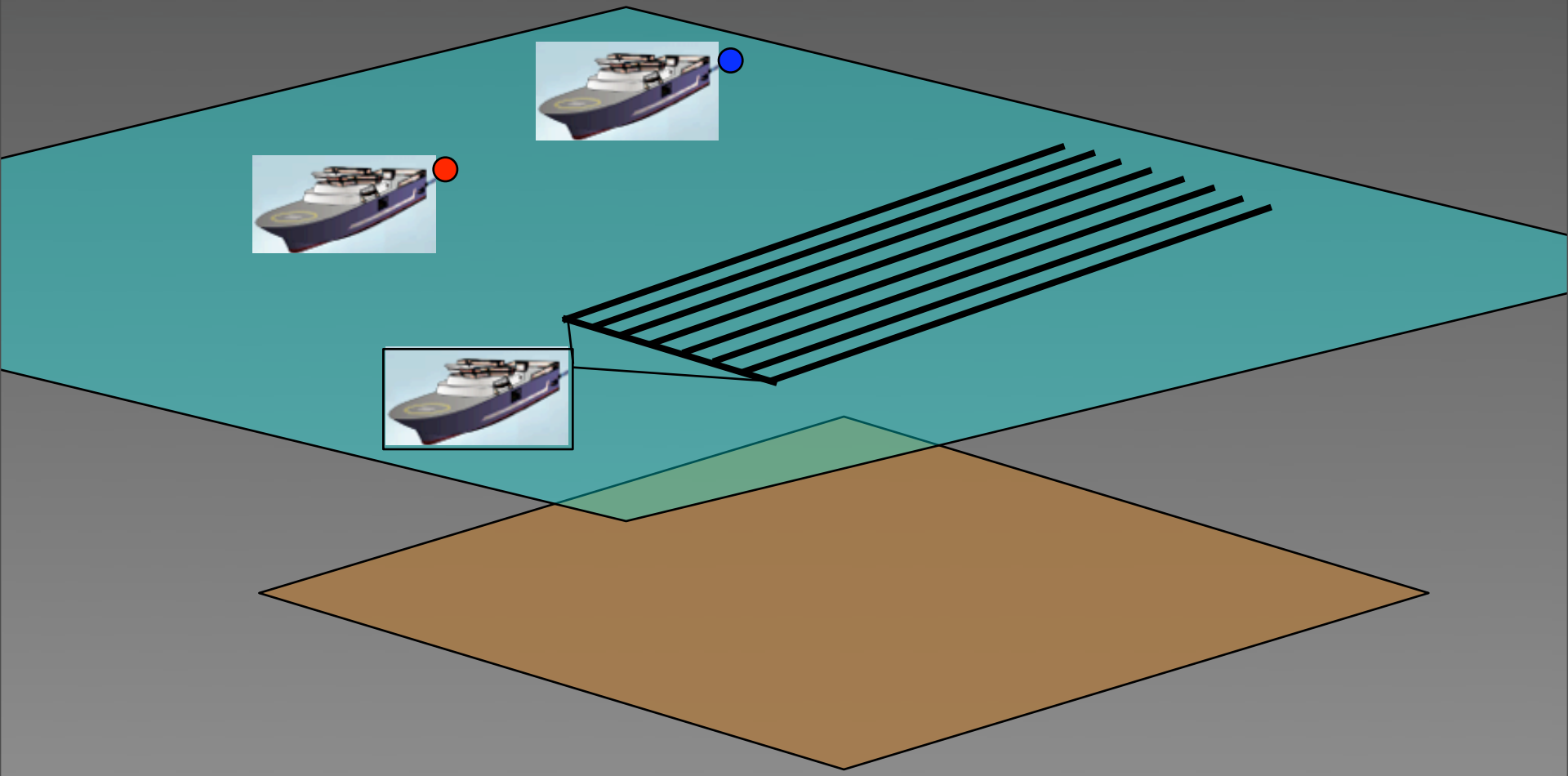

3D Wide azimuth acquisition

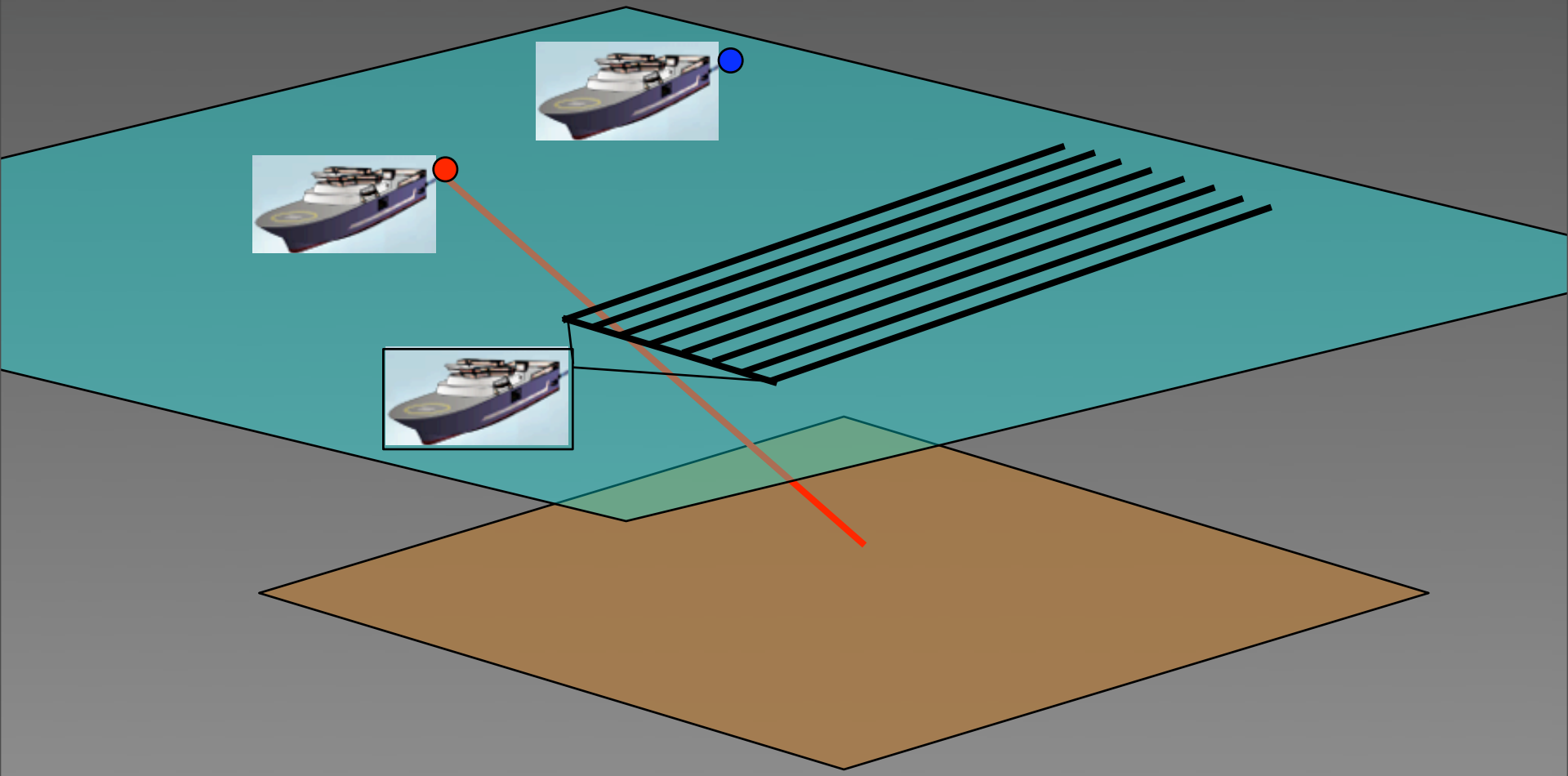

3D Wide azimuth acquisition

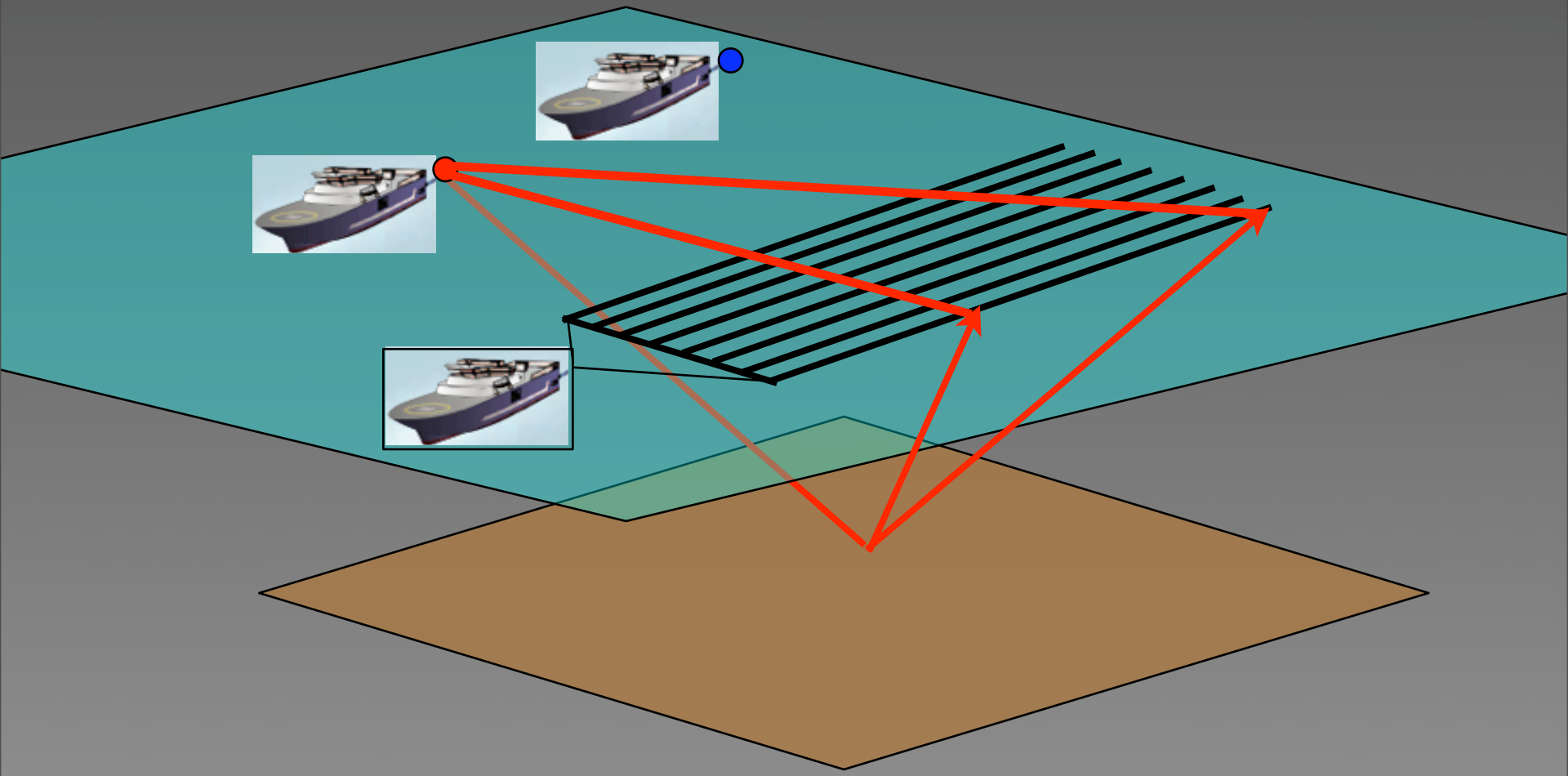

3D Wide azimuth acquisition

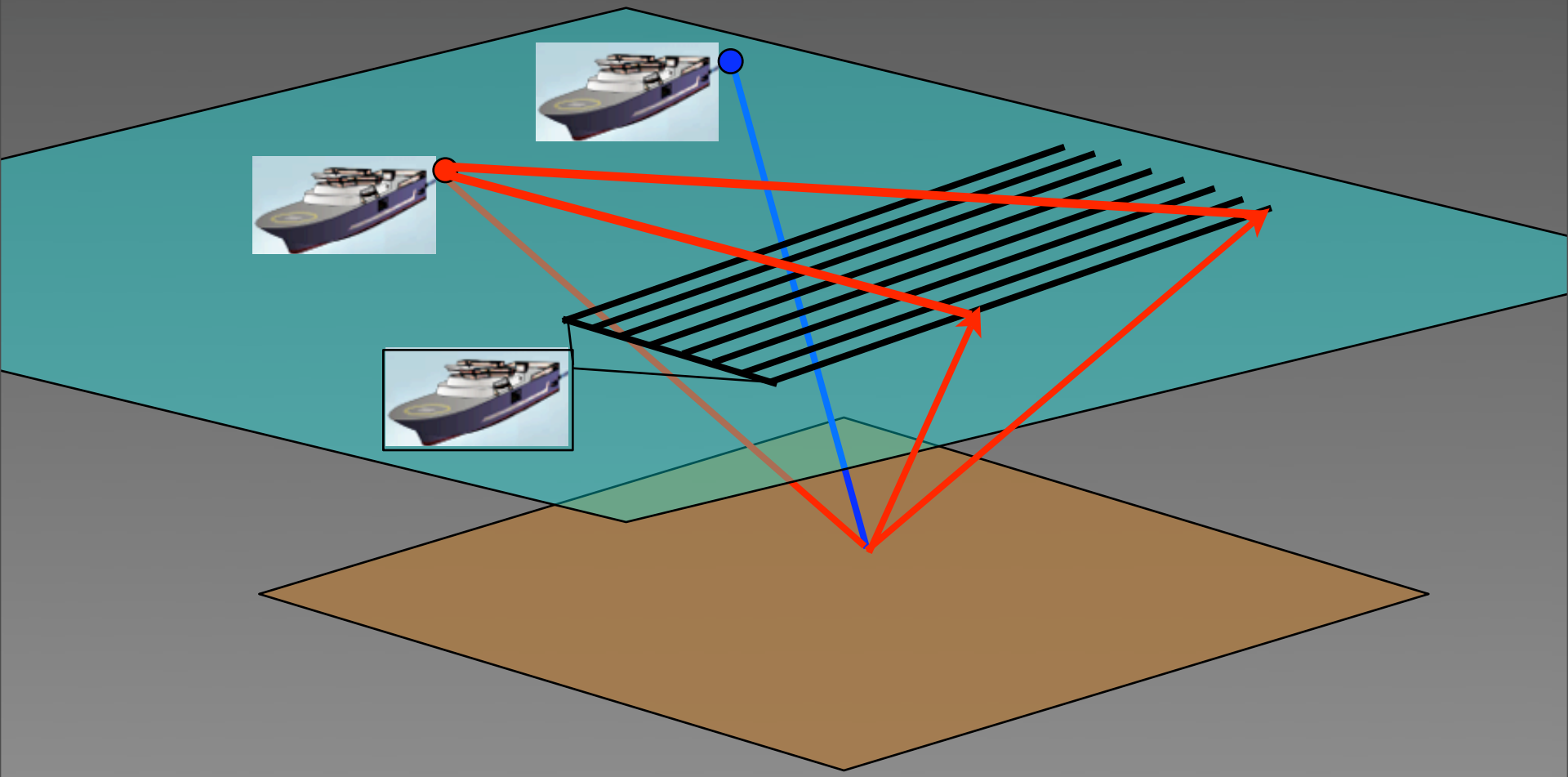

3D Wide azimuth acquisition

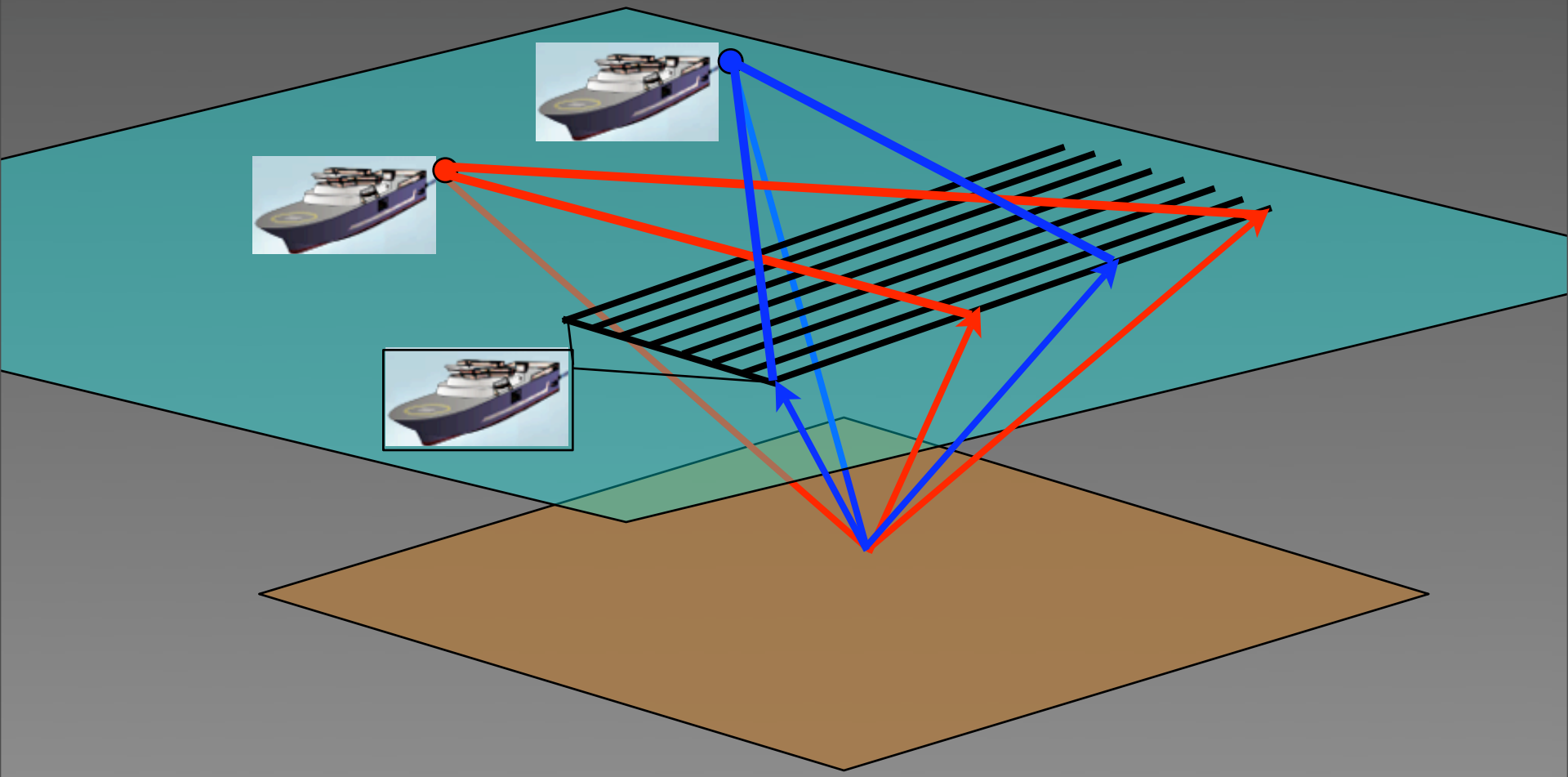

3D inversion angle stack $\varepsilon = 0.01$

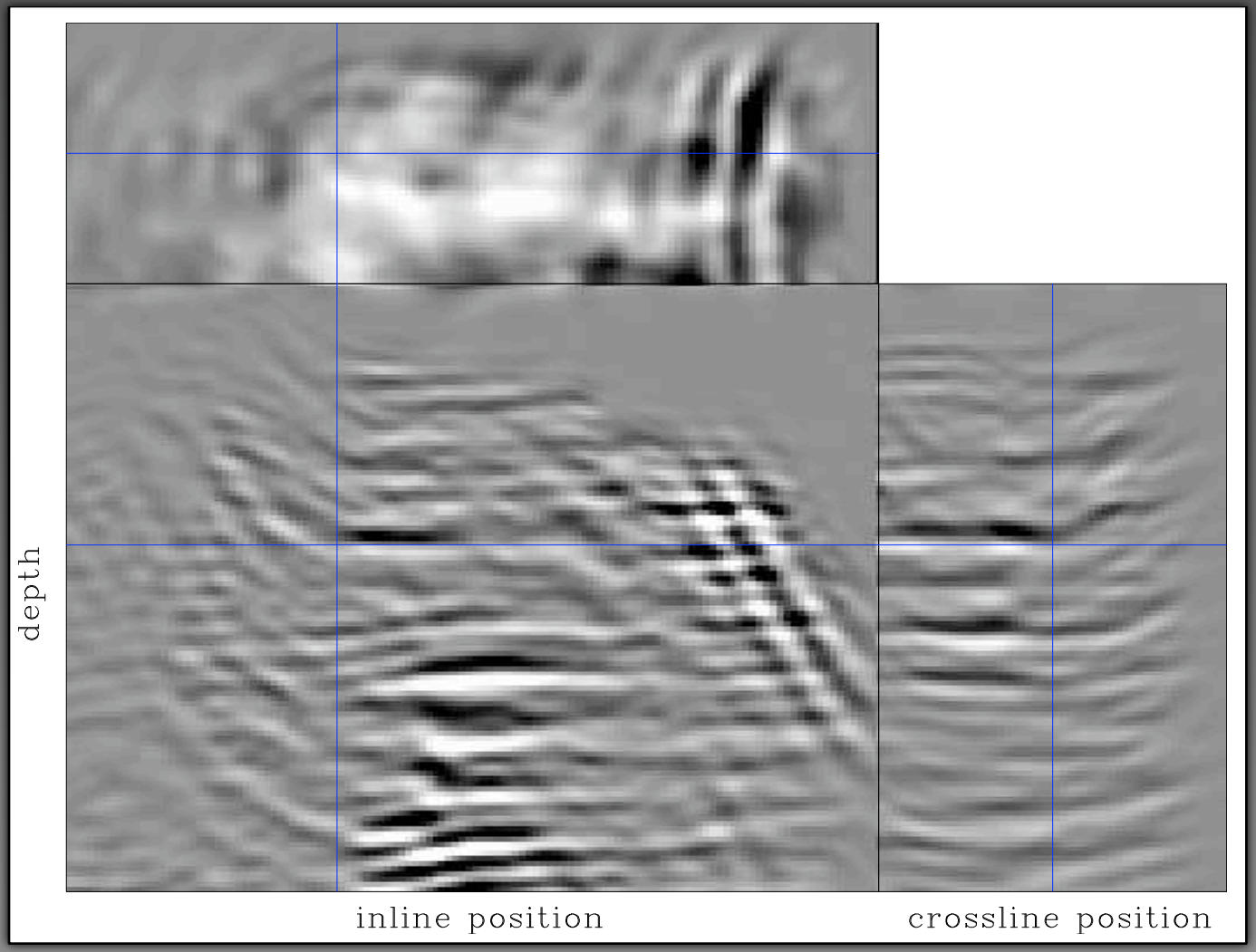

3D inversion angle stack $\varepsilon = 10$

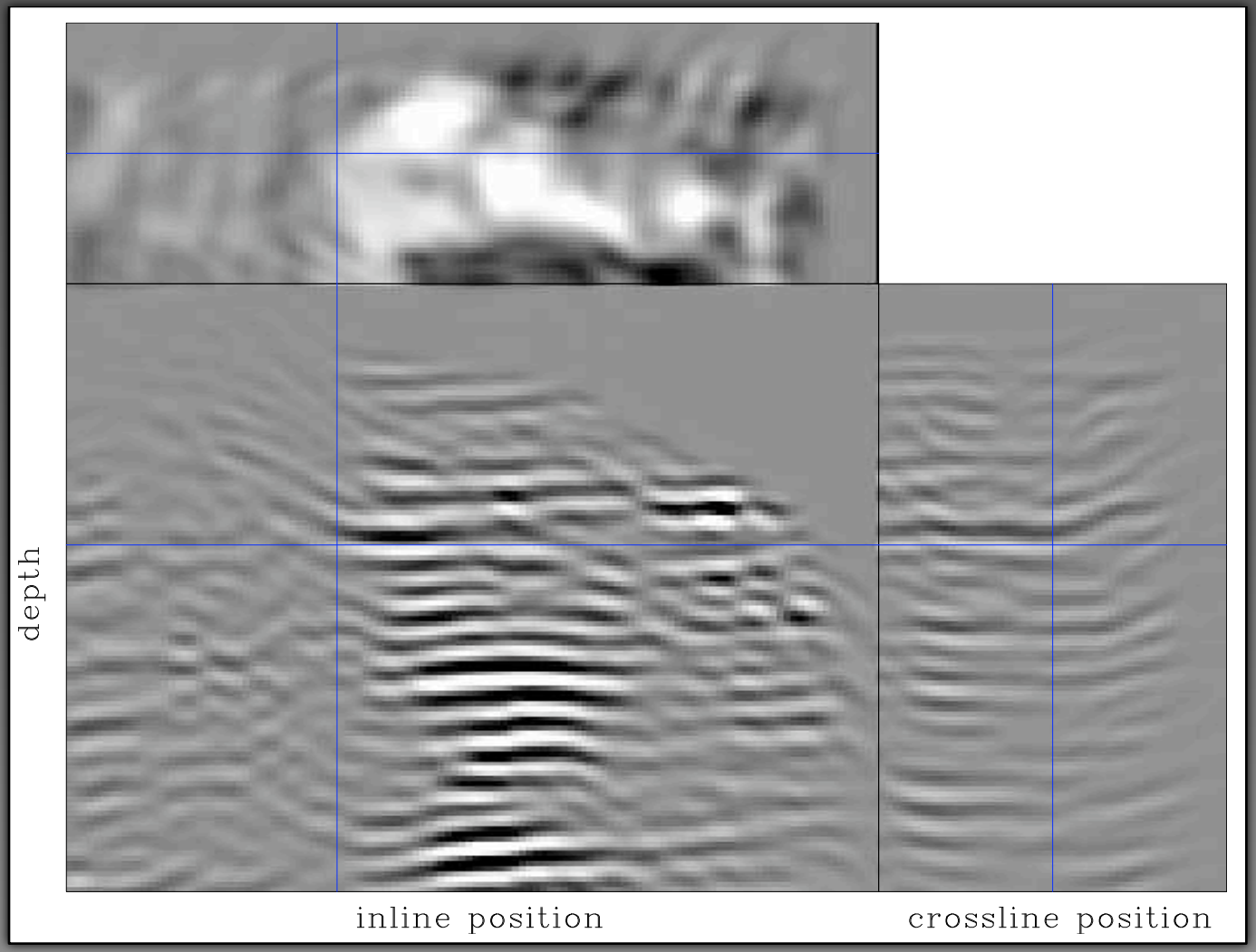

Target-oriented Hessian

$$\mathbf{H}(\mathbf{x}_T; \mathbf{x}'_T)$$

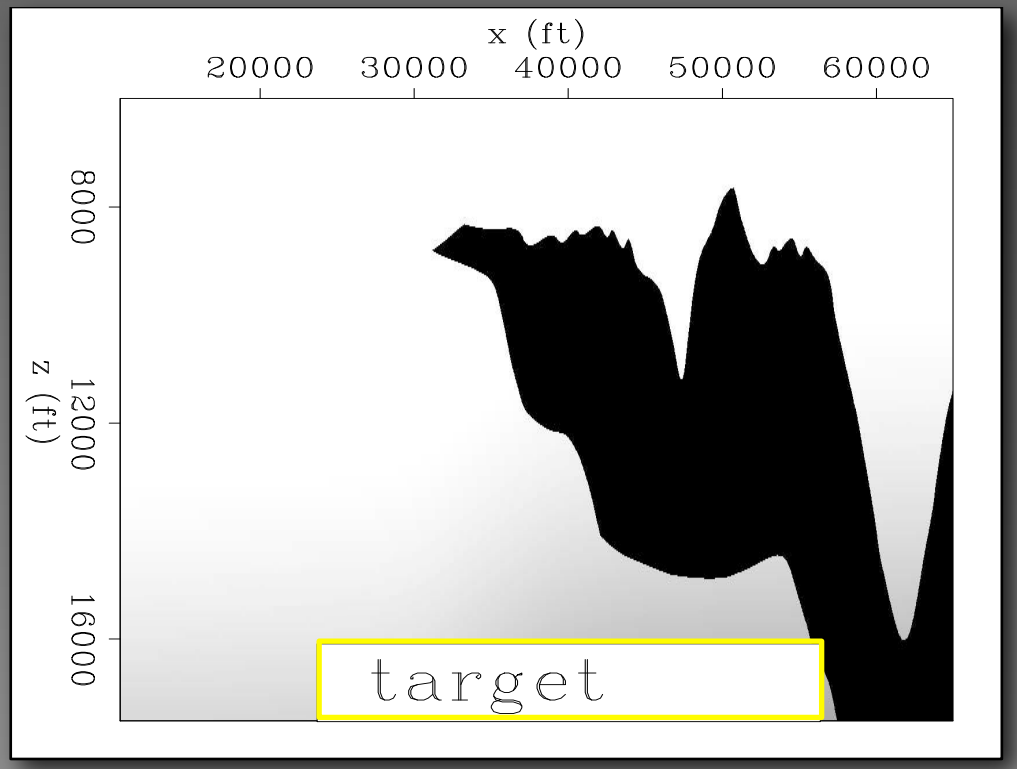

Hessian sparsity and structure

$$\mathbf{H}(\mathbf{x}_T, \mathbf{x}_T + \mathbf{a}_\mathbf{x}) = \sum_\omega \sum_{\mathbf{x}_s} \mathbf{G}'(\mathbf{x}_T, \mathbf{x}_s; \omega) \mathbf{G}(\mathbf{x}_T + \mathbf{a}_\mathbf{x}, \mathbf{x}_s; \omega)$$
$$\sum_{\mathbf{x}_r} \mathbf{G}'(\mathbf{x}_T, \mathbf{x}_r; \omega) \mathbf{G}(\mathbf{x}_T + \mathbf{a}_\mathbf{x}, \mathbf{x}_r; \omega)$$

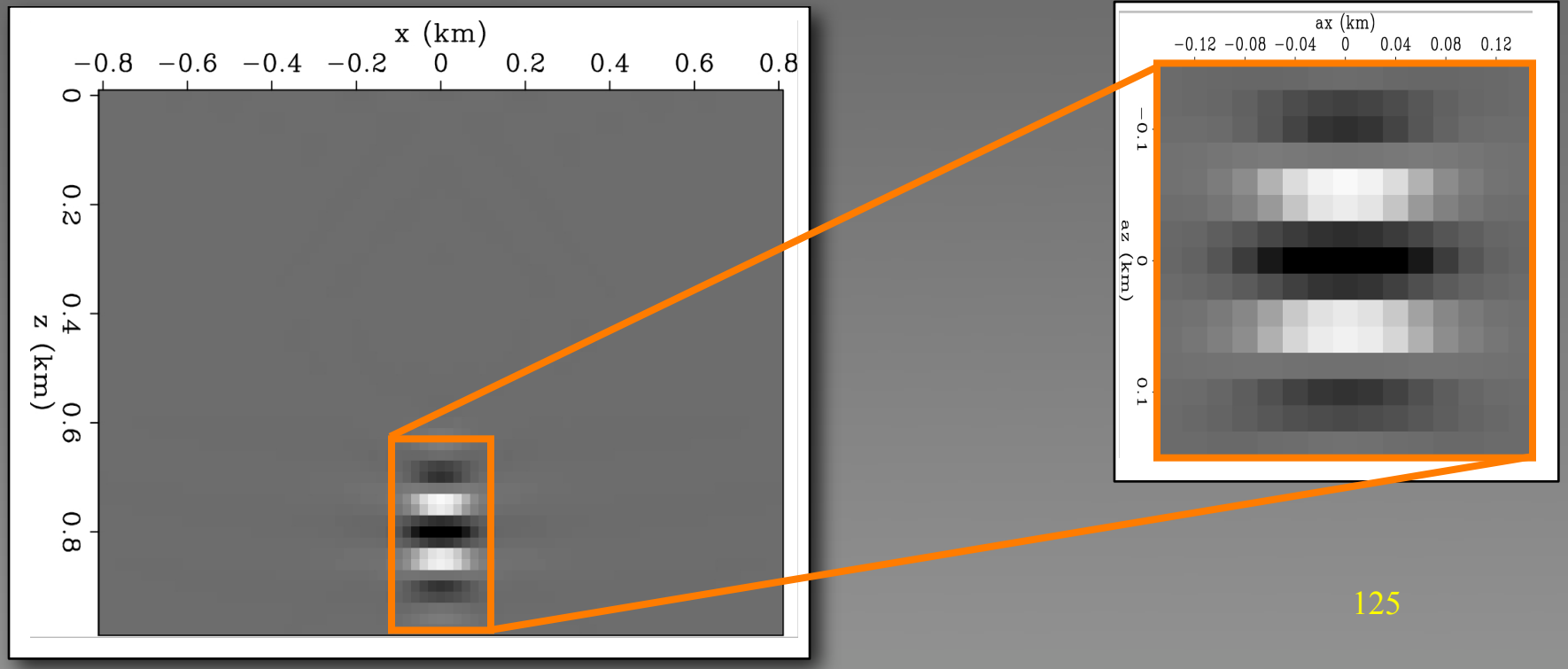

Acquisition geometry: OBC

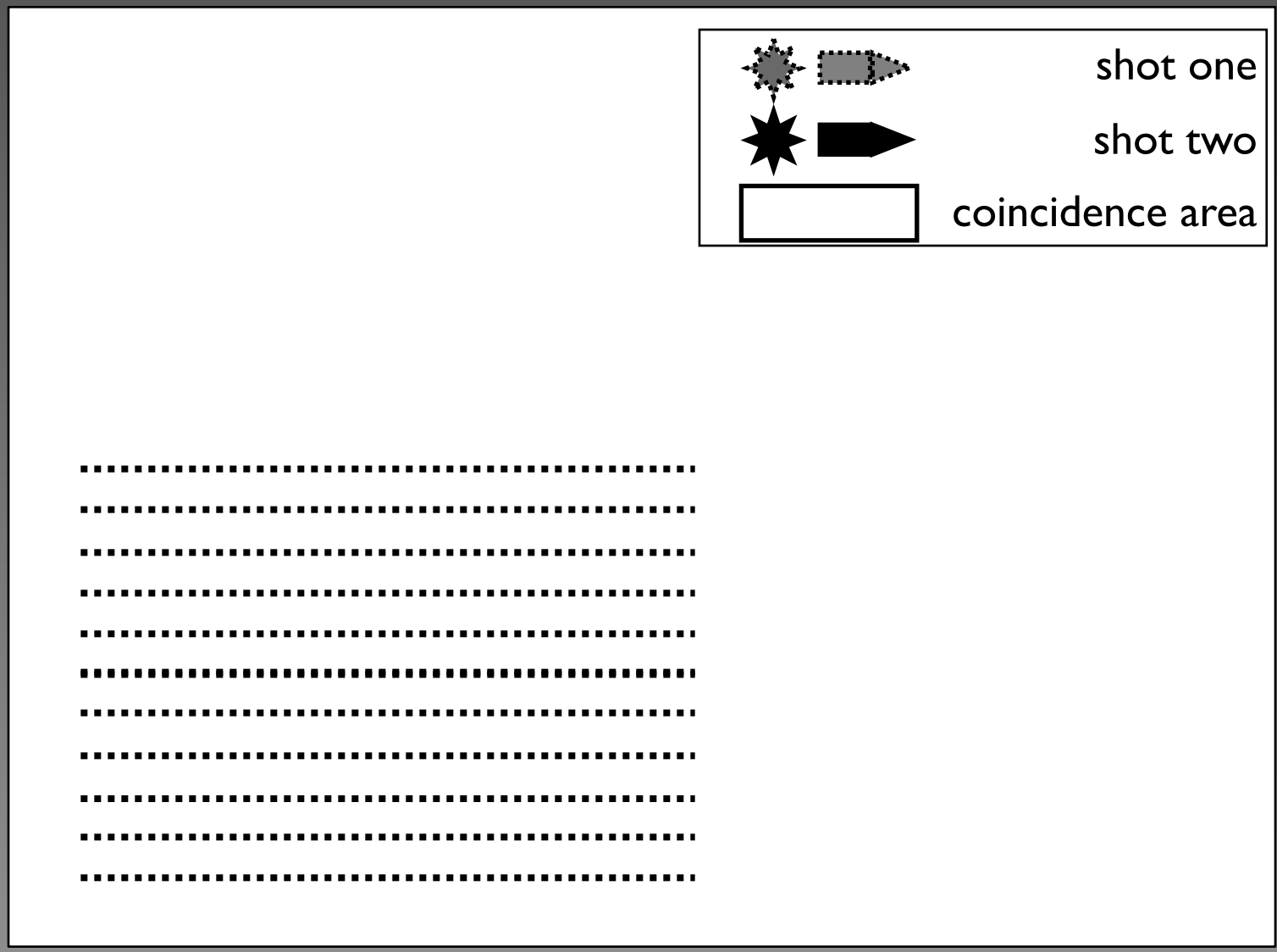

Acquisition geometry: OBC

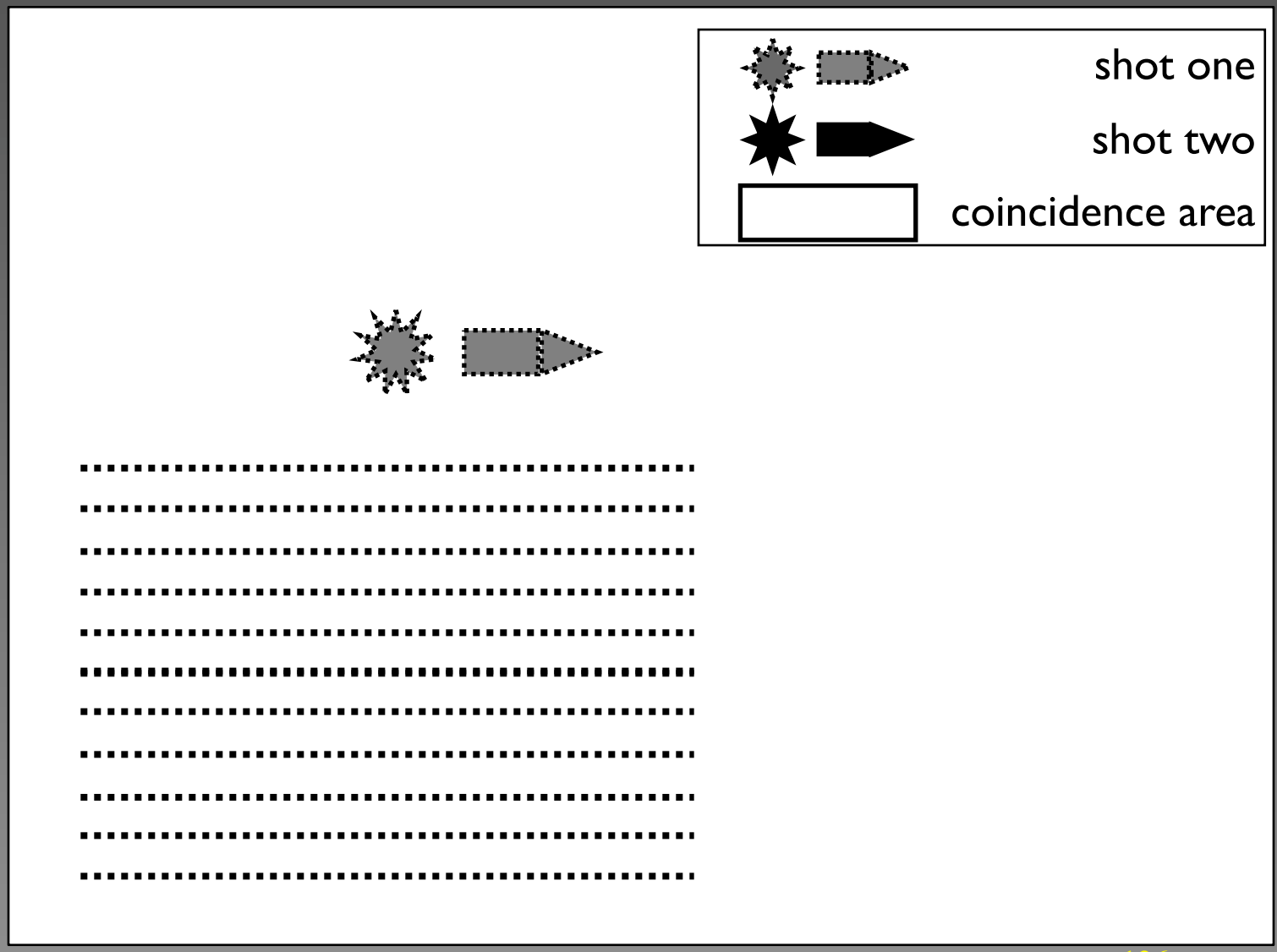

Acquisition geometry: OBC

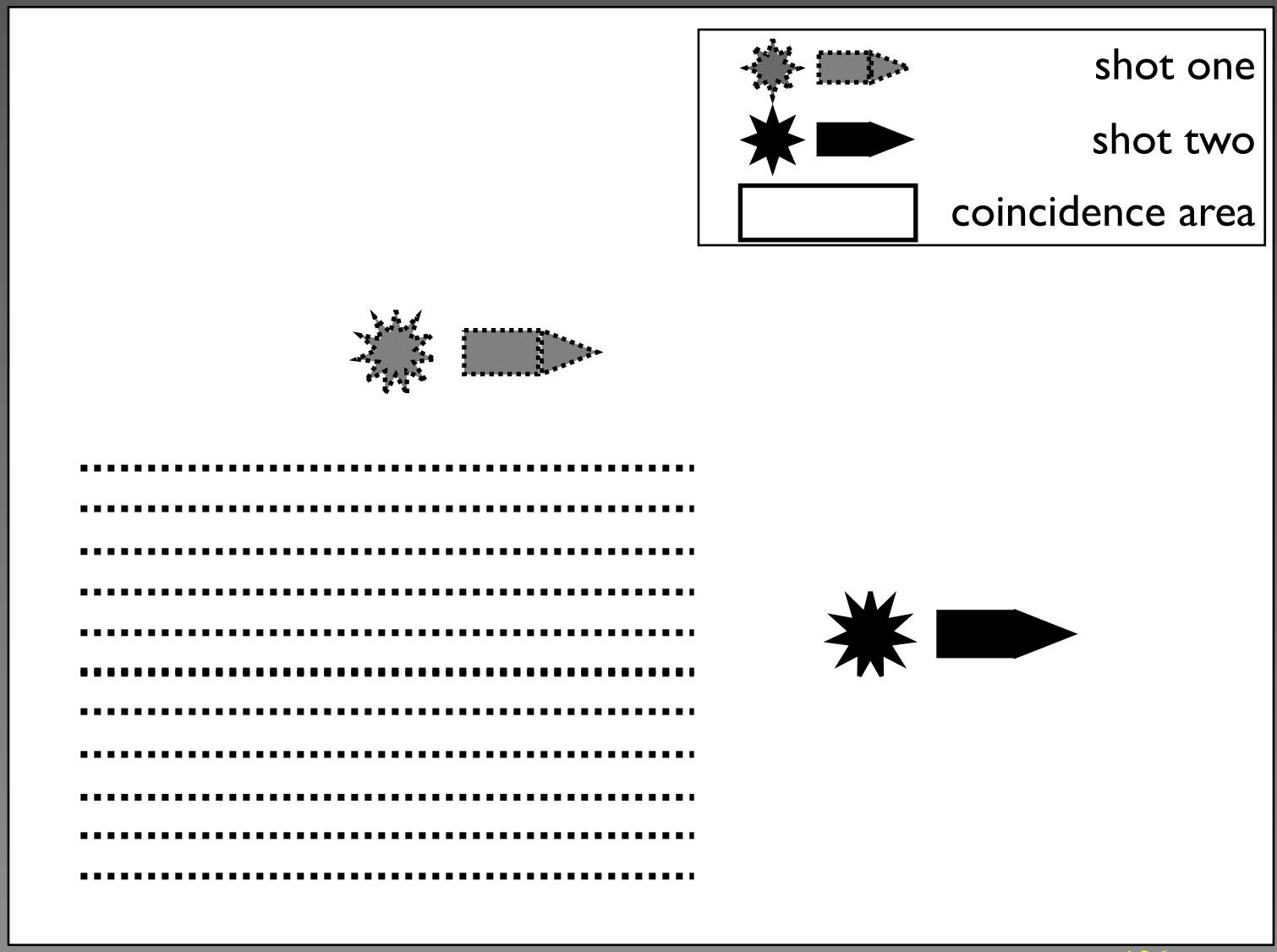

Acquisition geometry: OBC

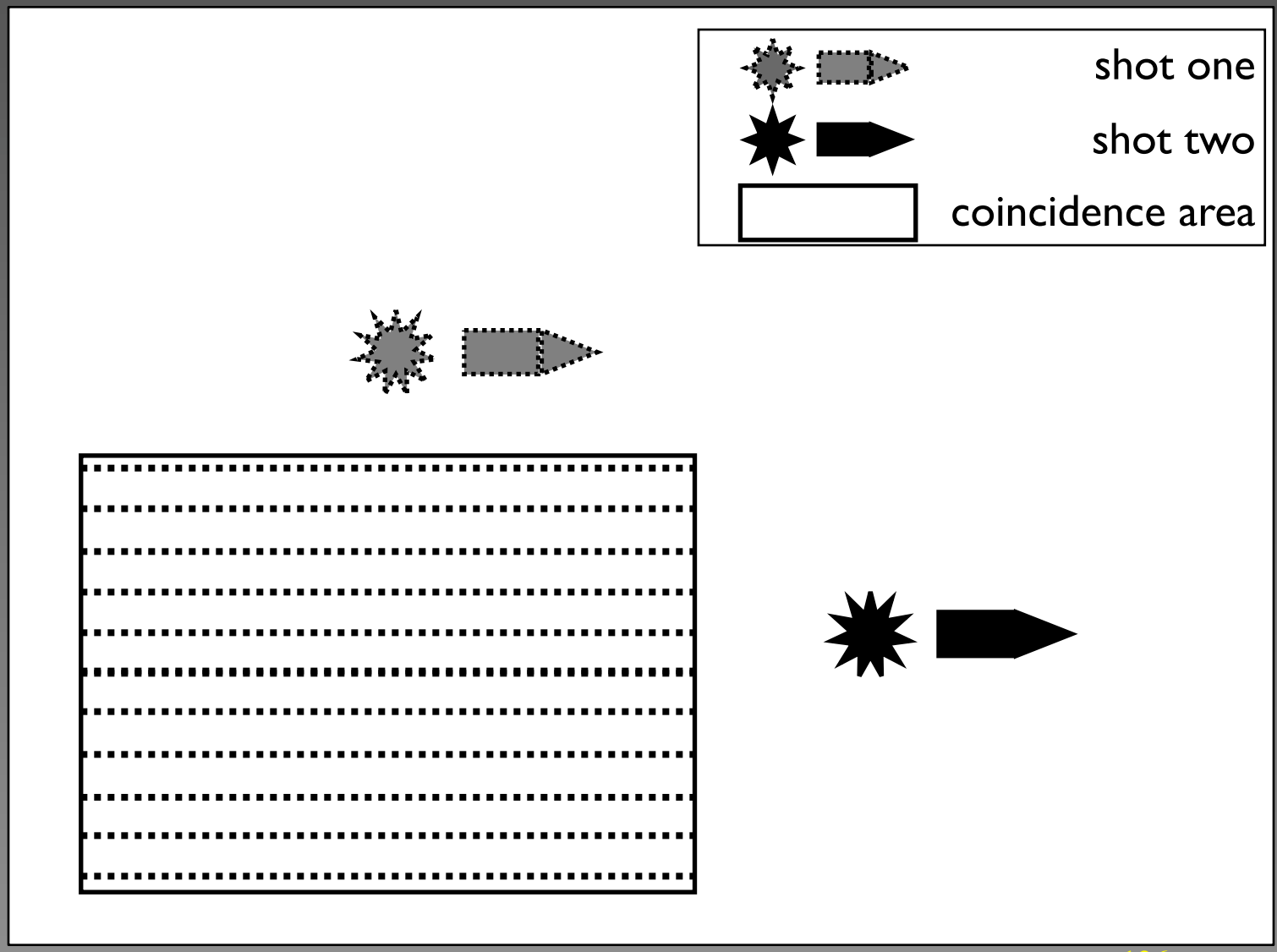

Acquisition geometry: towed streamers

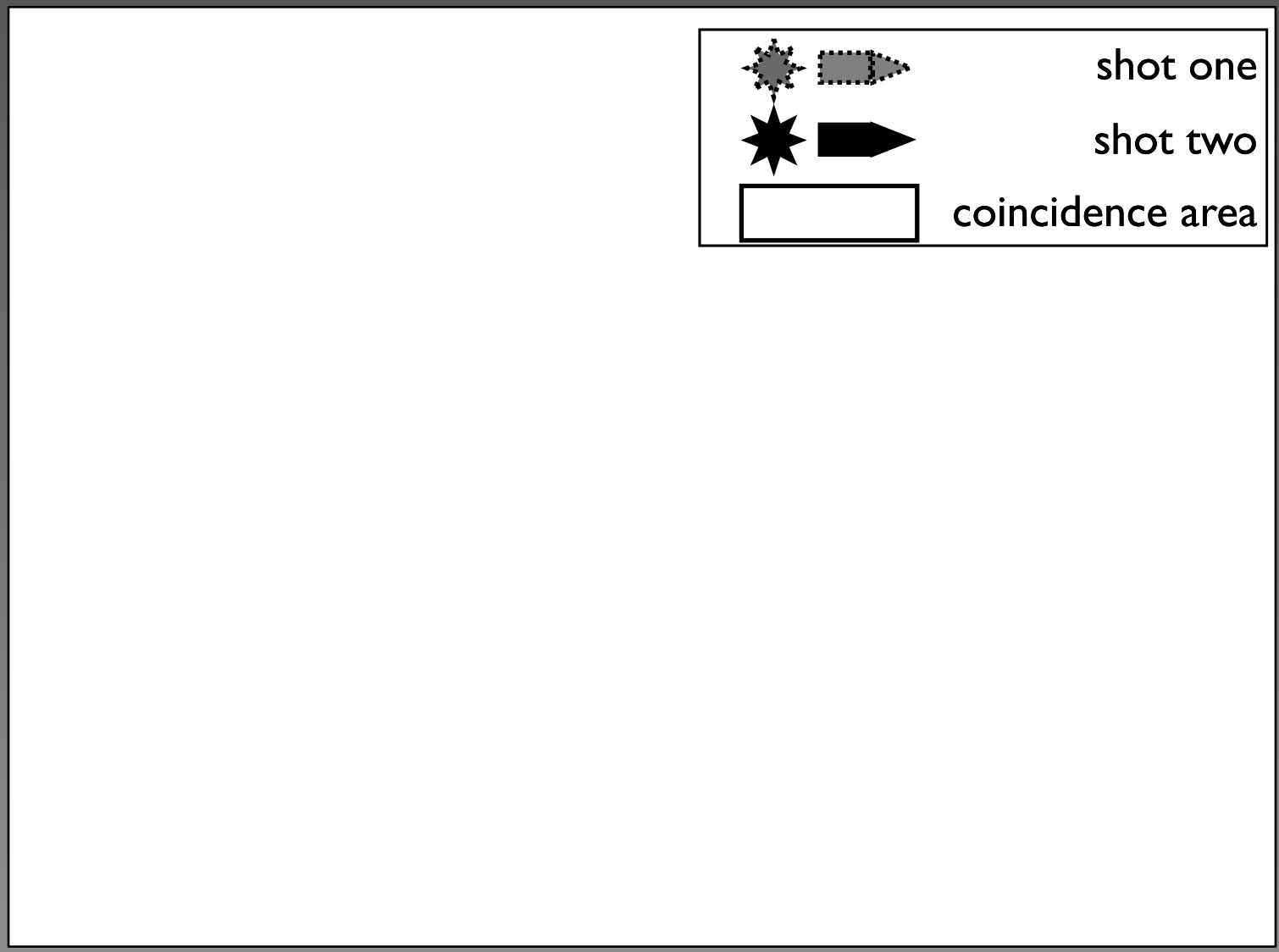

Acquisition geometry: towed streamers

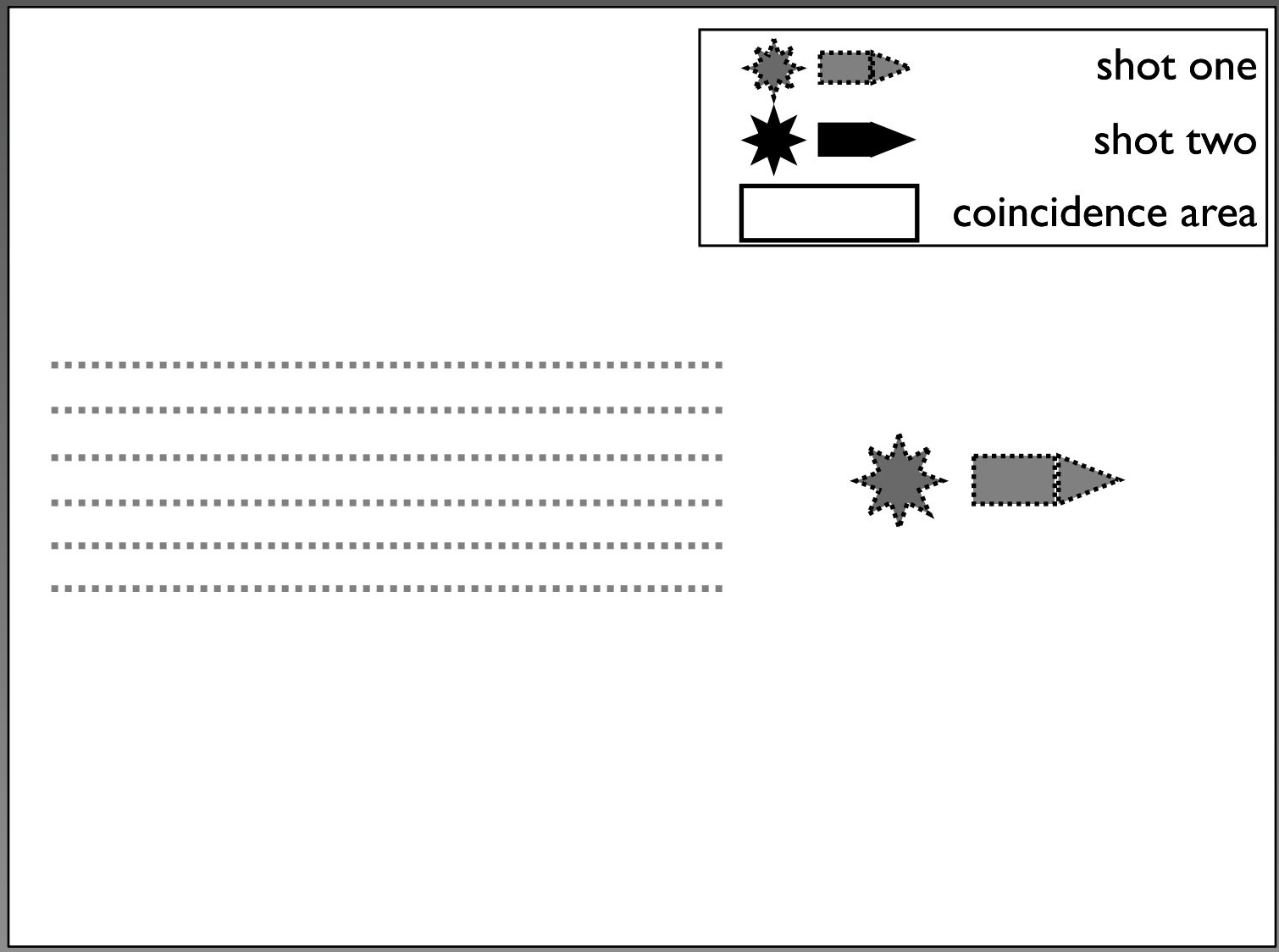

Acquisition geometry: towed streamers

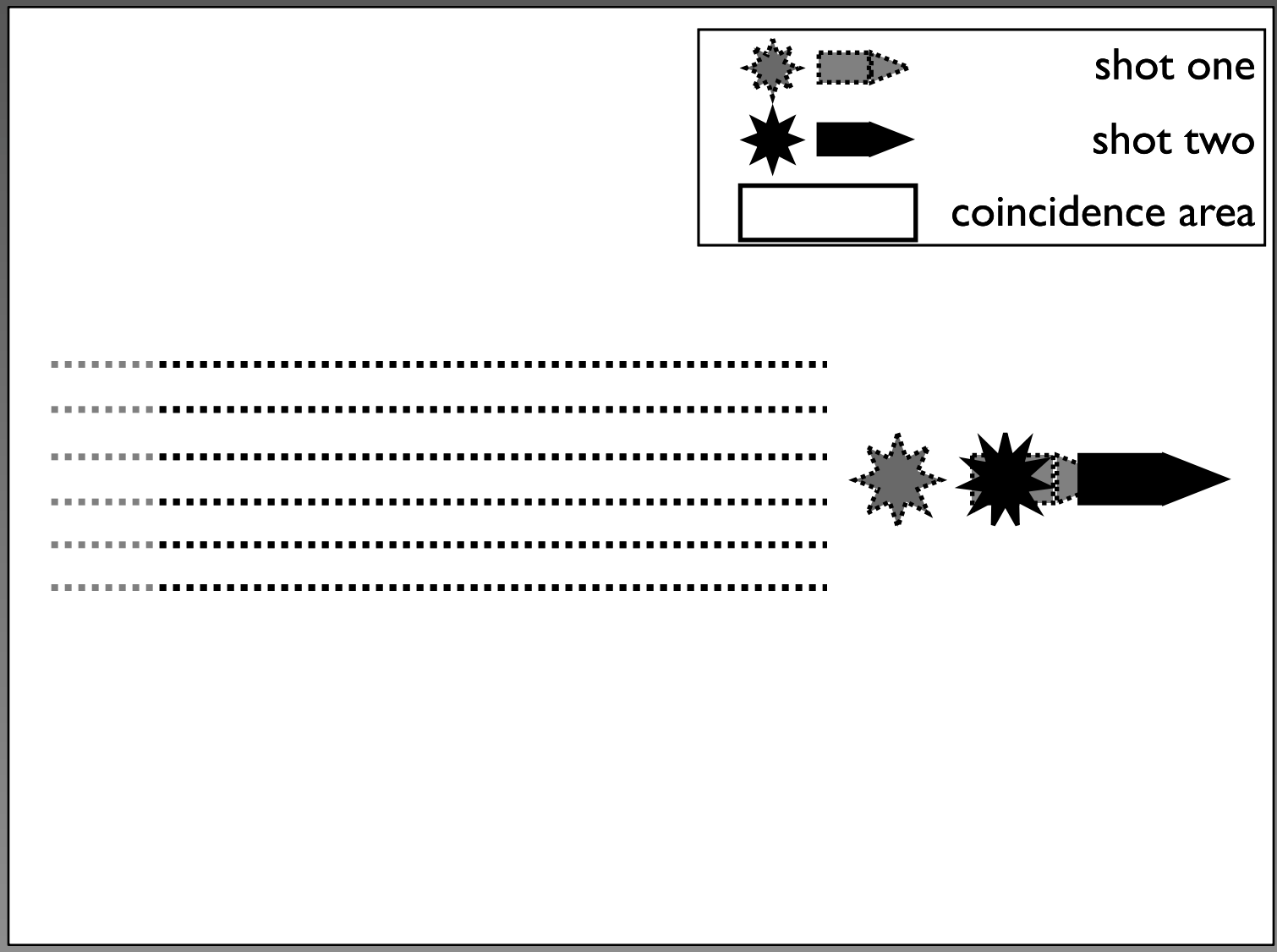

Acquisition geometry: towed streamers

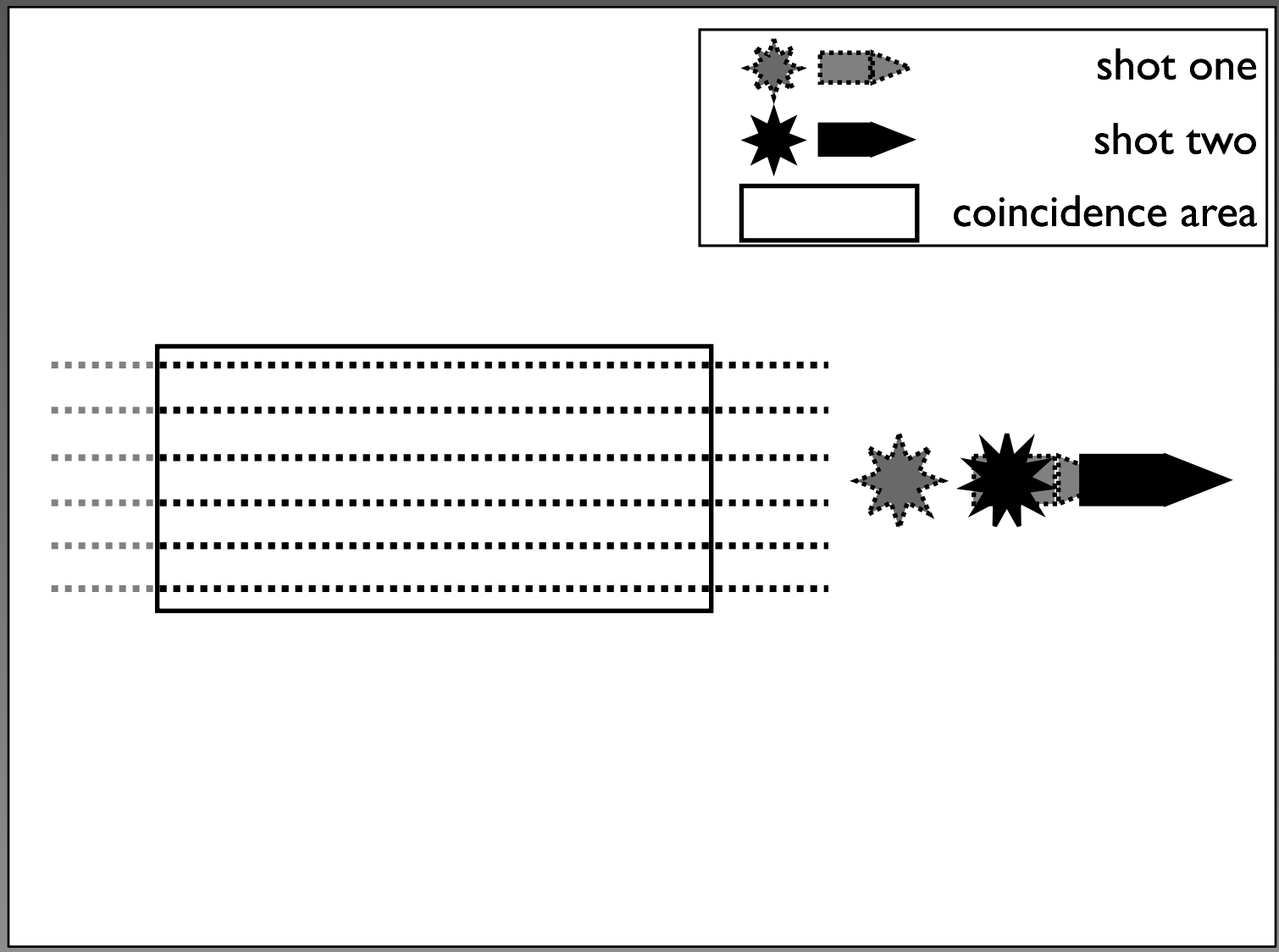

Frequency sampling $\Delta f = 2.44\,\mathrm{Hz}$

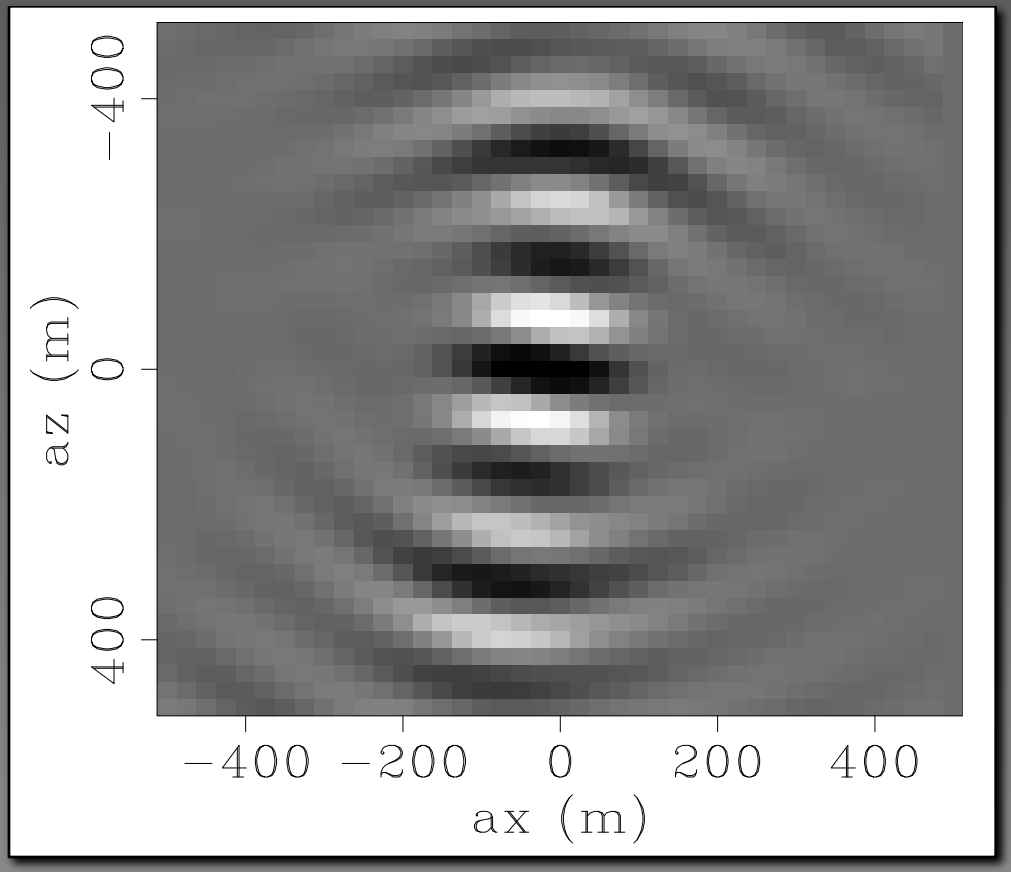

Frequency sampling $\Delta f = 2.19\,\mathrm{Hz}$

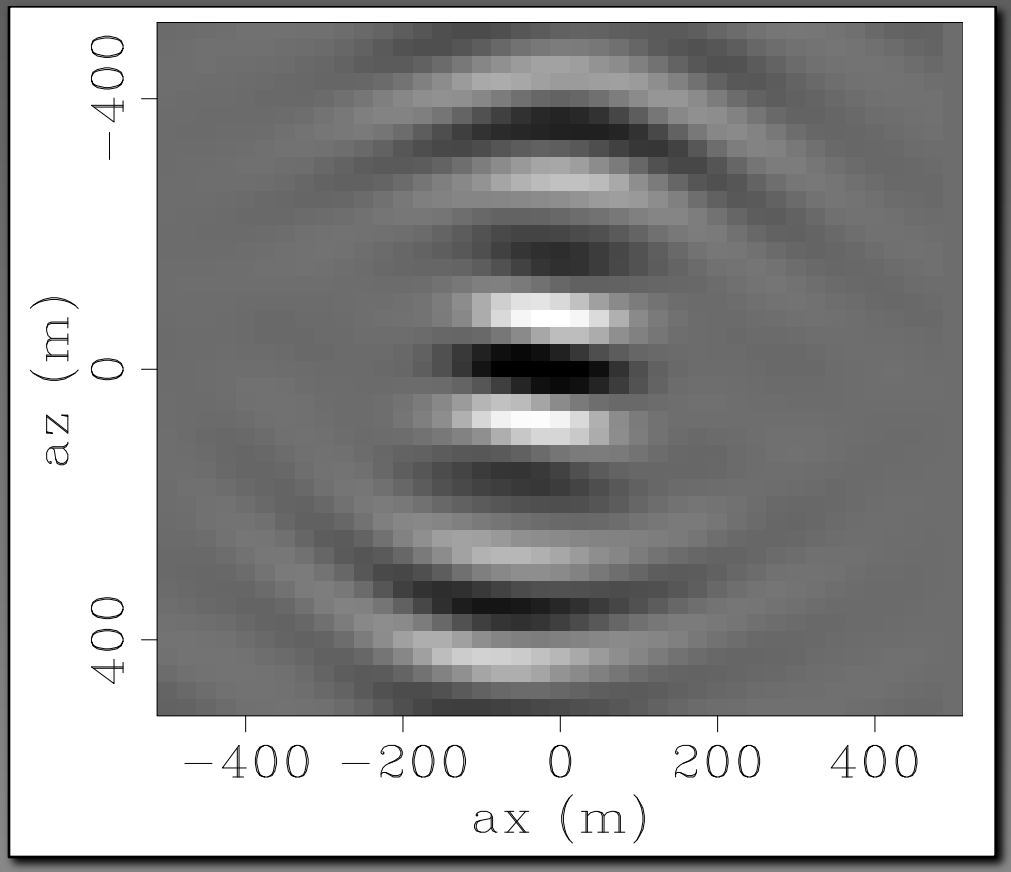

Frequency sampling $\Delta f = 1.95\,\mathrm{Hz}$

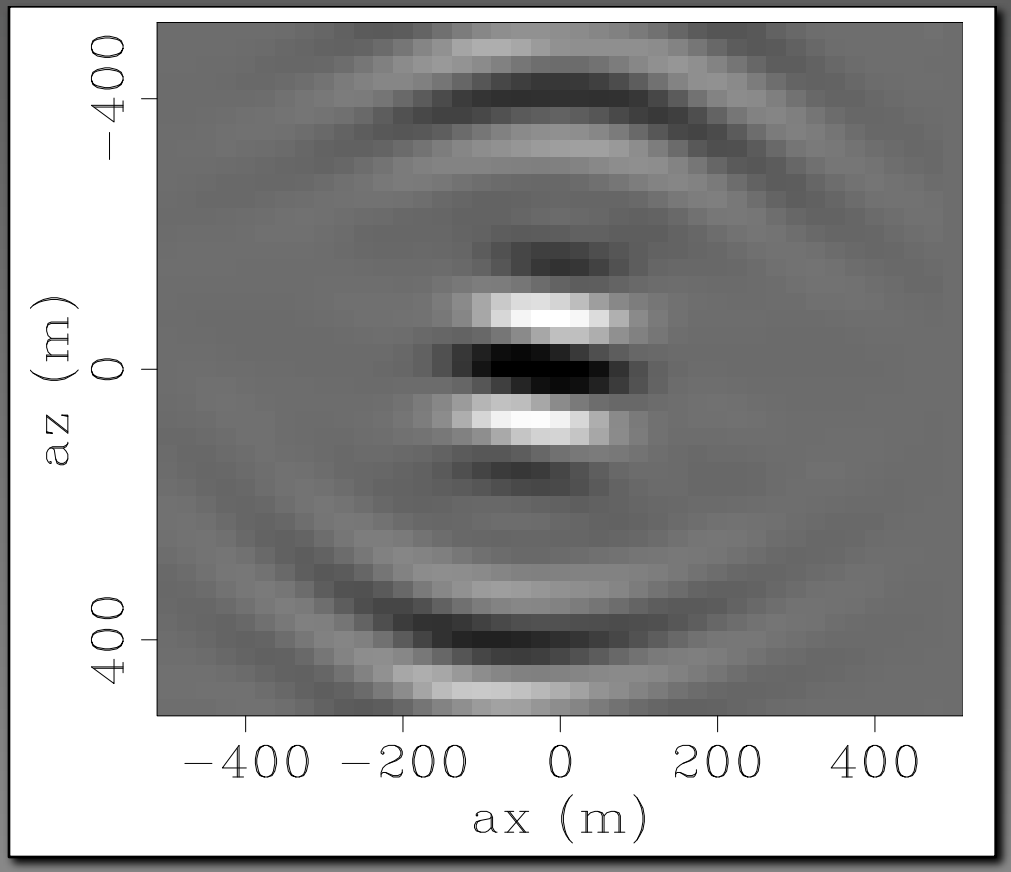

Frequency sampling $\Delta f = 1.71\,\mathrm{Hz}$

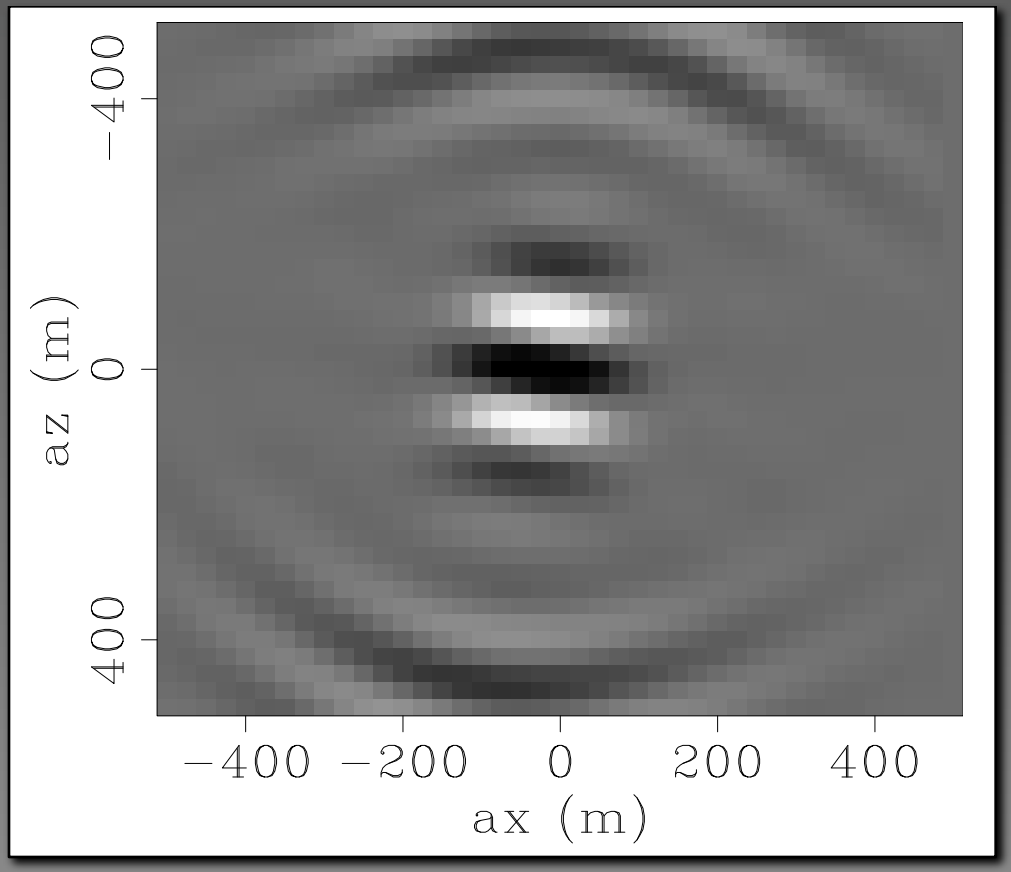

Frequency sampling $\Delta f = 1.46\,\mathrm{Hz}$

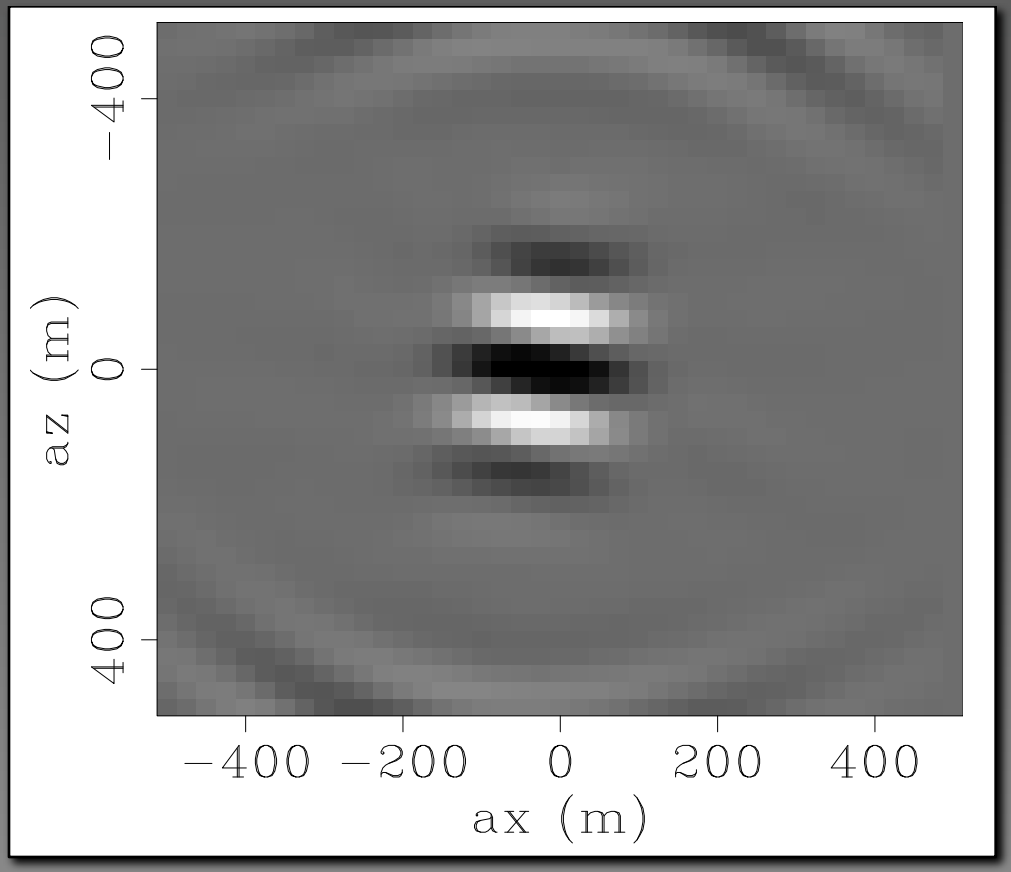

Frequency sampling $\Delta f = 1.22\,\mathrm{Hz}$

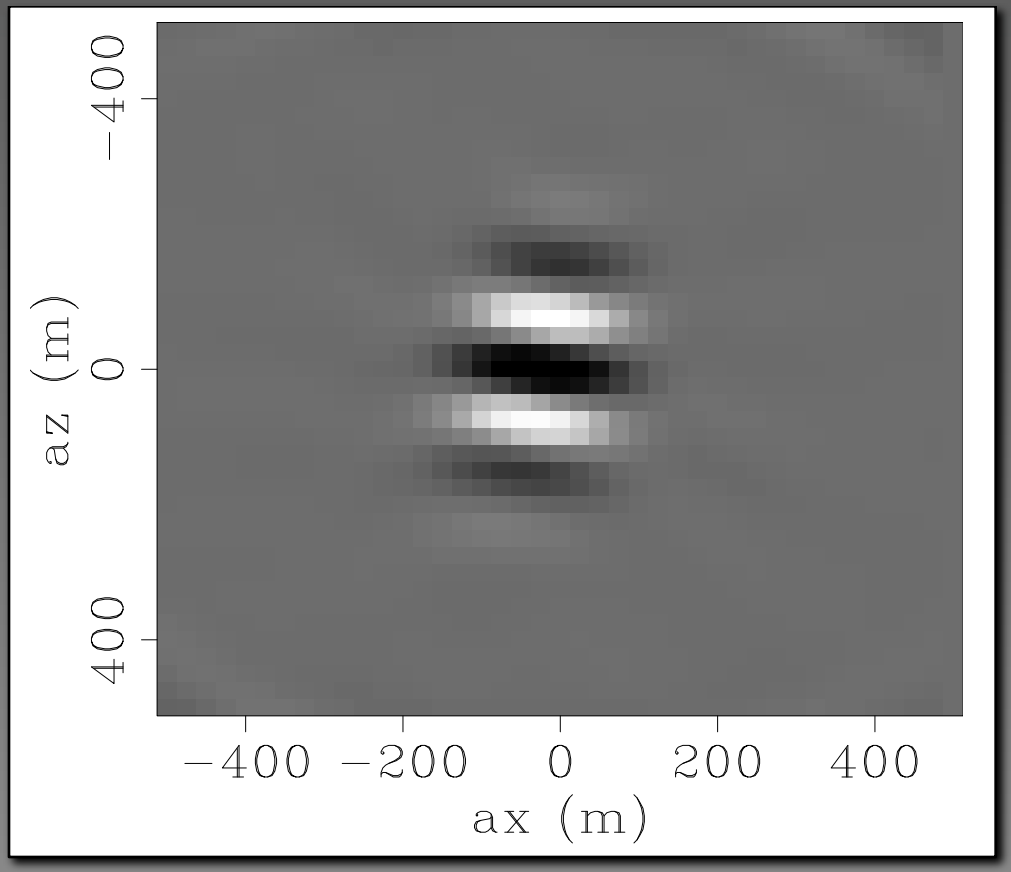

Frequency sampling $\Delta f = 0.97\,\mathrm{Hz}$

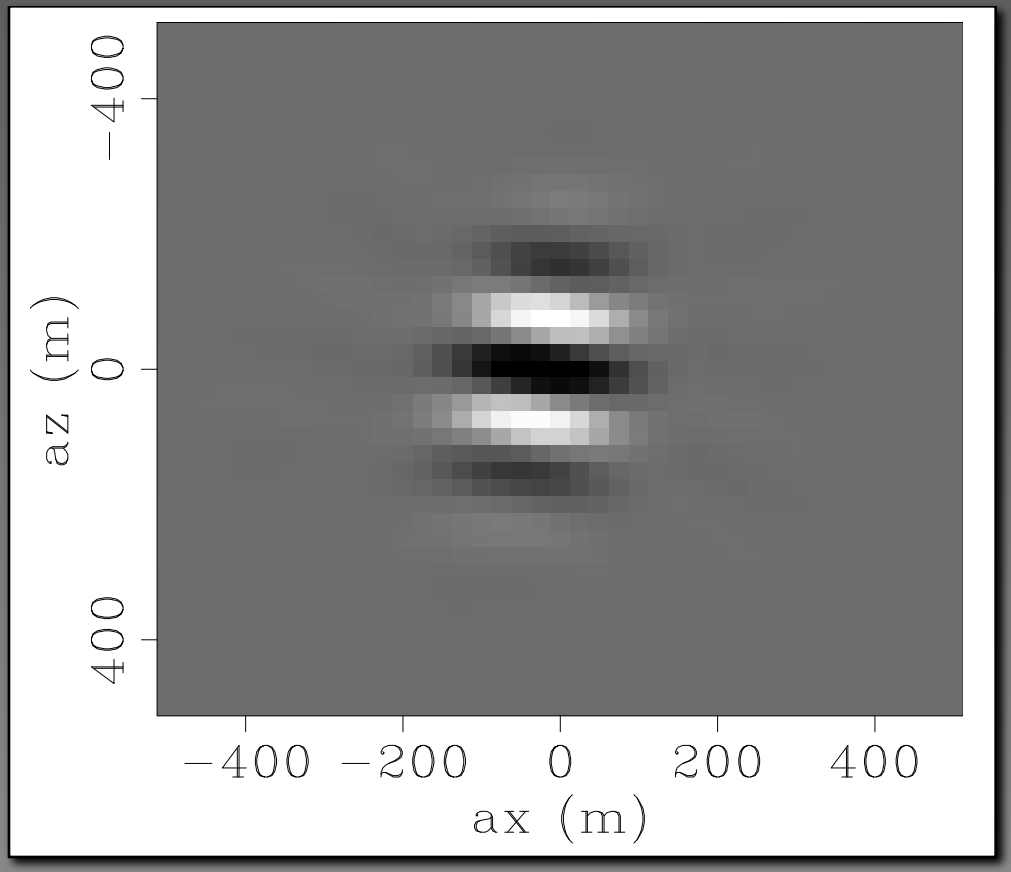

“illumination” from all shots: subsurface offset

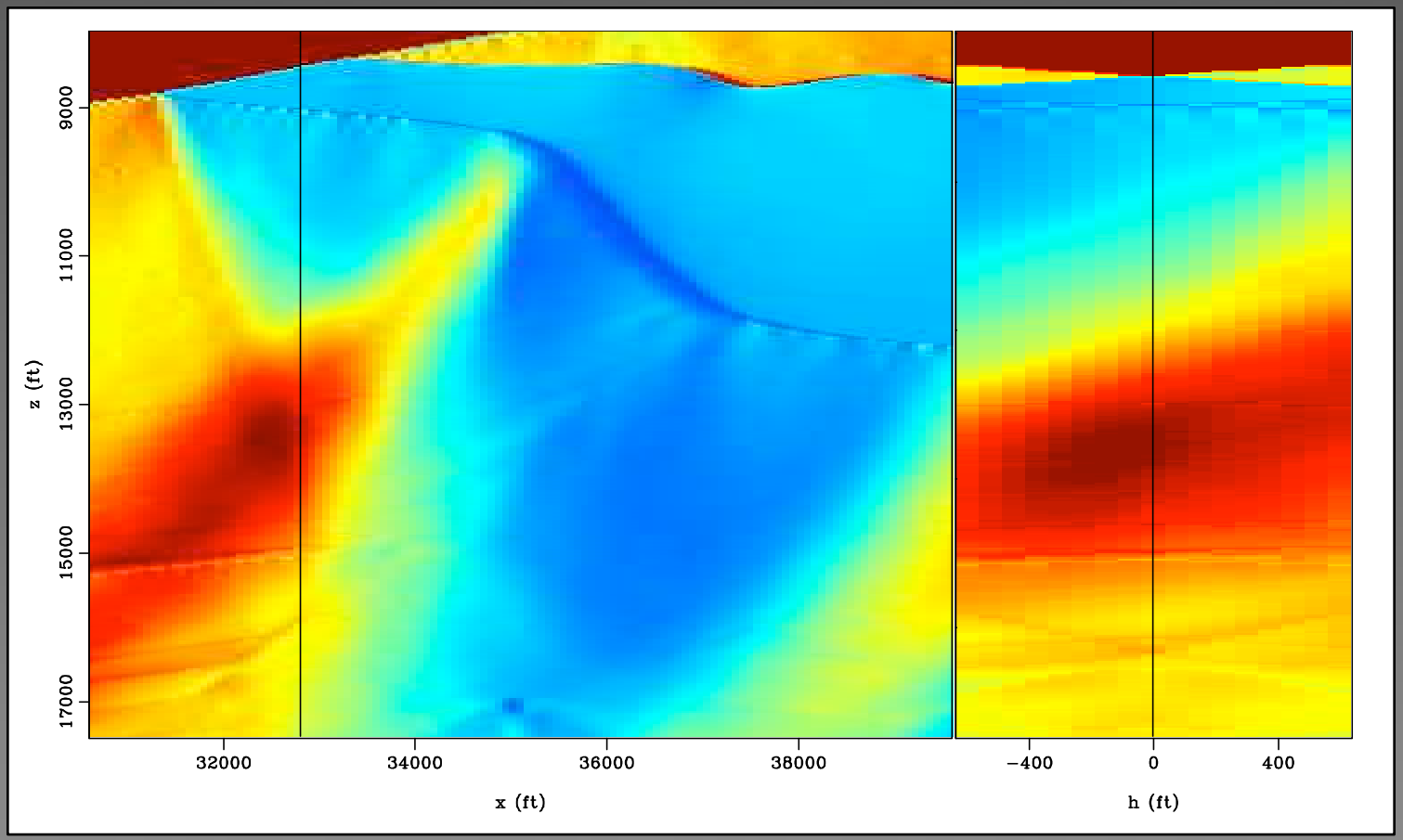

Point Spread Function: subsurface offset